

## CHAPTER 2

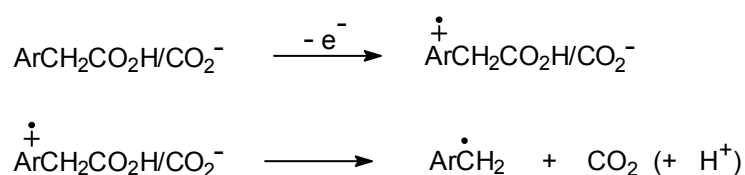
---

- 2.1. Spectroscopic Detection, Reactivity and Acid-Base Behavior of Ring-Dimethoxylated Phenylethanoic Acid Radical Cations and Radical Zwitterions in Aqueous Solution.**
  
  - 2.2. One-Electron Oxidation of 2-Aryl-2-Methyl Propanoic and 1-Arylcyclopropanecarboxylic Acids in Aqueous Solution. The Involvement of Aromatic Radical Cations and the Effect of an  $\alpha$ -Cyclopropyl Group.**
  
  - 2.3. One-Electron Oxidation of Ring Methoxylated 1-Arylcycloalkanecarboxylic Acids. The Involvement of Aromatic Radical Cations and the Effect of Ring Size on the Decarboxylation Rate Constant.**
-



## 2.1. Spectroscopic Detection, Reactivity and Acid-Base Behavior of Ring-Dimethoxylated Phenylethanoic Acid Radical Cations and Radical Zwitterions in Aqueous Solution.

The oxidative decarboxylation of aryloethanoic acids has attracted considerable attention. In aqueous solution the involvement of aromatic radical cations following the one-electron oxidation of aryloethanoic acids has been proposed in several studies,<sup>1,2</sup> but clear evidence in this respect has been obtained only for relatively electron rich substrates such as 1-naphthylethanoic acid,<sup>3</sup> 4-dimethylaminophenylethanoic acid and its  $\alpha$ -methyl and  $\alpha$ -hydroxy derivatives, and 2,4,5-trimethoxymandelic acid.<sup>4</sup> With these substrates a mechanism proceeding through a direct electron transfer from the aromatic ring with formation of an intermediate radical cation (or radical zwitterion) has been proposed. The radical cation then undergoes decarboxylation leading to the corresponding benzylic-type radicals as described in Scheme 2.1.1.

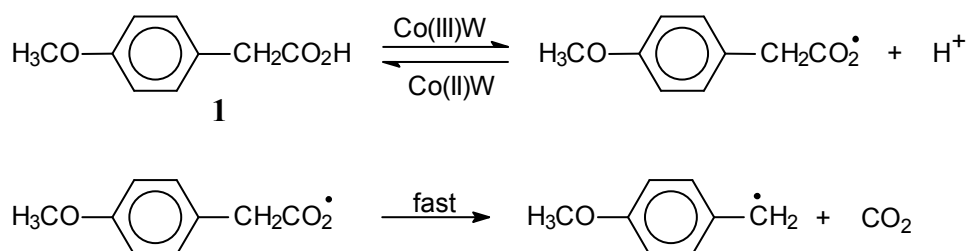


Scheme 2.1.1

With a less electron rich substrate such as 4-methoxyphenylethanoic acid (**1**), a number of product studies led to the conclusion that one electron oxidation proceeds through an analogous mechanism with formation of  $\mathbf{1}^{\bullet+}$ .<sup>1a,1c,2</sup> The formation of an intermediate aromatic radical cation, which then undergoes rapid decarboxylation leading to a benzylic radical was the conclusion of Steenken and Gilbert who studied the oxidative decarboxylation of 4-methylphenylethanoic and 4-methoxyphenylethanoic (**1**) acids in a laser flash photolysis (LFP) study in aqueous solution.<sup>3</sup> Lower limits for the decarboxylation rates of the two acids were provided ( $k_{\text{dec}} 10^7 \text{ s}^{-1}$ ), following the formation of the 4-methoxy and 4-methylbenzyl radical. However no direct evidence for the formation of an intermediate radical cation but only of the 4-methylbenzyl and 4-methoxybenzyl radicals was provided.<sup>5</sup> This observation suggests that no radical cation intermediates are formed or that their lifetimes are too short to allow their detection under the experimental conditions employed. In the same study, it was

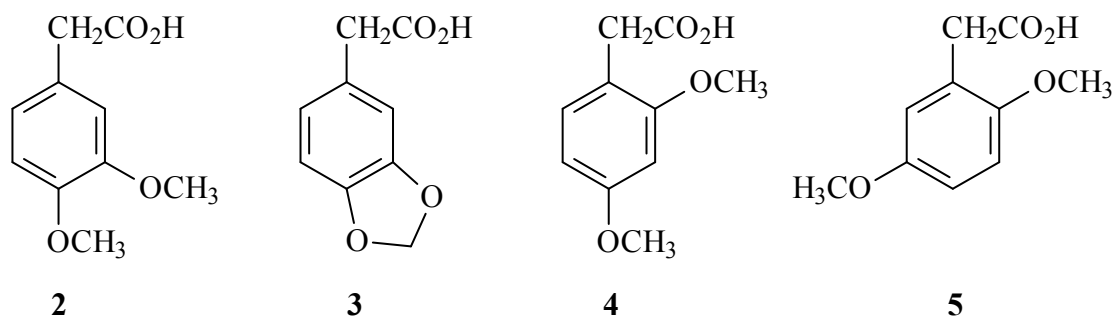
also shown that the decarboxylation rate constants, measured by following the formation of the corresponding benzyl radicals, increase by increasing pH, indicating that decarboxylation is faster when the carboxyl group is ionized.

Additional information comes from a recent indirect kinetic study of the effect of pH on the oxidation of **1** induced by potassium 12-tungstocobalt(III)ate (from now on simply indicated as Co(III)W).<sup>6</sup> This study led to the conclusion that no aromatic radical cation is formed as a reaction intermediate, suggesting that electron removal from the aromatic ring is instead concerted with an intramolecular side-chain to ring electron transfer, directly leading to a carboxyl radical which then undergoes rapid decarboxylation to give the 4-methoxybenzyl radical (Scheme 2.1.2).



Scheme 2.1.2

Along this line, in order to obtain a deeper understanding on the actual role of aromatic radical cations in these processes we have carried out a product and time-resolved kinetic study at different pH values on the one-electron oxidation of a series of ring dimethoxylated phenylalkanoic acids (**2**, **3**, **4**, **5**), characterized by oxidation potentials which are intermediate between that of **1**, and those of 1-naphthylethanoic acid, 4-dimethylaminophenylethanoic acid and its  $\alpha$ -methyl and  $\alpha$ -hydroxy derivatives described above.



In this respect, the one-electron oxidation potentials determined in aqueous solution for anisole, 1,2-, 1,3- and 1,4-dimethoxybenzene by means of redox pulse radiolysis (1.66, 1.44,

1.58 and 1.30 V/NHE, respectively)<sup>7</sup> can be taken as reasonable values for the oxidation potentials of **1**, **2** (and **3**), **4** and **5**, respectively.

## Results and Discussion

### Spectral properties and acid-base behavior

The transients produced after LFP or PR (see pag. 23 "Generation of Radical Cations") of acidic aqueous solutions ( $\text{pH} \leq 2$ ) containing **2-5** showed UV and visible absorption bands centered around 270-310 and 420-480 nm which are analogous to those observed for the corresponding ring dimethoxylated aromatic radical cations.<sup>8-10</sup> As an example, Figure 2.1.1 shows the time-resolved absorption spectrum observed after PR of an argon-saturated aqueous solution ( $\text{pH} = 1.7$ ) containing **5** (0.2 mM), 2-methyl-2-propanol (0.1 M) and  $\text{K}_2\text{S}_2\text{O}_8$  (10 mM). Visible are two bands, centered around 310 and 450 nm that are very similar to those observed previously for 1,4-dimethoxybenzene radical cation.<sup>8</sup> An identical spectrum was obtained after 248 nm LFP of an argon-saturated aqueous solution ( $\text{pH} = 2.0$ ) containing  $\text{K}_2\text{S}_2\text{O}_8$  (0.1 M) and **5** (0.4 mM).

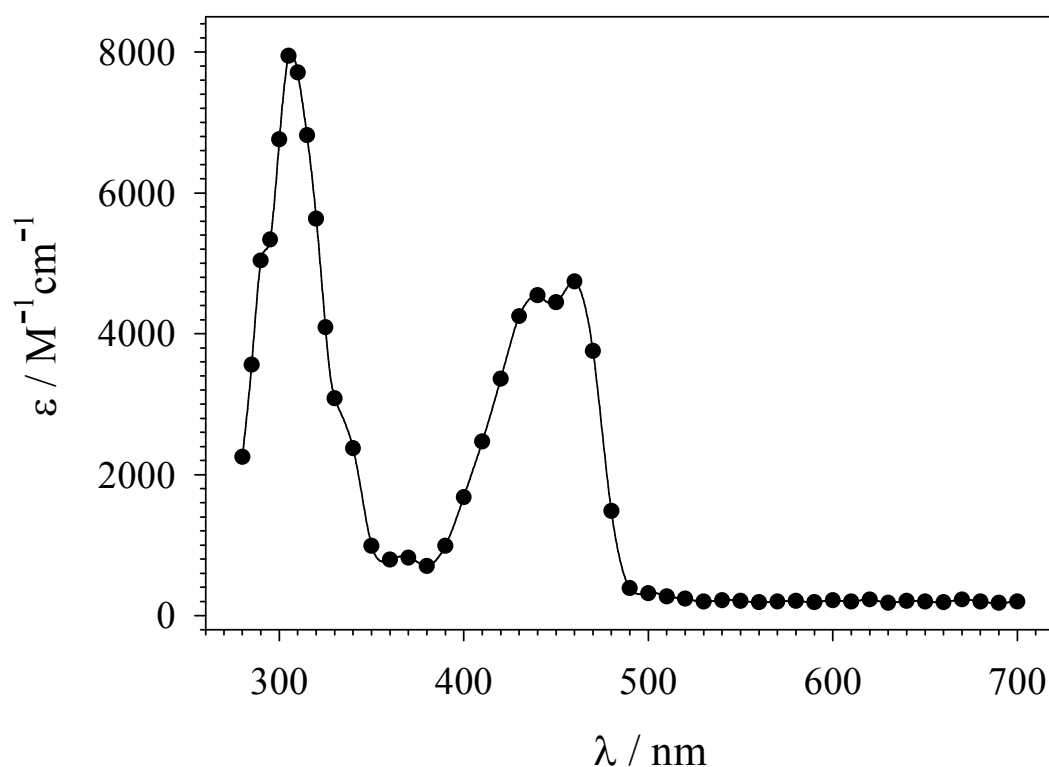


**Figure 2.1.1** Time-resolved absorption spectrum observed on reaction of  $\text{SO}_4^{\bullet-}$  with **5** (0.2 mM) recorded after pulse radiolysis of an argon-saturated aqueous solution ( $\text{pH} = 1.7$ ), containing 0.1 M 2-methyl-2-propanol and 10 mM  $\text{K}_2\text{S}_2\text{O}_8$ , at 8  $\mu\text{s}$  after the 300 ns, 10-MeV electron pulse. For the determination of the extinction coefficient,  $G(\text{radical cation}) = G(\text{SO}_4^{\bullet-}) = 3.1 \times 10^{-7} \text{ mol J}^{-1}$  was used.<sup>11,12</sup>

On the basis of these observations, the transients described above can be reasonably assigned to the dimethoxylated phenylethanoic acid radical cations  $2^{\bullet+}$ - $5^{\bullet+}$ , formed by  $\text{SO}_4^{\bullet-}$  or  $\text{Ti}^{2+}$  induced one-electron oxidation of the neutral substrates as described in eq 2.1.1.



Thus, these results clearly indicate that, differently than with 4-methoxyphenylethanoic acid (**1**), where no intermediate radical cation was detected,<sup>3</sup> the increased electron density on the aromatic ring determined by the presence of an additional methoxy group now allows the direct observation of the intermediate radical cations.

By increasing the pH of the solution to  $\approx 7$ , the spectra obtained after  $\text{SO}_4^{\bullet-}$  induced one-electron oxidation of **2-5** were similar to those obtained in acidic solution. However, a broadening of the radical cation visible absorption band accompanied in some cases by a slight red shift in its position (between 15 and 30 nm) was observed, a behavior that is attributed to the formation of the radical zwitterions  $^{-}2^{\bullet+}$ - $^{-}5^{\bullet+}$ .<sup>13</sup> As an example, Figure 2.1.2 shows the time-resolved absorption spectra observed after 248 nm LFP of argon-saturated aqueous solutions containing **4** (2 mM) and  $\text{K}_2\text{S}_2\text{O}_8$  (0.1 M) at pH = 2.2 (filled circles) and pH = 7.8 (empty circles).

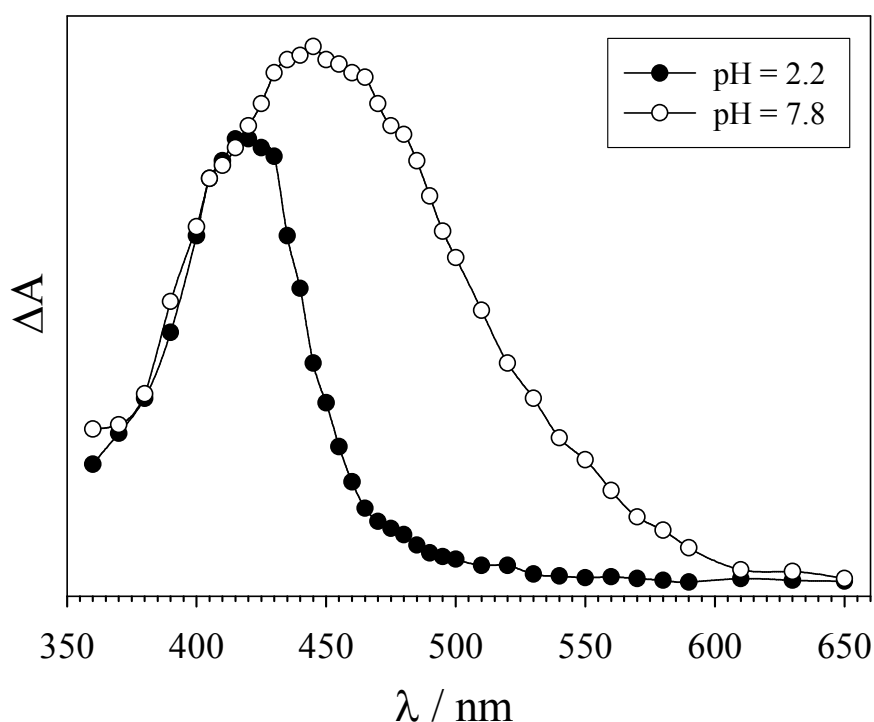


**Figure 2.1.2.** Time-resolved absorption spectra observed after 248 nm LFP of argon-saturated aqueous solutions containing 0.1 M  $\text{K}_2\text{S}_2\text{O}_8$  and 2 mM **2**, recorded at pH = 2.2 (filled circles), and pH = 7.8 (empty circles), 1  $\mu\text{s}$  after the 20 ns, 5 mJ laser flash. The broadening of the visible absorption band is accompanied by a 30 nm red shift of its position on going from  $2^{\bullet+}$  to  $2^{\bullet-}$ .

By measuring the absorption at a suitable wavelength (where the difference in absorption between radical cation and radical zwitterion is sufficiently large) as a function of pH, the  $\text{p}K_a$  values for the acid-base equilibria between the radical cations and the corresponding radical zwitterions (eq 2.1.2) were determined.

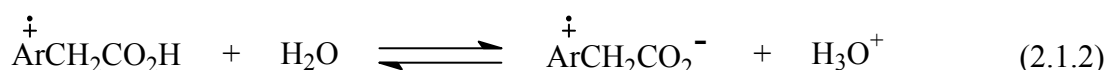
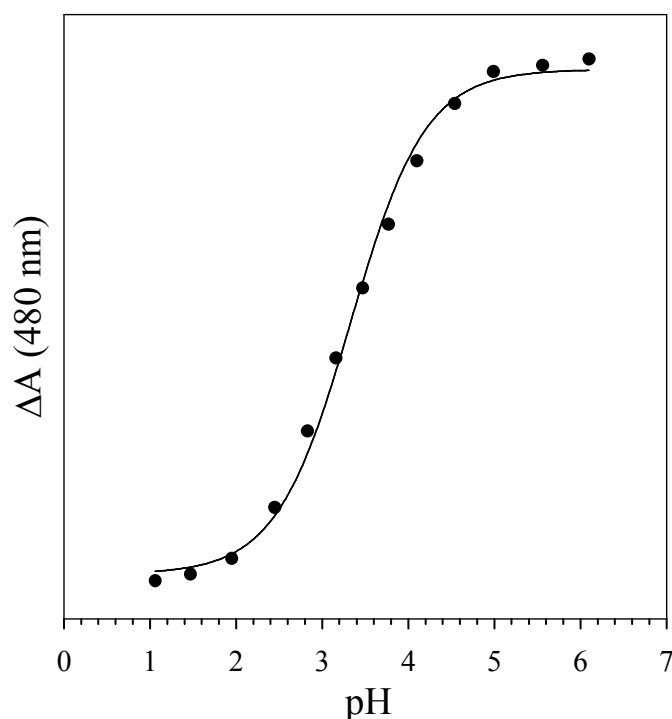


Figure 2.1.3 shows the plot of  $\Delta A$  (monitored at 480 nm) vs pH for the acid-base equilibrium between  $5^{\bullet+}$  and  $5^{\bullet-}$ .



**Figure 2.1.3.** Plot of  $\Delta A$  monitored at 480 nm vs pH for  $5^{\bullet+}/5^{\bullet-}$ , generated after 248 nm LFP of an argon-saturated aqueous solution containing 0.1 M  $\text{K}_2\text{S}_2\text{O}_8$  and 0.4 mM **5**. From the curve fit:  $\text{p}K_a = 3.33 \pm 0.04$  ( $r = 0.997$ ).

The  $\text{p}K_a$  values thus obtained for  $2^{\bullet+}$ - $5^{\bullet+}$  are collected in Table 1.1, together with the visible absorption band maxima for the radical cations and radical zwitterions.

With the exception of the equilibrium between  $4^{\bullet+}$  and  $4^{\bullet-}$  where the latter was too reactive (see later) to allow a reliable  $\text{p}K_a$  determination, similar  $\text{p}K_a$  values (between 3.34 and 3.67)

were obtained for  $2^{\bullet+}$ ,  $3^{\bullet+}$  and  $5^{\bullet+}$ . On the basis of a  $pK_a$  value of 4.33 measured for **2**,<sup>14</sup> it appears that in  $2^{\bullet+}$  the increased electron withdrawing effect determined by the presence of an electron hole on the aromatic ring leads to an increase in acidity of almost one  $pK_a$  unit. In this context, the slight difference observed between  $2^{\bullet+}$  (and  $3^{\bullet+}$ ) and  $5^{\bullet+}$  may reflect the fact that the 2-methoxy group (in  $5^{\bullet+}$ ) is closer to the acidic center than the 3-methoxy group (in  $2^{\bullet+}$ ).

**Table 2.1.1.** Visible absorption band maxima for radical cations and radical zwitterions generated from substrates **2-5**,<sup>a</sup> and corresponding  $pK_a$  values for their acid-base equilibria, measured at room temperature.

substrate	$\lambda_{\max}$ (r. c.) <sup>b</sup> (nm)	$\lambda_{\max}$ (r. z.) <sup>c</sup> (nm)	$\lambda_{\text{monit}}$ <sup>d</sup> (nm)	[substrate] (mM)	$pK_a$ <sup>e</sup>
<b>2</b>	420	450	460	2	3.49±0.05
<b>3</b>	430	450	470	2	3.67±0.07
<b>4</b>	455, 480	480 <sup>f</sup>	g	-	-
<b>5</b>	450	450	480	0.4	3.34±0.02

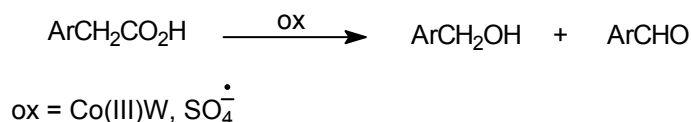
<sup>a</sup>Generated by 248 nm LFP as described above. <sup>b</sup>Visible absorption band maxima for radical cations  $2^{\bullet+}$ - $5^{\bullet+}$ . <sup>c</sup>Visible absorption band maxima for radical zwitterions  $2^{\bullet+}$ - $5^{\bullet+}$ . <sup>d</sup>Monitoring wavelength for  $pK_a$  determination. <sup>e</sup>Based on the average of two or three independent measurements. <sup>f</sup>Shoulder at 455 nm. <sup>g</sup>The radical zwitterion  $4^{\bullet+}$  is not sufficiently stable (see later) to allow a reliable  $pK_a$  determination.

It is also interesting to compare the values collected in Table 2.1.1 with those reported in the literature for monosubstituted ethanoic acids, showing that the increase in acidity determined by the positively charged ring is significantly smaller than that determined by  $\alpha$ -chloro ( $pK_a = 2.86$ ) and  $\alpha$ -cyano ( $pK_a = 2.46$ ) groups, being instead comparable with that resulting from the presence of an  $\alpha$ -methoxy group ( $pK_a = 3.54$ ).<sup>15</sup> An even more pronounced effect is observed when the comparison is made with a positively charged acid such as the protonated form of the  $\alpha$ -aminoacid glycine,  $H_3N^+CH_2CO_2H$ , for which  $pK_{a1} = 2.35$ .<sup>15</sup> The relatively large difference in acidity between glycine and  $2^{\bullet+}$  is likely to reflect the fact that in  $2^{\bullet+}$  the positive charge is delocalized over a relatively extended dimethoxyphenyl system and the resulting electron withdrawing effect is relatively weak, while in  $H_3N^+CH_2CO_2H$  the extent of charge delocalization is instead limited resulting in a much stronger electron withdrawing effect.



## Product studies

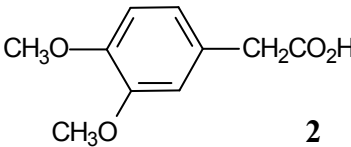
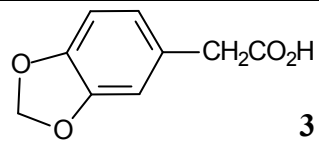
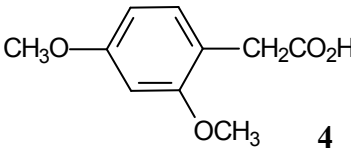
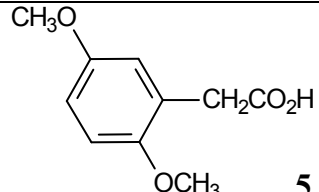
The oxidation reactions of substrates **2-5** were carried out in argon saturated aqueous solution (pH = 1.0 and 6.7) at room temperature, employing Co(III)W or  $\text{SO}_4^{\bullet-}$  (generated by steady state 254 nm photolysis as described in eq 1) as the oxidant. For all substrates product analysis, both at pH = 1.0 and 6.7, showed the formation of the corresponding benzyl alcohol as the major reaction product accompanied by small amounts of benzaldehyde (Scheme 2.1.3), and similar results were obtained with the two oxidants.



Scheme 2.1.3

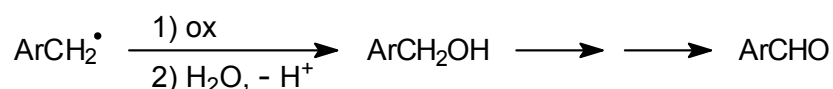
Experiments carried out increasing the Co(III)W/substrate molar ratio (from 0.5 to 2) confirmed that benzaldehyde is a product of over oxidation of the first formed benzyl alcohol. Good to excellent mass balances ( $\geq 85\%$ ) were obtained in all experiments. The results of the Co(III)W-induced oxidation reactions of substrates **2-5** are collected in Table 2.1.2.

**Table 2.1.2.** Product distributions observed in the Co(III)W-induced oxidation reactions of substrates **2-5**, carried out in argon saturated aqueous solution at  $T = 25\text{ }^\circ\text{C}$ .<sup>a</sup>

Substrate	pH <sup>b</sup>	Recovered Substrate (%)	Benzylalcohol (%)	Benzaldehyde (%)
 <b>2</b>	1.0	83	15	2
	1.0 <sup>c</sup>	18	67	15
	6.7	72	25	3
 <b>3</b>	1.0	78	20	2
	6.7	81	19	-
 <b>4</b>	1.0	87	13	-
	6.7	86	14	-
 <b>5</b>	1.0	77	20	3
	6.7	73	26	1

<sup>a</sup>[substrate] =  $5 \times 10^{-3}$  M, [Co(III)W] =  $2.5 \times 10^{-3}$  M. <sup>b</sup>For the experiments at pH = 1.0 a 0.1 M HClO<sub>4</sub> solution was employed. For the experiments at pH = 6.7 NaH<sub>2</sub>PO<sub>4</sub> (0.1 M) was added to the solution and the pH was adjusted with NaOH. <sup>c</sup>[substrate] =  $5 \times 10^{-3}$  M, [Co(III)W] =  $1.0 \times 10^{-2}$  M.

These results, together with those of the time-resolved experiments described above, are consistent with the mechanism shown in Scheme 1.1: formation of an intermediate radical cation or zwitterion followed by decarboxylation to give a benzyl radical. Oxidation of the benzyl radical in the reaction medium leads to the benzyl alcohol, which eventually can be further oxidized to give the corresponding benzaldehyde, as described in Scheme 2.1.4.<sup>6,16,17</sup>



Scheme 2.1.4

### Kinetic studies

Time-resolved kinetic studies were carried out using the PR and LFP techniques. The decay rates of the radical cations  $2^{\bullet+}$ - $5^{\bullet+}$  and zwitterions  $^{-}2^{\bullet+}$ - $^{-}5^{\bullet+}$  were measured spectrophotometrically, following the decrease in optical density at the visible absorption band maxima (420-480 nm), and were found to follow first order kinetics in a reaction which, on the basis of product analysis results, is assigned to decarboxylation. All the rate constants for decarboxylation of the radical cations and radical zwitterions ( $k_{\text{dec}}$ ) measured at different pH values are collected in Table 2.1.3.

**Table 2.1.3.** First order rate constants ( $k_{\text{dec}}$ ) for the decarboxylation of radical cations  $2^{\bullet+}$ - $5^{\bullet+}$  and radical zwitterions  $^{-}2^{\bullet+}$ - $^{-}5^{\bullet+}$  generated by pulse radiolysis of the parent substrates in aqueous solution, measured at room temperature.

substrate	pH <sup>a</sup>	transient	oxidant	$\lambda_{\text{det}}^{\text{b}}$ / nm	$k_{\text{dec}}$ / s <sup>-1</sup>
2	1.7	$2^{\bullet+}$	SO <sub>4</sub> <sup>•-</sup>	425	$5.2 \times 10^3$
	1.7	$2^{\bullet+}$	TI <sup>+2</sup>	425	$5.2 \times 10^3$
	7.1-10.2	$^{-}2^{\bullet+}$	SO <sub>4</sub> <sup>•-</sup>	450	$6.5 \times 10^4$
3	1.7	$3^{\bullet+}$	TI <sup>+2</sup>	425	$3.8 \times 10^3$
	7.0-10.2	$^{-}3^{\bullet+}$	SO <sub>4</sub> <sup>•-</sup>	450	$6.6 \times 10^4$
4	1.4	$4^{\bullet+}$	SO <sub>4</sub> <sup>•-</sup>	460	$5.6 \times 10^4$
	6.3	$^{-}4^{\bullet+}$	SO <sub>4</sub> <sup>•-</sup>	480	$2.0 \times 10^6$ <sup>c</sup>
5	1.7	$5^{\bullet+}$	TI <sup>+2</sup>	450	$< 10^2$ <sup>d</sup>
	7.4-10.8	$^{-}5^{\bullet+}$	SO <sub>4</sub> <sup>•-</sup>	450	$< 10^2$ <sup>d</sup>

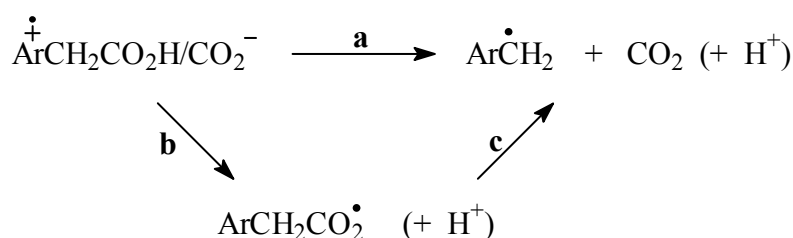
<sup>a</sup>For the experiments carried out at pH < 2 the pH was adjusted with HClO<sub>4</sub>. For the experiments carried out at pH > 6.3 Na<sub>2</sub>HPO<sub>4</sub> ( $2 \times 10^{-3}$  M) was added to the solution and

the pH was adjusted with HClO<sub>4</sub> or NaOH. <sup>b</sup>Monitoring wavelength. <sup>c</sup>4<sup>•+</sup> was generated by 266 nm LFP of an argon saturated aqueous solution (pH = 6.3) containing **5** (10 mM) and K<sub>2</sub>S<sub>2</sub>O<sub>8</sub> (0.1 M), as described above (page 23, eqs 1.2 and 1.3). <sup>d</sup>The time-resolution of the instrument did not allow the measurement of the decarboxylation rate constant and only an upper limit is provided ( $k_{\text{dec}} < 10^2 \text{ s}^{-1}$ ).

Interestingly, reactivity parallels radical cation stability,  $k_{\text{dec}}$  increasing in the order: **5**<sup>•+</sup>  $\ll$  **2**<sup>•+</sup>  $\cong$  **3**<sup>•+</sup>  $<$  **4**<sup>•+</sup>.<sup>7</sup> This reactivity order can be rationalized in terms of the ease of the intramolecular side-chain to ring electron transfer required for decarboxylation, which is influenced by the extent of stabilization of the positive charge on the aromatic ring and hence by the number and relative position of methoxy groups. Thus, **5**<sup>•+</sup> displays the lower reactivity in line with the greater stabilization of the positive charge in the 2,5-dimethoxyphenyl system as compared to the 2,4- and 3,4-dimethoxyphenyl ones.<sup>7,9</sup> In other words the intramolecular side-chain to ring electron transfer is significantly more costly in **5**<sup>•+</sup> as compared to **2**<sup>•+</sup>, **3**<sup>•+</sup> and **4**<sup>•+</sup>, and accordingly its reactivity is strongly depressed.

For **2**, **3** and **4** a significant increase in  $k_{\text{dec}}$  was observed on going from the radical cation (pH  $\leq$  1.7) to the corresponding radical zwitterion (pH  $>$  6), and no significant difference in reactivity was observed between pH 6 and 10. The lower decarboxylation rate constants measured for Ar<sup>•+</sup>CH<sub>2</sub>CO<sub>2</sub>H as compared to Ar<sup>•+</sup>CH<sub>2</sub>CO<sub>2</sub><sup>-</sup> can be again rationalized in terms of the kinetic barrier for intramolecular side-chain to ring electron transfer which should be higher for the former, since in this case an additional proton transfer to the medium is required.<sup>6</sup>

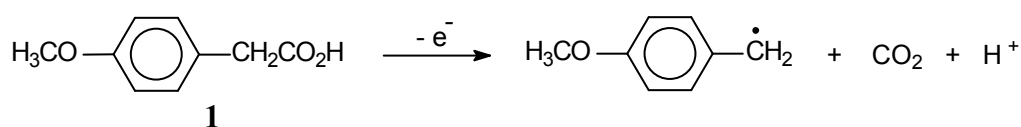
Unfortunately, these data do not provide any information on whether decarboxylation occurs directly from the radical cation or zwitterion (Scheme 1.5, path **a**) or if an intermediate arylacetoxyl radical is involved (paths **b** and **c**), as previously shown in the case of benzoic acids.<sup>18</sup>



Scheme 1.5

Accordingly, rate constants  $k \geq 1.5 \times 10^9 \text{ s}^{-1}$  have been measured for the decarboxylation of a series of phenylacetoxyl radicals,<sup>19,20</sup> showing moreover that no significant effect on

reactivity results from the presence of ring substituents.<sup>20</sup> These values are at least three orders of magnitude higher than those reported in Table 1.3 for decarboxylation of the radical cations and radical zwitterions. Thus, the extremely fast rate constants measured independently for reaction **c** do not allow us to distinguish between the concerted (path **a**) or stepwise (through paths **b** and **c**) nature of the conversion of the radical cation (zwitterion) into the benzyl radical. In light of this observation, in the mechanism shown in Scheme 1.2 for the Co(III)W induced oxidation of 4-methoxyphenylethanoic acid (**1**),<sup>6</sup> the possibility that decarboxylation is coupled with electron removal from the aromatic ring, bypassing 4-methoxyphenylacetoxy radical formation, should also be considered (Scheme 1.6).



Scheme 1.6

In conclusion this work clearly shows that aromatic radical cations and radical zwitterions are intermediates in the one-electron oxidation of ring-dimethoxylated phenylethanoic acids, providing moreover for the first time pK<sub>a</sub> values for their acid-base equilibria. The radical cations undergo decarboxylation with rate constants that depend on the stabilization of the positive charge on the aromatic ring, i.e. on the height of the kinetic barrier for side-chain to ring intramolecular electron transfer, and a significant increase in reactivity is observed on going from the radical cations to the corresponding radical zwitterions. More importantly, these results provide a detailed mechanistic picture for the one-electron oxidation of aryloethanoic acids in aqueous solution, a process that is governed by the interplay between electron removal from the aromatic ring and intramolecular side-chain to ring electron transfer required for decarboxylation. Along this line, it can be proposed that with **1** (and with less electron rich aryloethanoic acids such as 4-methylphenylethanoic acid), electron removal is relatively costly and is thus coupled with the intramolecular electron transfer, i.e. no radical cation intermediate is formed. By increasing ring electron density (as in substrates **2-5**), electron removal becomes easier while the rate of intramolecular electron transfer is depressed and a stepwise mechanism, proceeding through the formation of a radical cation (or radical zwitterion) followed by decarboxylation occurs. It is however important to point out that also the redox properties of oxidant employed (compare for example Co(III)W and SO<sub>4</sub><sup>•-</sup>, see above, page 23) may play an important role in this mechanistic picture.

## References

- (1) (a) Maki, Y.; Sako, M.; Oyabu, I.; Murase, T.; Kitade, Y.; Hirota, K. *J. Chem. Soc.; Chem. Commun.* **1989**, 1780-1782. (b) Gilbert, B. C.; Scarratt, C. J.; Thomas, C. B.; Young, J. *J. Chem. Soc., Perkin Trans. 2* **1987**, 371-380. (c) Walling, C.; El-Taliawi, G. M.; Amarnath, K. *J. Am. Chem. Soc.* **1984**, *106*, 7573-7578. (d) Walling, C.; Camaioni, D. M. *J. Org. Chem.* **1978**, *43*, 3266-3271. (e) Dessau, R. M.; Heiba, E. I. *J. Org. Chem.* **1975**, *40*, 3647-3649.
- (2) (a) Jönsson, L. *Acta Chem. Scand.* **1983**, *B37*, 761-768. (b) Jönsson, L. *Acta Chem. Scand.* **1981**, *B35*, 683-689. (c) Trahanovsky, W. S.; Cramer, J.; Brix ius, D. W. *J. Am. Chem. Soc.* **1974**, *96*, 1077-1081.
- (3) Steenken, S.; Warren, C. J.; Gilbert, B. C. *J. Chem. Soc., Perkin Trans. 2* **1990**, 335-342.
- (4) Gould, I. R.; Lenhard, J. R.; Muentner, A. A.; Godleski, S. A.; Farid, S. *J. Am. Chem. Soc.* **2000**, *122*, 11934-11943.
- (5) It is however important to point out that in acetonitrile solution direct evidence for the formation of 4-methoxyphenylethanoic acid radical cation ( $\mathbf{1}^{\bullet+}$ ) has been obtained by LFP. See: Freccero, M.; Pratt, A.; Albini, A.; Long, C. *J. Am. Chem. Soc.* **1998**, *120*, 284-297.
- (6) Baciocchi, E.; Bietti, M. *J. Chem. Soc., Perkin Trans. 2* **2002**, 720-722.
- (7) Jonsson, M.; Lind, J.; Reitberger, T.; Eriksen, T. E.; Merényi, G. *J. Phys. Chem.* **1993**, *97*, 11278-11282.
- (8) O'Neill, P.; Steenken, S.; Schulte-Frohlinde, D. *J. Phys. Chem.* **1975**, *79*, 2773-2779.
- (9) Baciocchi, E.; Bietti, M.; Gerini, M. F.; Manduchi, L.; Salamone, M.; Steenken, S. *Chem. Eur. J.* **2001**, *7*, 1408-1416.
- (10) No direct spectroscopic evidence for the formation of the ring-dimethoxylated benzyl radicals was obtained. It is however possible that under oxidative conditions, due to their very low oxidation potential, these radicals are rapidly oxidized to the corresponding cations. See for example: Wayner, D. D. M.; Sim, B. A.; Dannenberg, J. *J. J. Org. Chem.* **1991**, *56*, 4853-4858.
- (11) Faria, J. L.; Steenken, S. *J. Phys. Chem.* **1992**, *96*, 10869-10874.
- (12) Where  $G$  is the radiation chemical yield defined as the number of radicals produced by 100 eV of absorbed radiation ( $1 \text{ molecule}/100 \text{ eV} = 1.036 \times 10^{-7} \text{ mol J}^{-1}$ ). For further details see: Spinks, J. W. T.; Woods, R. J. *An Introduction to Radiation Chemistry 3<sup>rd</sup> Ed.*; Wiley: New York, 1990.

- (13) This notation represents an oversimplification because, as compared to the radical cations, the corresponding radical zwitterions lack the presence of the carboxylic proton.
- (14) Kortüm, G.; Vogel, W.; Andrussov, K. *Dissociation Constants of Organic Acids in Aqueous Solution*; Butterworths: London, 1961.
- (15) Streitwieser, A.; Heathcock, C. H.; Kosower, E. M. *Introduction to Organic Chemistry 4<sup>th</sup> Ed.*; Prentice Hall: Upper Saddle River, 1998.
- (16) Baciocchi, E.; Bietti, M.; Putignani, L.; Steenken, S. *J. Am. Chem. Soc.* **1996**, *118*, 5952-5960.
- (17) Baciocchi, E.; Bietti, M.; Mattioli, M. *J. Org. Chem.* **1993**, *58*, 7106-7110. Ebersson, L. *J. Am. Chem. Soc.* **1983**, *105*, 3192-3199.
- (18) Ashworth, B.; Gilbert, B. C.; Holmes, R. G. G.; Norman, R. O. C. *J. Chem. Soc., Perkin Trans. 2* **1978**, 951-956. Steenken, S.; O'Neill, P.; Schulte-Frohlinde, D. *J. Phys. Chem.* **1977**, *81*, 26-30.
- (19) Hilborn, J. W.; Pincock, J. A. *J. Am. Chem. Soc.* **1991**, *113*, 2683-2686.
- (20) Bockman, T. M.; Hubig, S. M.; Kochi, J. K. *J. Org. Chem.* **1997**, *62*, 2210-2221.

## 2.2 One-Electron Oxidation of 2-Aryl-2-Methyl Propanoic and 1-Arylcyclopropanecarboxylic Acids in Aqueous Solution. The Involvement of Aromatic Radical Cations and the Effect of an $\alpha$ -Cyclopropyl Group.

Following the study of the one-electron oxidation reactions of ring-dimethoxylated phenylethanoic acids **2-5** discussed in Chapter 2.1, in order to obtain a deeper understanding of the role of structural effects on the one-electron oxidation of aryloethanoic acids and in particular on the possible involvement of aromatic radical cations in these processes, we have carried out a product and time-resolved kinetic study at different pH values on the one-electron oxidation of 2-(4-methoxyphenyl)-2-methyl propanoic acid (**6**), 1-(4-methoxyphenyl)-1-cyclopropanecarboxylic acid (**7**), 2-(3,4-dimethoxyphenyl)-2-methyl propanoic acid (**8**), and 1-(3,4-dimethoxyphenyl)-1-cyclopropanecarboxylic acid (**9**); structurally related substrates derived from the side-chain modification of 4-methoxyphenylethanoic acid (**1**) and 3,4-dimethoxyphenylethanoic acid (**2**), respectively, whose structures are shown in Chart 2.2.1. In order to obtain additional information, we have also studied the one-electron oxidation of the methyl esters of acids **6**, **7** and **9** (substrates **10**, **11** and **12**, respectively), and of 1-(4-methoxyphenyl)cyclopropanol (**7a**).

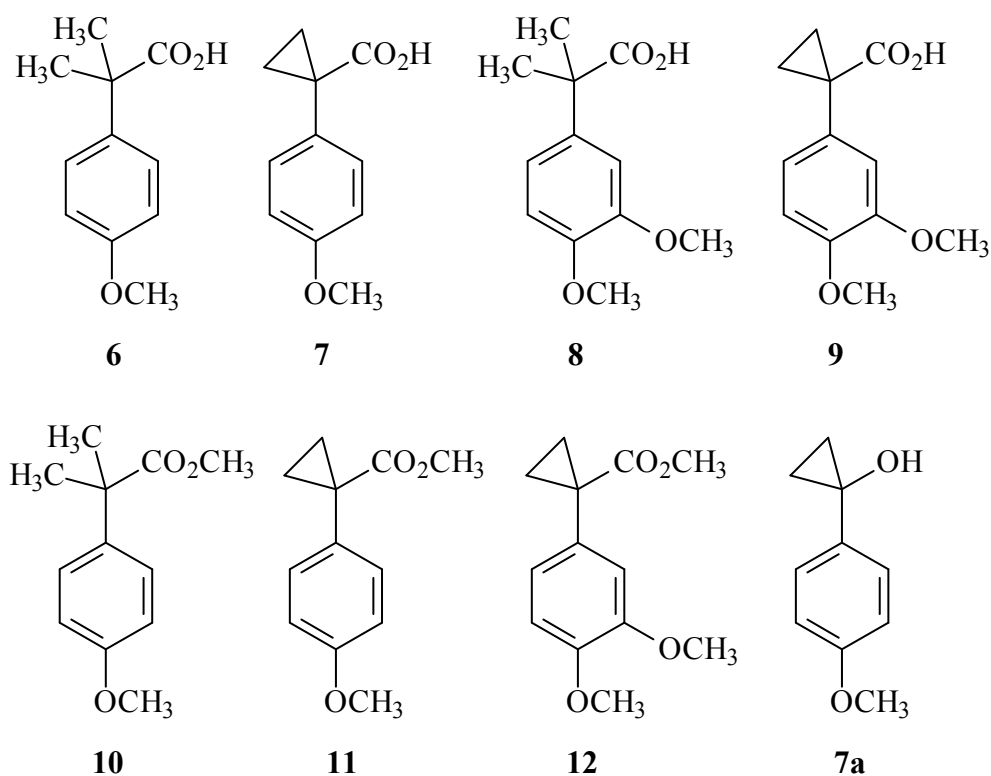
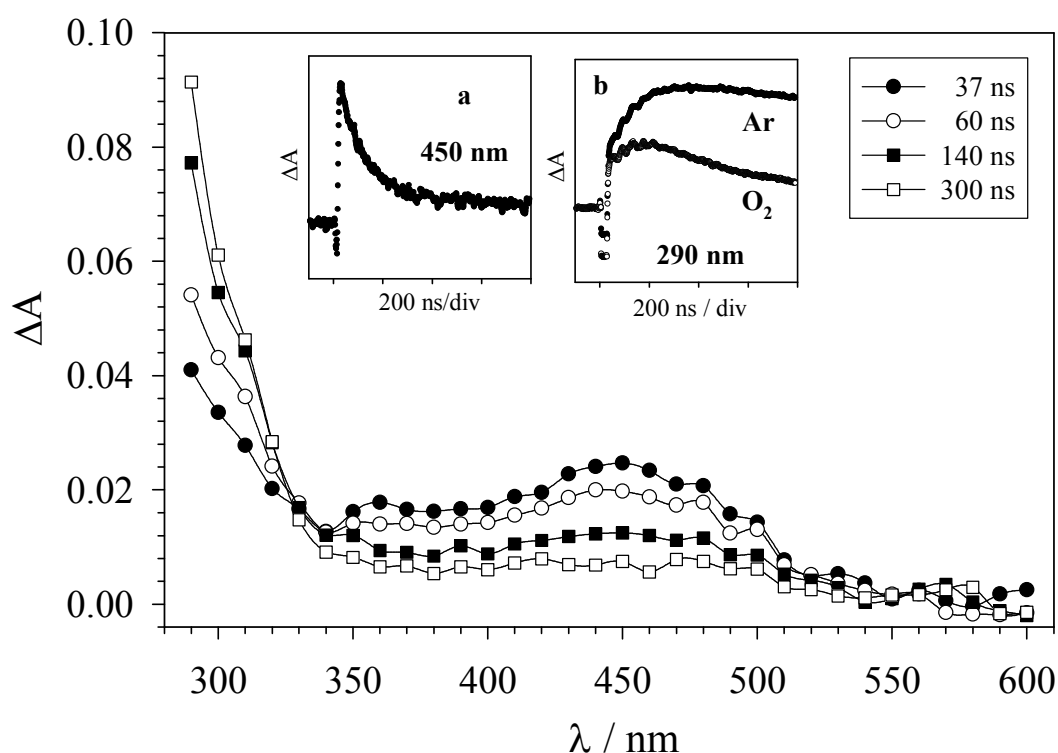


Chart 2.2.1

## Results

**Spectral properties.** Argon or nitrogen saturated aqueous solutions of substrates **6-12** (0.2-5 mM) were photolysed in the presence of 0.1 M  $K_2S_2O_8$  at  $pH \approx 2$  and  $pH \approx 7$ , employing 266 nm laser flash photolysis (LFP). Alternatively, time-resolved studies were carried out by pulse radiolysis (PR) of argon saturated aqueous solutions containing substrates **6-12** (0.2-2 mM),  $K_2S_2O_8$  (10 mM) and 2-methyl-2-propanol (0.1 M).

Figure 2.2.1 displays the time-resolved absorption spectra observed after LFP of an argon-saturated aqueous solution ( $pH = 1.7$ ) containing 2-(4-methoxyphenyl)-2-methyl propanoic acid (**6**) (2.0 mM) and  $K_2S_2O_8$  (0.1 M).



**Figure 2.2.1.** Time-resolved absorption spectra observed after 266 nm LFP of an argon-saturated aqueous solution ( $T = 25\text{ }^\circ\text{C}$ ,  $pH = 1.7$ ) containing 0.1 M  $K_2S_2O_8$  and 2 mM 2-(4-methoxyphenyl)-2-methyl propanoic acid (**6**), recorded at 37 (filled circles), 60 (empty circles), 140 (filled squares) and 300 ns (empty squares) after the 8 ns, 10 mJ laser flash. Insets: (a) First-order decay monitored at 450 nm. (b) Corresponding first-order buildup of absorption at 290 nm, measured under argon (filled circles) and oxygen (empty circles).

The spectrum recorded 37 ns after the laser flash (filled circles) shows the formation of a broad absorption band between 350 and 520 nm, characterized by a maximum at 450 nm, that, by comparison with literature data,<sup>1,2</sup> and with the time-resolved absorption spectrum of  $SO_4^{\bullet-}$ , obtained after 266 nm LFP of a nitrogen-saturated aqueous solution ( $pH = 1.7$ ) containing 0.1 M  $K_2S_2O_8$  (Figure 2.2.2), can be assigned to  $SO_4^{\bullet-}$ , formed as described in eq



1.3. The decay of this broad absorption band (inset **a**) occurs with  $k_{\downarrow}(450 \text{ nm}) = 1.0 \times 10^7 \text{ s}^{-1}$  and is accompanied by the formation of a species ( $k_{\uparrow}(290 \text{ nm}) = 1.1 \times 10^7 \text{ s}^{-1}$ ) characterized by an absorption in the UV region of the spectrum extending from  $< 290 \text{ nm}$  to  $340 \text{ nm}$  (an isosbestic point is visible at  $330 \text{ nm}$ ). The decay of this band is accelerated by the presence of oxygen (inset **b**), and in an oxygen saturated solution occurs with an observed rate constant  $k_{\text{obs}} = 2.2 \times 10^6 \text{ s}^{-1}$ . Given that the solubility of oxygen in water is  $1.27 \times 10^{-3} \text{ M}$  at  $T = 25 \text{ }^\circ\text{C}$ ,<sup>3</sup> a second order rate constant for reaction of this transient with oxygen can be derived as  $k = 1.7 \times 10^9 \text{ M}^{-1} \text{ s}^{-1}$ .

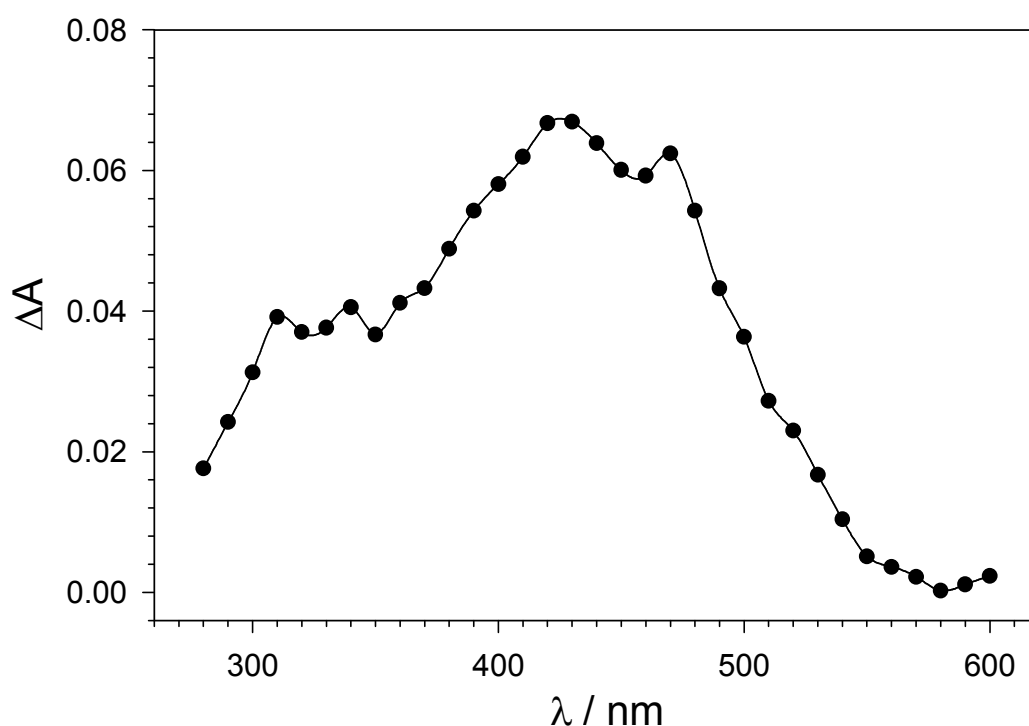
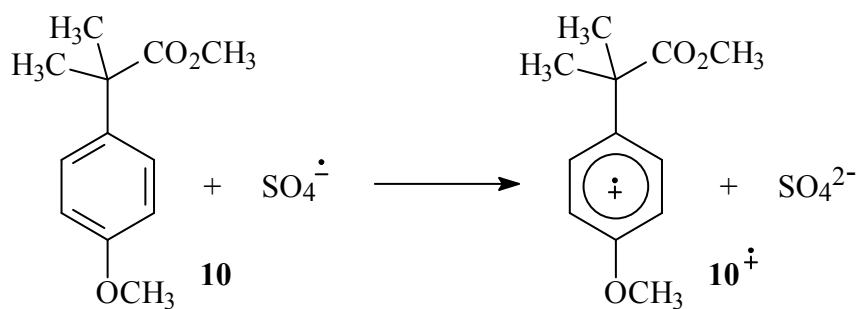


**Figure 2.2.2.** Time-resolved absorption spectrum observed after 266 nm LFP of a nitrogen-saturated aqueous solution ( $T = 25 \text{ }^\circ\text{C}$ ,  $\text{pH} = 1.7$ ) containing  $0.1 \text{ M K}_2\text{S}_2\text{O}_8$  recorded 90 ns after the 8 ns, 10 mJ laser flash.

Figure 2.2.3 displays the time-resolved absorption spectrum observed after 266 nm LFP of a nitrogen-saturated aqueous solution ( $\text{pH} = 7.0$ ) containing  $0.1 \text{ M K}_2\text{S}_2\text{O}_8$  and  $0.2 \text{ mM}$  methyl 2-(4-methoxyphenyl)-2-methyl propanoate (**10**). Visible are two bands, centered at 290 and 450 nm that are very similar to those observed previously for the radical cations of 4-methoxyalkylbenzenes and 1-(4-methoxyphenyl)alkanols.<sup>4-7</sup> An identical spectrum was obtained after PR of an argon-saturated aqueous solution ( $\text{pH} = 7.0$ ) containing  $10 \text{ mM K}_2\text{S}_2\text{O}_8$ ,  $0.2 \text{ mM}$  **10** and  $0.1 \text{ M}$  2-methyl-2-propanol. On the basis of these observations, this species can be reasonably assigned to the aromatic radical cation **10**<sup>•+</sup>, formed by  $\text{SO}_4^{\bullet-}$  induced one-electron oxidation of the neutral substrate **10** as described in Scheme 2.2.1.



Scheme 2.2.1

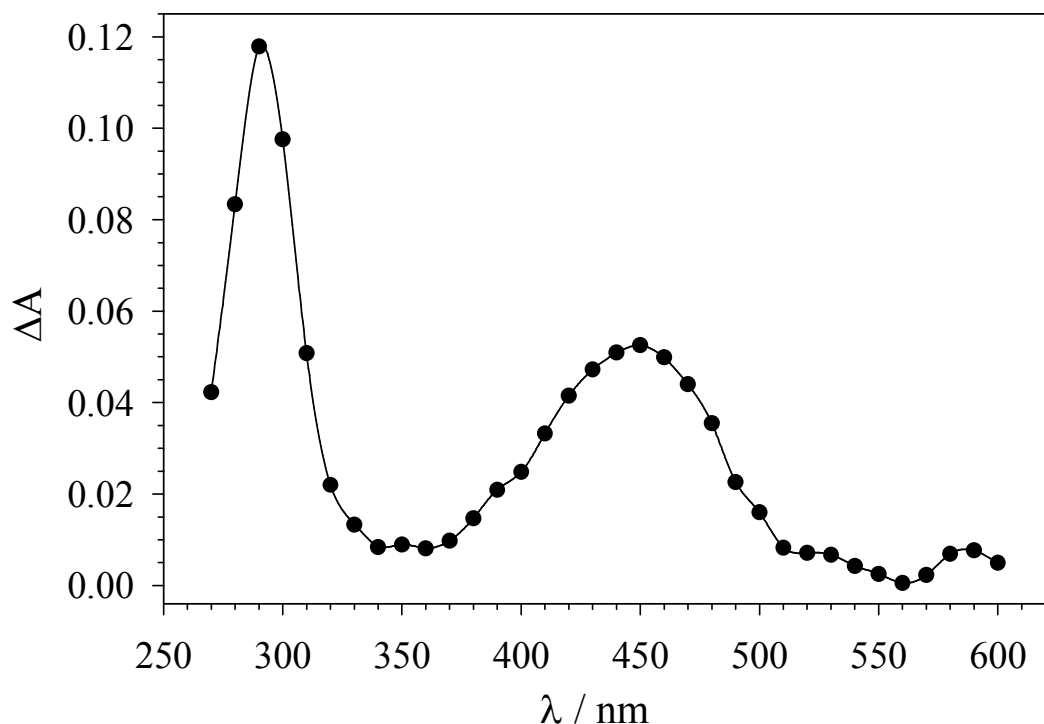


**Figure 2.2.3.** Time-resolved absorption spectrum observed after 266 nm LFP of a nitrogen-saturated aqueous solution ( $T = 25\text{ }^{\circ}\text{C}$ ,  $\text{pH} = 7.0$ ) containing  $0.1\text{ M K}_2\text{S}_2\text{O}_8$  and  $0.2\text{ mM}$  methyl 2-(4-methoxyphenyl)-2-methyl propanoate (**10**), recorded  $2.1\text{ }\mu\text{s}$  after the  $8\text{ ns}$ ,  $10\text{ mJ}$  laser flash.

The time-resolved absorption spectra observed after LFP of an argon saturated aqueous solution ( $\text{pH} = 1.7$ ) containing 1-(4-methoxyphenyl)cyclopropanecarboxylic acid (**7**) ( $1\text{ mM}$ ) and  $\text{K}_2\text{S}_2\text{O}_8$  ( $0.1\text{ M}$ ) are displayed in Figure 2.2.4. The spectrum recorded  $64\text{ ns}$  after the laser flash (filled circles) shows the formation of a broad absorption band between  $350$  and  $550\text{ nm}$ , that, as discussed above, is assigned to  $\text{SO}_4^{\bullet-}$  (see Figure 2.2.2). The decay of this band is accompanied by the formation of two bands centered at  $320$  and  $490\text{ nm}$  (two isosbestic points are visible at  $350$  and  $440\text{ nm}$ ) whose decay is not affected by the presence of oxygen. An analogous spectrum, characterized by two absorption bands centered at  $320$  and  $500\text{ nm}$ , was observed after PR of an argon-saturated aqueous solution containing **7** ( $0.5\text{ mM}$ ),  $\text{K}_2\text{S}_2\text{O}_8$  ( $10\text{ mM}$ ) and 2-methyl-2-propanol ( $0.1\text{ M}$ ) at  $\text{pH} = 1.7$  (Figure 2.2.5, filled circles).

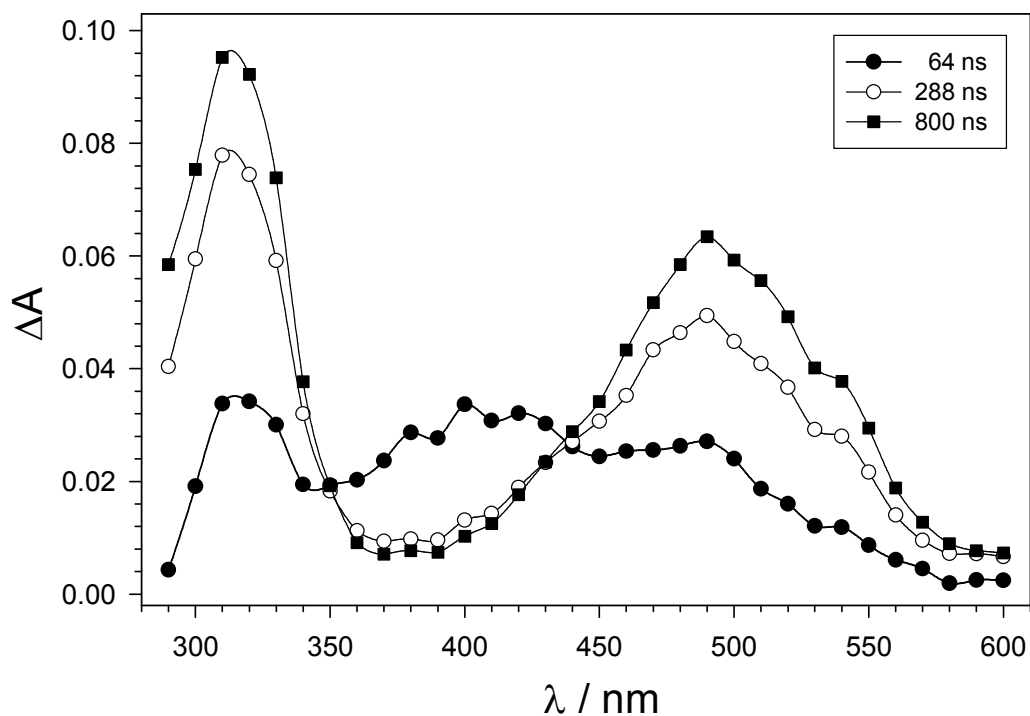


**Figure 2.2.4.** Time-resolved absorption spectra observed after 266 nm LFP of an argon-saturated aqueous solution ( $T = 25\text{ }^{\circ}\text{C}$ ,  $\text{pH} = 1.7$ ) containing  $0.1\text{ M K}_2\text{S}_2\text{O}_8$  and  $1\text{ mM}$  1-(4-methoxyphenyl)-1-cyclopropanecarboxylic acid (**7**), recorded at 64 (filled circles), 288 (empty circles) and 800 ns (filled squares) after the 8 ns, 10 mJ laser flash.

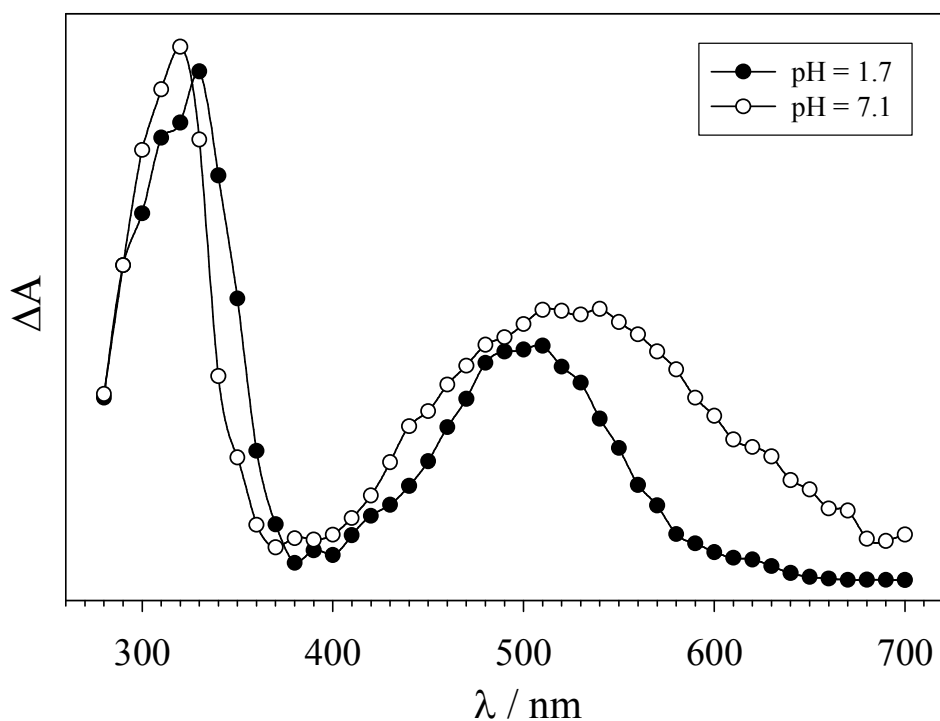


**Figure 2.2.5.** Time-resolved absorption spectra observed on reaction of  $\text{SO}_4^{\bullet-}$  with 1-(4-methoxyphenyl)-1-cyclopropanecarboxylic acid (**7**) ( $0.5\text{ mM}$ ) recorded after PR of argon-saturated aqueous solutions at  $\text{pH} = 1.7$  (filled circles), and  $\text{pH} = 7.1$  (empty circles), containing  $0.1\text{ M}$  2-methyl-2-propanol and  $10\text{ mM K}_2\text{S}_2\text{O}_8$ ,  $2\text{ }\mu\text{s}$  after the 300 ns, 10-MeV electron pulse.

An analogous spectrum, characterized by UV and visible absorption bands centered at 300 and 500 nm, was also observed after PR of an argon-saturated aqueous solution (pH = 4.0) containing methyl 1-(4-methoxyphenyl)-1-cyclopropanecarboxylate (**11**) (0.2 mM), K<sub>2</sub>S<sub>2</sub>O<sub>8</sub> (10 mM) and 2-methyl-2-propanol (0.1 M) (Figure 2.2.6).

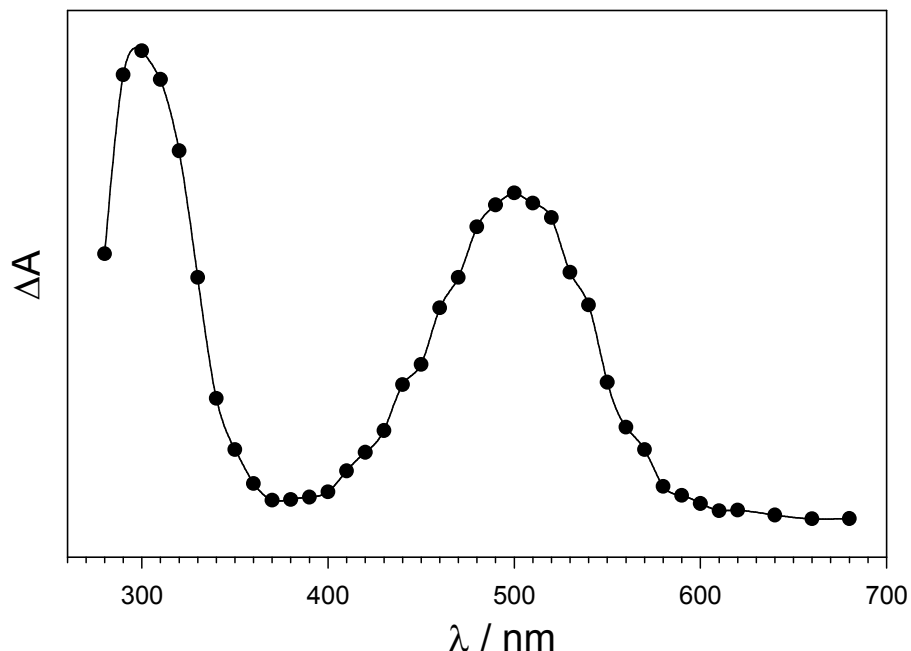
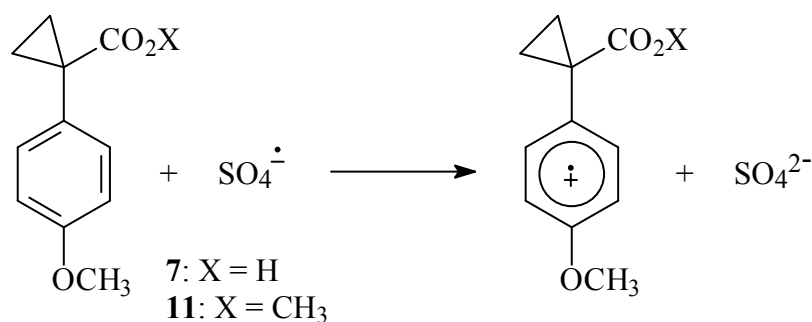


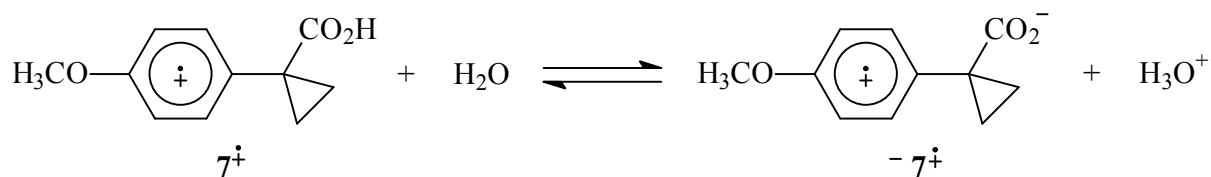
**Figure 2.2.6.** Time-resolved absorption spectrum observed on reaction of SO<sub>4</sub><sup>•-</sup> with methyl 1-(4-methoxyphenyl)-1-cyclopropanecarboxylate (**11**) (0.2 mM) recorded after PR of an argon-saturated aqueous solution (pH = 4.0), containing 0.1 M 2-methyl-2-propanol and 10 mM K<sub>2</sub>S<sub>2</sub>O<sub>8</sub>, 4 μs after the 300 ns, 10-MeV electron pulse.

It is well known that the radical cations of arylcyclopropanes are characterized by an absorption band in the visible region of the spectrum centered between 510 and 580 nm depending on the nature of the aromatic ring substituent.<sup>8,9</sup> Along this line, the UV and visible absorption bands described above for the transients observed in the oxidation reactions of substrates **7** and **11**, can be reasonably assigned to the radical cations **7**<sup>•+</sup> and **11**<sup>•+</sup>, formed by one-electron oxidation of the neutral substrates as described in Scheme 2.2.2.



Scheme 2.2.2

By increasing the pH of the solution to  $\approx 7$ , the spectrum obtained after  $\text{SO}_4^{\bullet-}$  induced one-electron oxidation of **7** was similar to that obtained in acidic solution. However, as described previously for ring-methoxylated phenylethanoic acid radical cations (see Chapter 2.1), a broadening of the radical cation visible absorption band, accompanied by a 25 nm red-shift in its position was observed (Figure 2.2.5, empty circles). This behavior is attributed to the formation of the radical zwitterion  ${}^{-}\mathbf{7}^{\bullet+}$  as described in Scheme 2.2.3.<sup>10</sup> Quite importantly, no significant spectral variation was instead observed for  $\mathbf{11}^{\bullet+}$  between pH 4 and 10.



Scheme 2.2.3

Figure 2.2.7 displays the time-resolved absorption spectra observed after LFP of a nitrogen-saturated aqueous solution (pH = 1.7) containing 2-(3,4-dimethoxyphenyl)-2-methyl propanoic acid (**8**) (2.0 mM) and  $\text{K}_2\text{S}_2\text{O}_8$  (0.1 M).

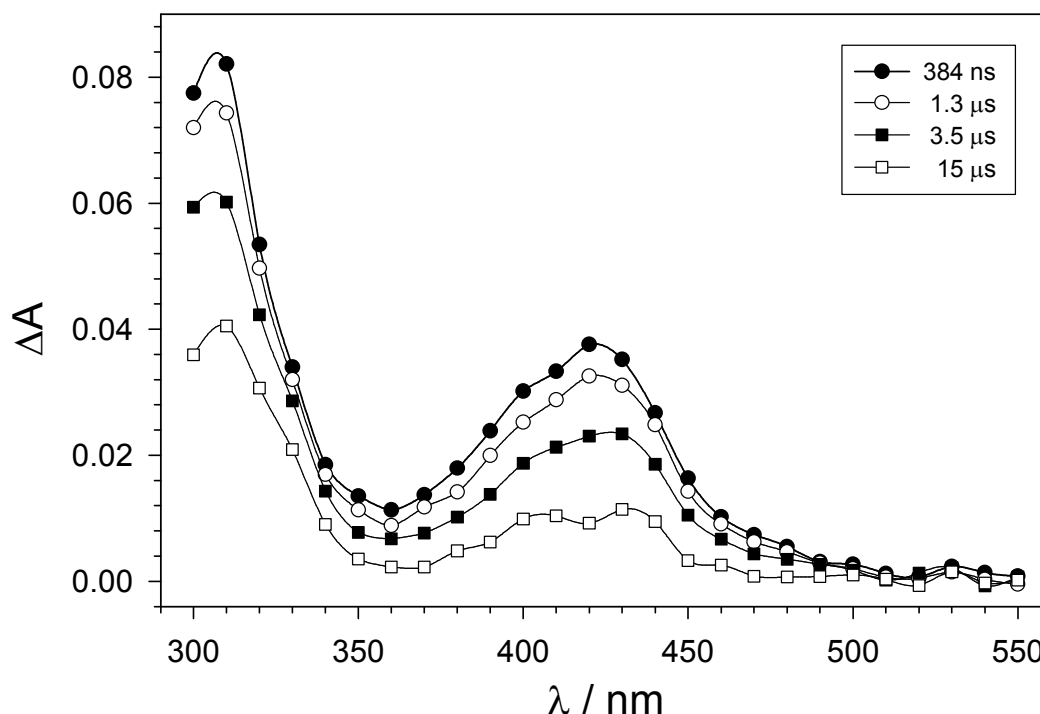


**Figure 2.2.7.** Time-resolved absorption spectra observed after 266 nm LFP of a nitrogen-saturated aqueous solution ( $T = 25\text{ }^\circ\text{C}$ , pH = 1.7) containing 0.1 M  $\text{K}_2\text{S}_2\text{O}_8$  and 2 mM 2-(3,4-dimethoxyphenyl)-2-methyl propanoic acid (**8**), recorded at 384 ns (filled circles), 1.3  $\mu\text{s}$  (empty circles), 3.5  $\mu\text{s}$  (filled squares) and 15  $\mu\text{s}$  (empty squares) after the 8 ns, 10 mJ laser flash.

The spectrum recorded 384 ns after the laser flash (filled circles) shows the formation of two absorption bands, centered at 310 and 420 nm that are very similar to those observed previously for the radical cations of 1,2-dimethoxybenzene,<sup>11</sup> 1-(3,4-dimethoxyphenyl)alkanols,<sup>12</sup> and 3,4-dimethoxyphenylethanoic acid (see Chapter 2.1). On the basis of this observation, the transient described above can be reasonably assigned to the radical cation  $\mathbf{8}^{\bullet+}$ , formed by  $\text{SO}_4^{\bullet-}$  induced one-electron oxidation of  $\mathbf{8}$ . Moreover, these two absorption bands were observed to decay following first-order kinetics and identical rate constants were measured for the decay of the two bands ( $k_{\downarrow} = 2.1 \times 10^5 \text{ s}^{-1}$ ), and their decay was not affected by the presence of oxygen, in line with their assignment to an aromatic radical cation.

Figure 2.2.8 displays the time-resolved absorption spectra observed after LFP of a nitrogen-saturated aqueous solution (pH = 6.8) containing 2-(3,4-dimethoxyphenyl)-2-methyl propanoic acid ( $\mathbf{8}$ ) (5.0 mM) and  $\text{K}_2\text{S}_2\text{O}_8$  (0.1 M). The spectrum recorded 28 ns after the laser flash (filled circles) shows again the formation of two bands, centered at 310 and 420 nm. However, as described previously for  $\mathbf{7}^{\bullet+}$  and for ring-methoxylated phenylethanoic acid radical cations (see Chapter 2.1), a broadening of the radical cation visible absorption band was observed on going from pH = 1.7 to pH = 6.8.

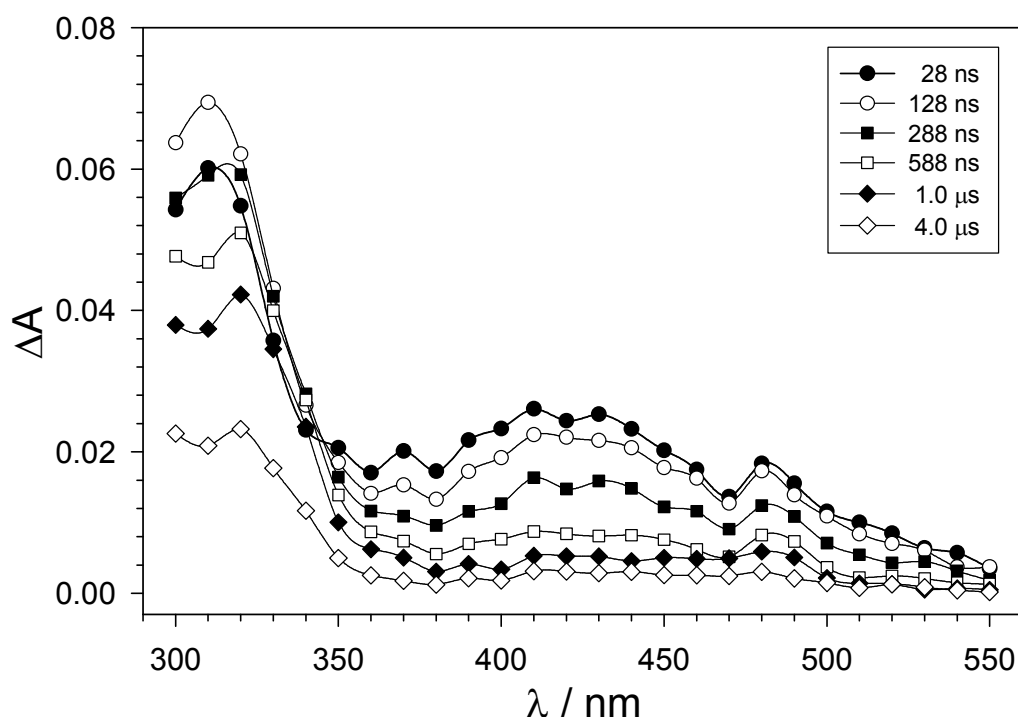


**Figure 2.2.8.** Time-resolved absorption spectra observed after 266 nm LFP of a nitrogen-saturated aqueous solution ( $T = 25 \text{ }^\circ\text{C}$ , pH = 6.8) containing 0.1 M  $\text{K}_2\text{S}_2\text{O}_8$  and 5 mM 2-(3,4-dimethoxyphenyl)-2-methyl propanoic acid ( $\mathbf{8}$ ), recorded at 28 ns (filled circles), 128 ns (empty circles), 288 ns (filled squares), 588 ns (empty squares), 1.0  $\mu\text{s}$  (filled diamonds) and 4.0  $\mu\text{s}$  (empty diamonds) after the 8 ns, 10 mJ laser flash.

This behavior is again attributed to the formation of the radical zwitterion  ${}^{-}\mathbf{8}^{\bullet+}$ , as described in Scheme 2.2.3 for  $\mathbf{7}^{\bullet+}$ .  ${}^{-}\mathbf{8}^{\bullet+}$  was observed to decay following first-order kinetics ( $k_{\downarrow}$  (420 nm) =  $2.6 \times 10^6 \text{ s}^{-1}$ ) and this decay was accompanied by the formation of a species that showed an absorption at 320 nm (an isosbestic point is visible at 340 nm).

The time-resolved absorption spectrum observed after PR of an argon saturated aqueous solution (pH = 1.7) containing 1-(3,4-dimethoxyphenyl)-1-cyclopropanecarboxylic acid (**9**) (1 mM),  $\text{K}_2\text{S}_2\text{O}_8$  (10 mM) and 2-methyl-2-propanol (0.1 M) recorded 5  $\mu\text{s}$  after the pulse shows the formation of two bands, centered at 310 and 445 nm, whose decay is not affected by the presence of oxygen, that can be reasonably assigned to the radical cation  $\mathbf{9}^{\bullet+}$ , formed by  $\text{SO}_4^{\bullet-}$  induced one-electron oxidation of **9**.

By increasing the pH of the solution to  $\approx 7$ , the spectrum observed after  $\text{SO}_4^{\bullet-}$  induced one-electron oxidation of **9** was similar to that obtained in acidic solution. However, as described previously for  $\mathbf{7}^{\bullet+}$  a broadening of the radical cation visible absorption band, accompanied by a 20 nm red-shift in its position was observed. This behavior is again attributed to the formation of the corresponding radical zwitterion  ${}^{-}\mathbf{9}^{\bullet+}$ , characterized by absorption bands at 310 and 465 nm.

Unfortunately, 266 nm LFP studies carried out on **9** showed the formation of transient species derived from the direct photochemistry of the substrate and this did not allow the use of this technique for the study of the one-electron oxidation of this substrate.

Figure 2.2.9 shows the time-resolved absorption spectrum observed after PR of an argon saturated aqueous solution (pH = 7.0) containing methyl 1-(3,4-dimethoxyphenyl)-1-cyclopropanecarboxylate (**12**) (0.3 mM),  $\text{K}_2\text{S}_2\text{O}_8$  (10 mM) and 2-methyl-2-propanol (0.1 M). The spectrum recorded 6  $\mu\text{s}$  after the pulse shows the formation of two bands, centered at 300 and 445 nm, that are very similar to those observed for  $\mathbf{9}^{\bullet+}$  and can be reasonably assigned to  $\mathbf{12}^{\bullet+}$ . As described previously for  $\mathbf{11}^{\bullet+}$ , also in this case no significant spectral variation was observed between pH 4 and 10.

The one-electron oxidation of 1-(4-methoxyphenyl)cyclopropanol (**7a**) was studied employing both PR and LFP. PR of an argon-saturated aqueous solution (pH = 5.0) containing 2 mM 1-(4-methoxyphenyl)cyclopropanol (**7a**), 0.1 M 2-methyl-2-propanol and 10 mM  $\text{K}_2\text{S}_2\text{O}_8$ , did not provide evidence for the formation of an intermediate radical cation, showing instead the fast formation of a product absorbing at  $\lambda < 370 \text{ nm}$ . A result that suggests that  $\mathbf{7a}^{\bullet+}$  is either not formed under these conditions or that its decomposition exceeds the time resolution of the PR equipment employed. Unfortunately, 266 nm LFP

experiments carried out on **7a** showed the formation of transient species derived from the direct photochemistry of the substrate and no further LFP investigation was carried out. Additional studies, are thus necessary in order to obtain information on the one-electron oxidation of this substrate.

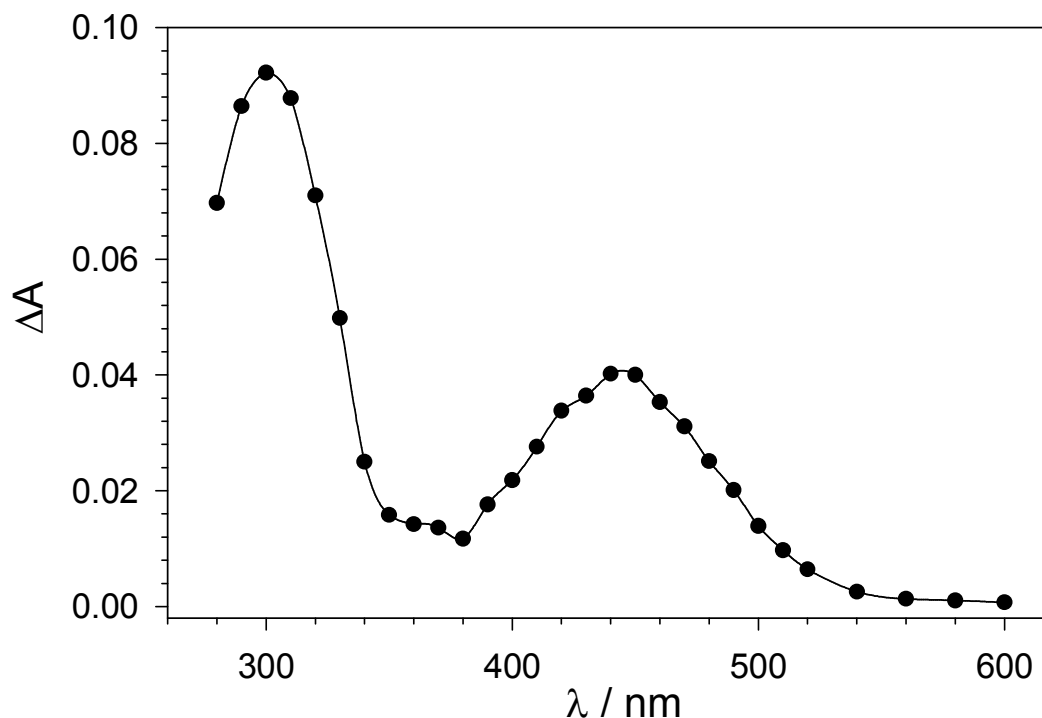
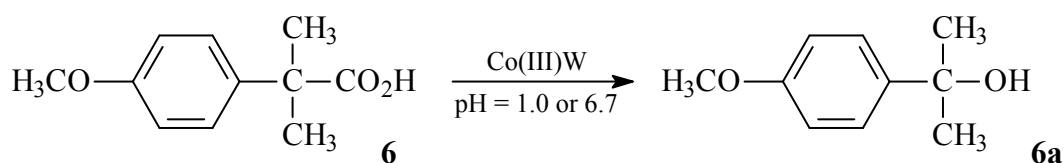


**Figure 2.2.9.** Time-resolved absorption spectrum observed on reaction of  $\text{SO}_4^{\bullet-}$  with methyl 1-(3,4-dimethoxyphenyl)-1-cyclopropanecarboxylate (**12**) (0.3 mM) recorded after pulse radiolysis of an argon-saturated aqueous solution (pH = 7.0), containing 0.1 M 2-methyl-2-propanol and 10 mM  $\text{K}_2\text{S}_2\text{O}_8$ , 6  $\mu\text{s}$  after the 300 ns, 10-MeV electron pulse.

**Product studies.** The one-electron oxidation reactions of substrates **6-12** and **7a** were carried out in argon saturated aqueous solution (pH = 1.0, 1.7 or 6.7) at  $T = 25$  or  $50$  °C, employing  $\text{SO}_4^{\bullet-}$  (generated by steady state photolysis as described in eq 1.3) and/or potassium 12-tungstocobalt(III)ate (Co(III)W) as the oxidant. The Co(III)W-induced oxidations were generally carried out until complete conversion of the oxidant. In the  $\text{SO}_4^{\bullet-}$ -induced oxidations, irradiation times were chosen in such a way as to avoid complete substrate consumption.

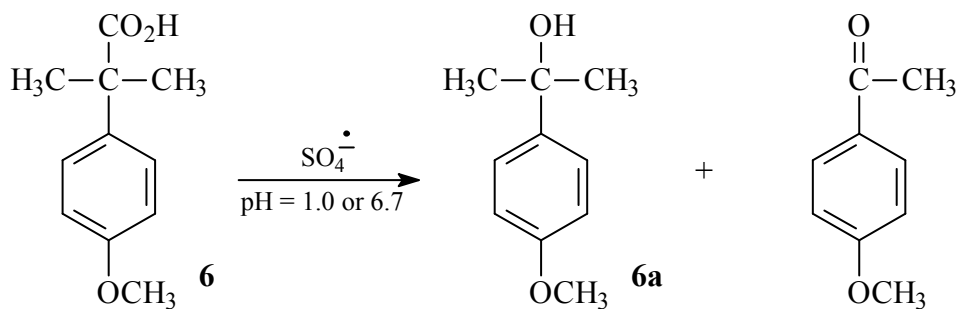


Scheme 2.2.4



With 2-(4-methoxyphenyl)-2-methyl propanoic acid (**6**) product studies, carried out both at pH = 1.0 and 6.7 using Co(III)W as the oxidant, showed the exclusive formation of 2-(4-methoxyphenyl)propan-2-ol (**6a**) as described in Scheme 2.2.4.

When  $\text{SO}_4^{\bullet-}$  was used as the oxidant, the reaction of **6**, both at pH = 1.0 and 6.7, showed the formation of **6a** as major product accompanied by 4-methoxyacetophenone (Scheme 2.2.5).



Scheme 2.2.5

The relative amount of 4-methoxyacetophenone was observed to increase on going from pH = 1.0 to pH = 6.7. The product distributions observed in the one-electron oxidation reactions carried out for **6** are collected in Table 2.2.1.

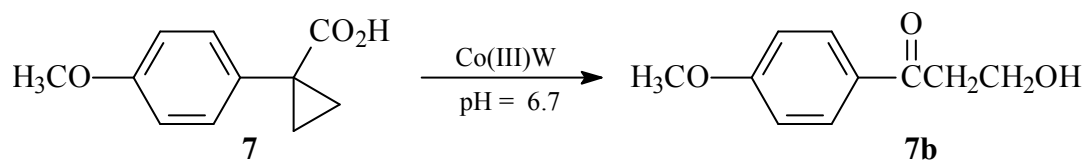
**Table 2.2.1.** Product distributions observed in the Co(III)W and  $\text{SO}_4^{\bullet-}$  induced oxidation of 2-(4-methoxyphenyl)-2-methylpropanoic acid (**6**), carried out in aqueous solution.<sup>a</sup>

entry	oxidant	pH <sup>b</sup>	recovered substrate ( <b>6</b> ) (%)	AnC(CH <sub>3</sub> ) <sub>2</sub> OH <sup>c</sup> ( <b>6a</b> ) (%)	AnCOCH <sub>3</sub> <sup>c</sup> (%)
1 <sup>d</sup>	Co(III)W	1 <sup>b</sup>	53	47	-
2 <sup>d</sup>	Co(III)W	6.7 <sup>b</sup>	40	60	-
3 <sup>e</sup>	$\text{SO}_4^{\bullet-}$	1 <sup>c</sup>	-	98	2
4 <sup>f</sup>	$\text{SO}_4^{\bullet-}$	6.7 <sup>d</sup>	-	89	11

<sup>a</sup>Good to excellent mass balances ( $\geq 90\%$ ) were observed in all experiments. <sup>b</sup>pH = 1.0 (HClO<sub>4</sub> 0.1 M); pH = 6.7 (NaH<sub>2</sub>PO<sub>4</sub> 0.1 M, adjusted with NaOH). <sup>c</sup>An = 4-MeOC<sub>6</sub>H<sub>4</sub>. <sup>d</sup>[substrate] = 5 mM, [Co(III)W] = 5 mM, *T* = 50 °C. <sup>e</sup>[substrate] = 2.5 mM, [K<sub>2</sub>S<sub>2</sub>O<sub>8</sub>] = 0.1 M, *T* = 25 °C, irradiation time = 30 sec. <sup>f</sup>[substrate] = 2.5 mM, [K<sub>2</sub>S<sub>2</sub>O<sub>8</sub>] = 0.1 M, *T* = 25 °C, irradiation time = 20 sec.

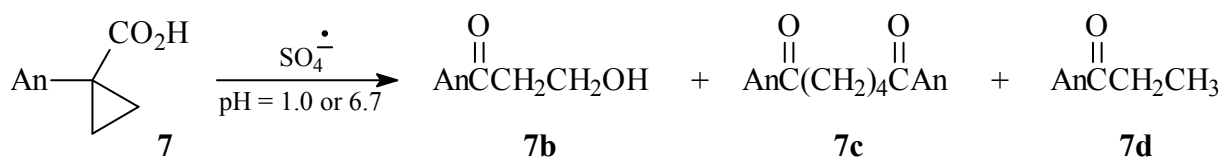
The Co(III)W induced oxidation of 1-(4-methoxyphenyl)-1-cyclopropanecarboxylic acid (**7**) was studied at pH = 1.0 and 6.7. At pH = 1.0 a very slow reaction was observed, (after 48 hrs at *T* = 50 °C, > 95 % of the substrate was recovered from the reaction mixture). At pH = 6.7 a

significantly faster reaction was observed, showing the exclusive formation of 1-(4-methoxyphenyl)-3-hydroxypropan-1-one (**7b**) as described in Scheme 2.2.6.



Scheme 2.2.6

The  $\text{SO}_4^{\bullet-}$ -induced oxidation of **7** was studied both at pH = 1.0 and 6.7. The analysis of the reaction mixture showed the formation of **7b**, 1,6-bis(4-methoxyphenyl)hexane-1,6-dione (**7c**) and 4-methoxypropiophenone (**7d**) as described in Scheme 2.2.7.



Scheme 2.2.7

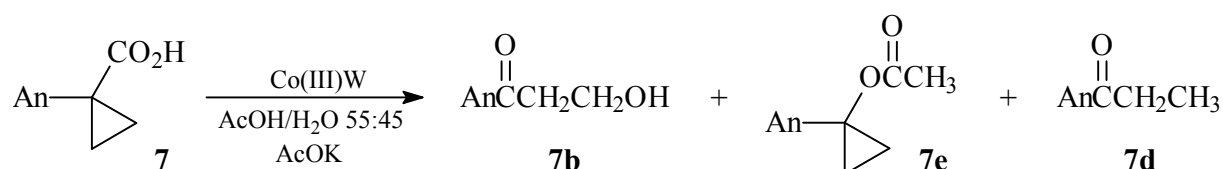
The product distributions observed in the one-electron oxidation reactions carried out for **7** are collected in Table 2.2.2.

**Table 2.2.2.** Product distributions observed in the Co(III)W and  $\text{SO}_4^{\bullet-}$  induced oxidation of 1-(4-methoxyphenyl)-1-cyclopropanecarboxylic acid (**7**), carried out in aqueous solution.<sup>a</sup>

Entry	oxidant	pH <sup>b</sup>	recovered substrate ( <b>7</b> ) (%)	<b>7b</b> (%)	<b>7c</b> (%)	<b>7d</b> (%)
1 <sup>c,d</sup>	Co(III)W	1.0	> 95	<sup>d</sup>	-	-
2 <sup>c</sup>	Co(III)W	6.7	55	45	-	-
3 <sup>e,f</sup>	$\text{SO}_4^{\bullet-}$	1.0	90	3	4	3
4 <sup>e,g</sup>	$\text{SO}_4^{\bullet-}$	6.7	90	1	6	4
5 <sup>e,h</sup>	$\text{SO}_4^{\bullet-}$	6.7	70	4	20	6
6 <sup>e,i</sup>	$\text{SO}_4^{\bullet-}$	6.7	38	7	46	9

<sup>a</sup>Good to excellent mass balances ( $\geq 85\%$ ) were observed in all experiments. <sup>b</sup>pH = 1.0 ( $\text{HClO}_4$  0.1 M); pH = 6.7 ( $\text{NaH}_2\text{PO}_4$  0.1 M, adjusted with NaOH). <sup>c</sup>[substrate] = 2.5 mM, [Co(III)W] = 2.5 mM,  $T = 50\text{ }^\circ\text{C}$ . <sup>d</sup>An almost complete recovery of the substrate was observed after 48 hrs and only traces of **7b** were observed. <sup>e</sup>[substrate] = 2.5 mM,  $[\text{K}_2\text{S}_2\text{O}_8] = 0.1\text{ M}$ ,  $T = 25\text{ }^\circ\text{C}$ . <sup>f</sup>Irradiation time = 60 sec. <sup>g</sup>Irradiation time = 30 sec. <sup>h</sup>Irradiation time = 120 sec. <sup>i</sup>Irradiation time = 360 sec.

The Co(III)W induced oxidation of **7** was also studied in AcOH/H<sub>2</sub>O 55:45 at  $T = 50\text{ }^{\circ}\text{C}$ , in the presence of 0.5 M AcOK. Under these conditions, the analysis of the reaction mixture showed the formation of **7b**, 1-(4-methoxyphenyl)cyclopropyl acetate (**7e**) and **7d** as described in Scheme 2.2.8 (An = 4-MeOC<sub>6</sub>H<sub>4</sub>). No quantitative analysis was carried out under these conditions.



Scheme 2.2.8

With 1-(4-methoxyphenyl)cyclopropanol (**7a**), product studies, carried out at pH = 6.7 using Co(III)W or SO<sub>4</sub><sup>•-</sup> as the oxidant, showed the formation of **7b**, **7c** and **7d**, i.e. of the same products observed in the SO<sub>4</sub><sup>•-</sup> induced oxidation of **7** described above in Scheme 2.2.7 and Table 2.2.2. The product distributions observed in the one-electron oxidation reactions carried out for **7a** are collected in Table 2.2.3.

**Table 2.2.3.** Product distributions observed in the Co(III)W and SO<sub>4</sub><sup>•-</sup> induced oxidation of 1-(4-methoxyphenyl)cyclopropanol (**7a**), carried out in aqueous solution (pH = 6.7) at  $T = 25\text{ }^{\circ}\text{C}$ .<sup>a</sup>

Entry	oxidant	Recovered substrate ( <b>7a</b> ) (%)	<b>7b</b> (%)	<b>7c</b> (%)	<b>7d</b> (%)
1 <sup>b</sup>	Co(III)W	74	11	9	6
2 <sup>c</sup>	SO <sub>4</sub> <sup>•-</sup>	70	1	22	7

<sup>a</sup>Good to excellent mass balances ( $\geq 95\%$ ) were observed in all experiments. <sup>b</sup>[substrate] = 2 mM, [Co(III)W] = 2 mM. <sup>c</sup>[substrate] = 1.5 mM, [K<sub>2</sub>S<sub>2</sub>O<sub>8</sub>] = 0.1 M, irradiation time = 40 sec.

The one-electron oxidation of 2-(3,4-dimethoxyphenyl)-2-methyl propanoic acid (**8**), was carried out in argon saturated aqueous solution (pH = 1.0 or 6.7) at  $T = 25\text{ }^{\circ}\text{C}$ , employing Co(III)W as the oxidant. At both pH = 1.0 and 6.7 the reaction showed the exclusive formation of 2-(3,4-dimethoxyphenyl)propan-2-ol (**8a**) in close analogy with the Co(III)W-induced oxidation of **6** described in Scheme 2.2.4.

The one-electron oxidation of 1-(3,4-dimethoxyphenyl)-1-cyclopropanecarboxylic acid (**9**) was carried out in argon saturated aqueous solution (pH = 1.0 or 6.7) at  $T = 25\text{ }^{\circ}\text{C}$ , employing Co(III)W as the oxidant. At both pH = 1.0 and 6.7 the reaction showed the exclusive formation of 1-(3,4-dimethoxyphenyl)-3-hydroxypropan-1-one (**9b**) in close analogy with the Co(III)W-induced oxidation of **7** described in Scheme 2.2.6.

The one-electron oxidations of methyl 2-(4-methoxyphenyl)-2-methyl propanoate (**10**), methyl 1-(4-methoxyphenyl)-1-cyclopropanecarboxylate (**11**) and methyl 1-(3,4-dimethoxyphenyl)-1-cyclopropanecarboxylate (**12**) were carried out in argon saturated aqueous solution (pH = 6.7) at  $T = 50\text{ }^{\circ}\text{C}$ , employing Co(III)W as the oxidant. Under these conditions complete recovery of the parent compound was observed for all substrates after reaction times  $\geq 24$  hrs. This observation clearly indicates that methyl esters **10-12** do not react under these experimental conditions. The lack of reactivity of these substrates is also evidenced by the fact that no change in color was observed for the Co(III)W/methyl ester reaction mixtures, whereas when the Co(III)W-induced oxidation reaction of aromatic compounds takes place, it is always accompanied by a color change from yellow to blue (indicative of the conversion of Co(III)W into its reduced form Co(II)W).<sup>13,14</sup>

**Time-resolved kinetic studies.** As mentioned above, no intermediate radical cation was detected in the time-resolved studies carried out for 2-(4-methoxyphenyl)-2-methyl propanoic acid (**6**), and 1-(4-methoxyphenyl)cyclopropanol (**7a**). Even though the mechanistic aspects of the one-electron oxidation of **6** and **7a** will be discussed in detail later on, it is important to point out that with **6** the kinetic data obtained by LFP indicate that if a radical cation is actually formed after one electron oxidation, its decay rate constant must exceed  $5 \times 10^7\text{ s}^{-1}$ , whereas with **7a** the kinetic data obtained by PR indicate that if a radical cation is actually formed, its decay rate constant must exceed  $1 \times 10^6\text{ s}^{-1}$ .<sup>15</sup>

The decay of the radical cations  $7^{\bullet+}$ - $9^{\bullet+}$  and of the corresponding radical zwitterions  $^{-}7^{\bullet+}$ - $^{-}9^{\bullet+}$  was measured spectrophotometrically in aqueous solution ( $T = 25\text{ }^{\circ}\text{C}$ , pH = 1.7 and  $\approx 7$ , respectively) following the decrease in optical density at the corresponding visible absorption band maximum (between 420 and 520 nm). In all cases the decay was observed to follow first order kinetics, and the rate constants thus obtained are collected in Table 2.2.4.

The decay of the radical cations  $10^{\bullet+}$ - $12^{\bullet+}$  was measured spectrophotometrically in aqueous solution ( $T = 25\text{ }^{\circ}\text{C}$ , pH  $\approx 7$ ) following the decrease in optical density at the corresponding visible absorption band maximum (between 450 and 500 nm). With these radical cations the decay was observed to be influenced by the radiation chemical dose and accordingly, only an

upper limit for their decay rate constant could be determined. The upper limits to the rate constants thus obtained are also collected in Table 2.2.4.

**Table 2.2.4.** First order rate constants ( $k$ ) for the decay of radical cations and radical zwitterions generated after PR and/or LFP of the parent substrates **7-12** in aqueous solution, measured at  $T = 25$  °C.

substrate	pH <sup>a</sup>	transient	generation	$\lambda_{\text{det}}^{\text{b}}$ / nm	$k / \text{s}^{-1}$
<b>7</b>	1.7	$7^{\bullet+}$	PR, $\text{SO}_4^{\bullet-}$ , Ar	500	$4.7 \times 10^3$
	1.7	$7^{\bullet+}$	PR, $\text{SO}_4^{\bullet-}$ , $\text{O}_2$	500	$4.4 \times 10^3$
	1.7	$7^{\bullet+}$	LFP, $\text{SO}_4^{\bullet-}$ , $\text{N}_2$	500	$4.5 \times 10^3$
	7.0	${}^{-}7^{\bullet+}$	PR, $\text{SO}_4^{\bullet-}$ , Ar	520	$2.2 \times 10^4$
	7.0	${}^{-}7^{\bullet+}$	LFP, $\text{SO}_4^{\bullet-}$ , $\text{N}_2$	520	$2.4 \times 10^4$
<b>8</b>	1.7	$8^{\bullet+}$	PR, $\text{SO}_4^{\bullet-}$ , Ar	420	$2.1 \times 10^5$
	1.7	$8^{\bullet+}$	PR, $\text{SO}_4^{\bullet-}$ , $\text{O}_2$	420	$1.8 \times 10^5$
	1.7	$8^{\bullet+}$	LFP, $\text{SO}_4^{\bullet-}$ , $\text{N}_2$	420	$2.1 \times 10^5$
	7.2	${}^{-}8^{\bullet+}$	PR, $\text{SO}_4^{\bullet-}$ , Ar	420	$> 1 \times 10^6$ <sup>c</sup>
	6.8	${}^{-}8^{\bullet+}$	LFP, $\text{SO}_4^{\bullet-}$ , $\text{N}_2$	420	$2.6 \times 10^6$
<b>9</b>	1.7	$9^{\bullet+}$	PR, $\text{SO}_4^{\bullet-}$ , Ar	445	$1.1 \times 10^4$
	7.0	${}^{-}9^{\bullet+}$	PR, $\text{SO}_4^{\bullet-}$ , Ar	465	$3.5 \times 10^4$
	7.0	${}^{-}9^{\bullet+}$	PR, $\text{SO}_4^{\bullet-}$ , $\text{O}_2$	465	$3.7 \times 10^4$
<b>10</b>	7.0	$10^{\bullet+}$	PR, $\text{SO}_4^{\bullet-}$ , Ar	450	$< 10^3$ <sup>d</sup>
<b>11</b>	7.2	$11^{\bullet+}$	PR, $\text{SO}_4^{\bullet-}$ , Ar	500	$< 10^3$ <sup>d</sup>
<b>12</b>	7.0	$12^{\bullet+}$	PR, $\text{SO}_4^{\bullet-}$ , Ar	445	$< 10^3$ <sup>d</sup>

<sup>a</sup>pH = 1.7 (adjusted with  $\text{HClO}_4$ ); pH  $\approx$  7 ( $\text{NaH}_2\text{PO}_4$  2 mM, adjusted with NaOH).

<sup>b</sup>Monitoring wavelength. <sup>c</sup>The time-resolution of the instrument did not allow the measurement of the decay rate constant and only an upper limit is provided. <sup>d</sup>The decay of the radical cations was observed to be influenced by the radiation chemical dose, and only an upper limit for the decay rate constant could be determined.

By monitoring the decay of the radical zwitterions  ${}^{-}7^{\bullet+}$  and  ${}^{-}9^{\bullet+}$ , and of the radical cations  $11^{\bullet+}$  and  $12^{\bullet+}$  at the visible absorption band maximum (between 445 and 520 nm) a significant increase in rate was observed when  ${}^{-}\text{OH}$  was added to the solution, and by plotting the observed rates ( $k_{\text{obs}}$ ) vs concentration of added base, a linear dependence was observed in all cases. (Figures 2.2.10 and 2.2.11, showing the  $k_{\text{obs}}$  vs  $[{}^{-}\text{OH}]$  plots for the reactions of  ${}^{-}7^{\bullet+}$  and  ${}^{-}9^{\bullet+}$ , respectively). From the slopes of these plots, the second-order rate constants for reaction of  ${}^{-}\text{OH}$  with  ${}^{-}7^{\bullet+}$ ,  ${}^{-}9^{\bullet+}$ ,  $11^{\bullet+}$  and  $12^{\bullet+}$  ( $k_{-}\text{OH}$ ) were determined. The second-order rate constants thus obtained are collected in Table 2.2.5.

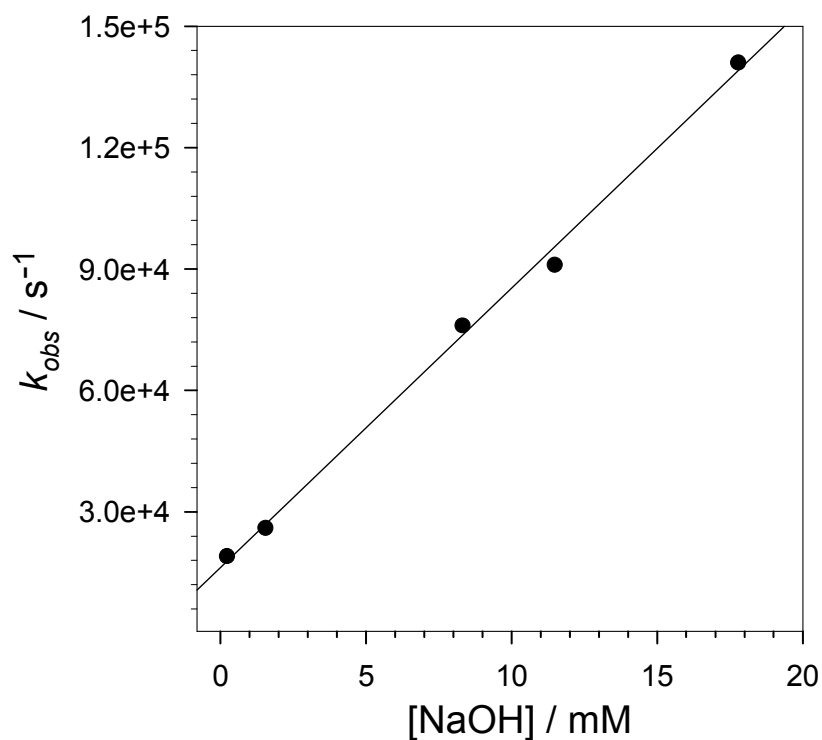


**Figure 2.2.10.** Plot of  $k_{obs}$  against concentration of NaOH for the reaction of radical zwitterion  $7^{\bullet+}$  with  $OH^-$ . From the linear regression analysis: intercept =  $1.6 \times 10^4 s^{-1}$ , slope =  $6.9 \times 10^6 M^{-1} s^{-1}$ ,  $r^2 = 0.9968$ .

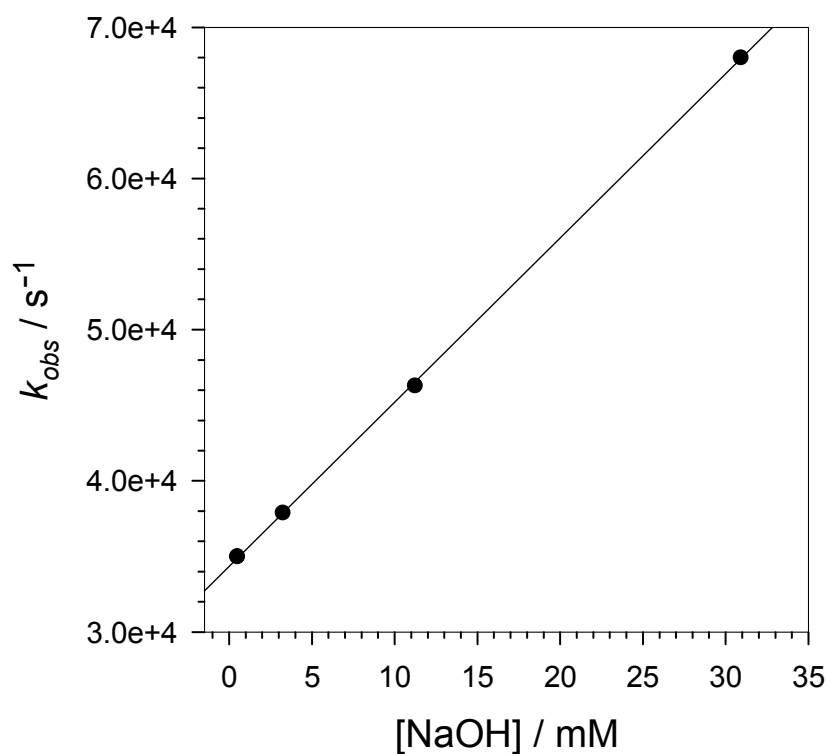


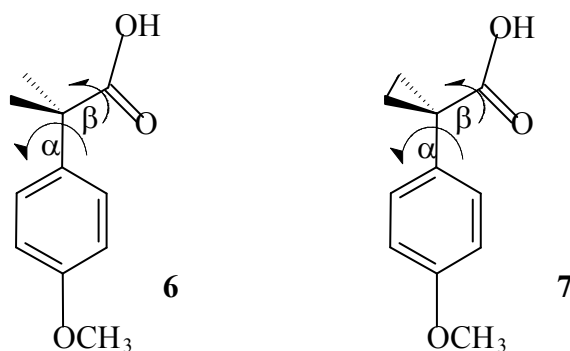
**Figure 2.2.11.** Plot of  $k_{obs}$  against concentration of NaOH for the reaction of radical zwitterion  $9^{\bullet+}$  with  $OH^-$ . From the linear regression analysis: intercept =  $3.4 \times 10^4 s^{-1}$ , slope =  $1.1 \times 10^6 M^{-1} s^{-1}$ ,  $r^2 = 0.9999$ .

**Table 2.2.5.** Second-order rate constants for the  $^{\ominus}\text{OH}$ -catalyzed ( $k_{\text{-OH}}$ ) decay of radical zwitterions  $^{-7}\bullet^{+}$  and  $^{-9}\bullet^{+}$ , and radical cations  $^{11}\bullet^{+}$  and  $^{12}\bullet^{+}$  generated by PR of the parent substrates in aqueous solution, measured at  $T = 25\text{ }^{\circ}\text{C}$ .

transient <sup>a</sup>	pH range <sup>b</sup>	$k_{\text{-OH}}^{\text{c}}$ ( $\text{M}^{-1}\text{ s}^{-1}$ )
$^{-7}\bullet^{+}$	10.2-12.3	$7.1 \times 10^6$
$^{-9}\bullet^{+}$	10.0-12.5	$1.0 \times 10^6$
$^{11}\bullet^{+}$	10.0-11.3	$5.4 \times 10^7$
$^{12}\bullet^{+}$	10.1-11.3	$5.7 \times 10^6$

<sup>a</sup>The radical cations and the radical zwitterions were generated by PR (dose  $\leq 5\text{ Gy/pulse}$ ) of argon saturated aqueous solutions containing the substrate (0.4-1.0 mM),  $\text{K}_2\text{S}_2\text{O}_8$  (10 mM), 2-methyl-2-propanol (0.1 M) and  $\text{Na}_2\text{B}_4\text{O}_7$  (1 mM). <sup>b</sup>pH range employed for the determination of  $k_{\text{-OH}}$ . <sup>c</sup>Obtained from the slopes of the  $k_{\text{obs}}$  vs  $[\text{NaOH}]$  plots, where  $k_{\text{obs}}$  was obtained following the decay of absorption at the radical cation or radical zwitterion visible absorption band maximum (between 445 and 520 nm). Average of at least two independent determinations. Error  $\leq 10\%$ . <sup>d</sup>The pH was limited to 11.3 because at  $\text{pH} > 11.5$  ester hydrolysis was observed

**DFT calculations.** Hybrid density functional (DFT) calculations with unrestricted MO formalism [UB3LYP/6-31G(d)] were carried out for 2-(4-methoxyphenyl)-2-methyl propanoic acid (**6**), 1-(4-methoxyphenyl)-1-cyclopropanecarboxylic acid (**7**) and for the corresponding radical cations  $^{6}\bullet^{+}$  and  $^{7}\bullet^{+}$ . The relaxed potential energy surface scans for the internal rotations about the  $\text{C}_{\text{Ar}}\text{-C}$  ( $\alpha$ ) and  $\text{C-CO}_2\text{H}$  ( $\beta$ ) bonds (depicted for the sake of clarity in Scheme 2.2.9) were carried out for **6** and **7** and for  $^{6}\bullet^{+}$  and  $^{7}\bullet^{+}$ , and those calculated for the radical cations are shown in Figures 2.2.12 and 2.2.13.



Scheme 2.2.9

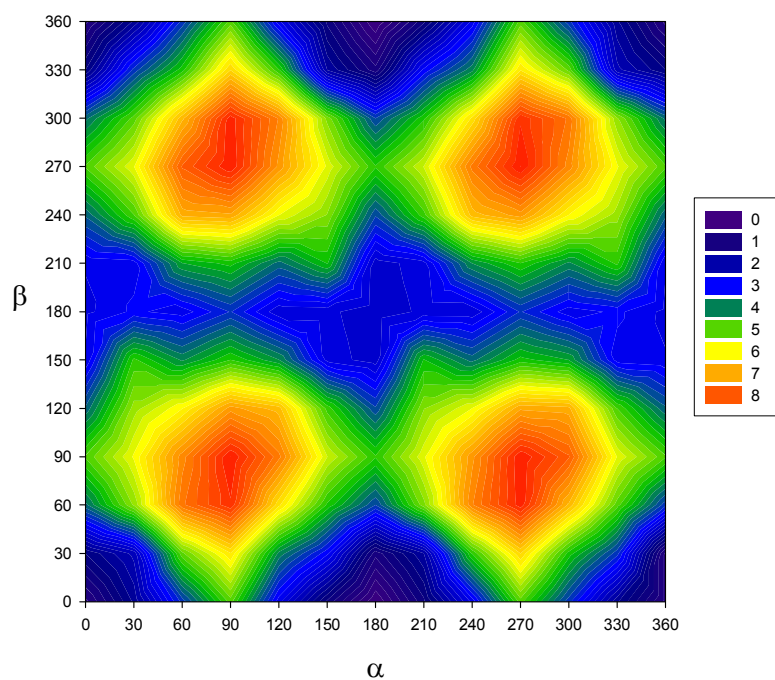


**Figure 2.2.12.** Relaxed potential energy surface scan for  $7^{*+}$  calculated at the UB3LYP/6-31G(d) level of theory.  $\alpha$  represents the dihedral angle between the plane of the aromatic ring and the plane that bisects the cyclopropyl ring.  $\beta$  is the dihedral angle between the plane that bisects the cyclopropyl ring and the plane of the CO<sub>2</sub>H group (see Scheme 2.2.9). The colored scale on the right hand side is in kcal mol<sup>-1</sup>.

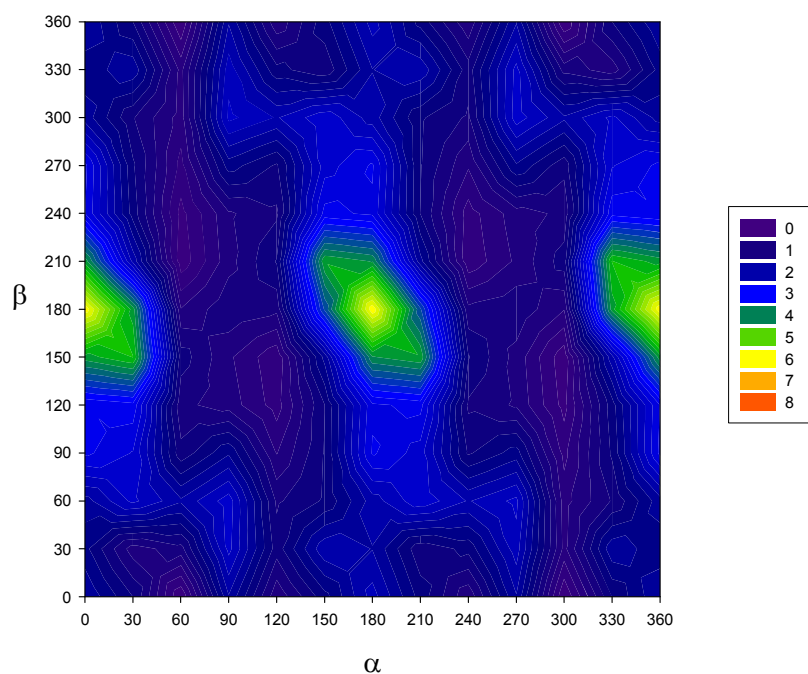
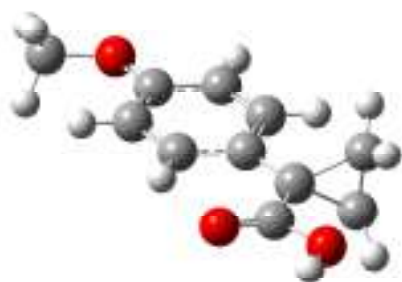


**Figure 2.2.13.** Relaxed potential energy surface scan for  $6^{*+}$  calculated at the UB3LYP/6-31G(d) level of theory.  $\alpha$  represents the dihedral angle between the plane of the aromatic ring and the plane that bisects the CH<sub>3</sub>CCH<sub>3</sub> angle.  $\beta$  is the dihedral angle between the plane that bisects the CH<sub>3</sub>CCH<sub>3</sub> angle and the plane of the CO<sub>2</sub>H group (see Scheme 2.2.9). The colored scale on the right hand side is in kcal mol<sup>-1</sup>.

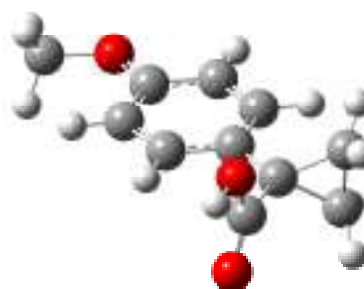


With the neutral substrates **6** and **7**, the most stable conformations were those characterized by dihedral angle values of  $\alpha = 60^\circ$ ,  $\beta = 90^\circ$  and  $\alpha = 90^\circ$ ,  $\beta = 180^\circ$ , respectively.

The analysis of Figure 2.2.12 clearly shows that the potential energy surface for **7<sup>•+</sup>** is strongly influenced by the relative orientation of the cyclopropyl and carboxylic groups. Accordingly, the most stable conformation for **7<sup>•+</sup>** is the one where the plane of the aromatic ring bisects the plane of the cyclopropyl ring ( $\alpha = 180^\circ$ ,  $\beta = 0^\circ$ : *bisected* conformation) (Scheme 2.2.10, structure **I**). This result is in line with the well known conformation-dependent  $\pi$ -donor properties of the cyclopropyl group.<sup>16</sup> In this conformation, orbital alignment between the aromatic  $\pi$ -system and the cyclopropyl HOMO is maximal and electron donation can occur. Quite interestingly, in this conformation the carboxylic group is coplanar with the aromatic ring, resulting in efficient orbital overlap between the carbonyl  $\pi$ -system and the cyclopropyl orbitals.



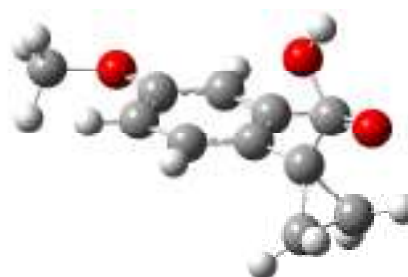
$\alpha = 180^\circ$ ,  $\beta = 0^\circ$  (structure **I**)  
 $\Delta E = 0.00$  (Kcal/mol)  
**Global minimum**



$\alpha = 180^\circ$ ,  $\beta = 90^\circ$  (structure **II**)  
 $\Delta E = 4.63$  (Kcal/mol)



$\alpha = 180^\circ$ ,  $\beta = 180^\circ$  (structure **III**)  
 $\Delta E = 2.24$  (Kcal/mol)

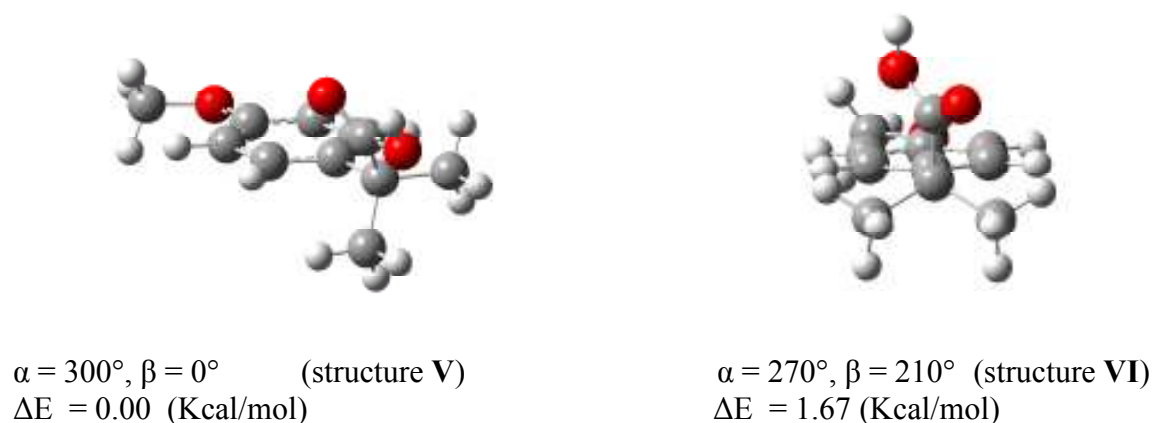


$\alpha = 90^\circ$ ,  $\beta = 180^\circ$  (structure **IV**)  
 $\Delta E = 3.21$  (Kcal/mol)

Scheme 2.2.10

In the alternative *perpendicular* conformation (Scheme 2.2.10, structure **IV**), the cyclopropyl HOMO is orthogonal to the  $\pi$ -system and no such overlap can be achieved.

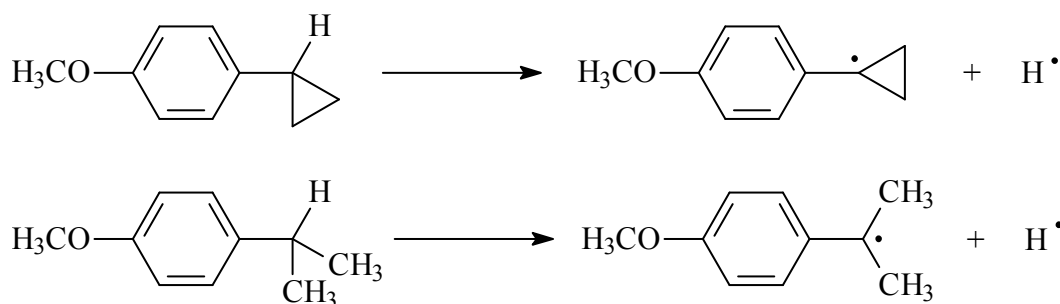
As compared to the potential energy surface calculated for **7<sup>•+</sup>** (Figure 2.2.12), the energy surface calculated for **6<sup>•+</sup>**, depicted in Figure 2.2.13, appears to be relatively flat. In this case significantly smaller energy differences between the alternative conformations were calculated (Scheme 2.2.11) indicating that the relative conformations of the aromatic ring and the C(CH<sub>3</sub>)<sub>2</sub> group play a minor role.



Scheme 2.2.11

The computed energies obtained for the most stable conformations of **6**, **7**, **6<sup>•+</sup>** and **7<sup>•+</sup>** were then used to evaluate the adiabatic ionization potentials (IPs) of **6** and **7**. IP values of 7.48 and 7.33 eV, for **6** and **7**, respectively, were thus obtained from the energy difference between the radical cation and the neutral precursor.

DFT calculations at the UB3LYP/6-31G(d) level of theory were also carried out in order to obtain information on the stability of the 1-(4-methoxyphenyl)cyclopropyl radical and of the 4-methoxycumyl radical, expressed in terms of the benzylic C–H bond dissociation enthalpies (BDEs) of the parent compounds (4-methoxycyclopropylbenzene and 4-methoxycumene, respectively, Scheme 2.2.12).



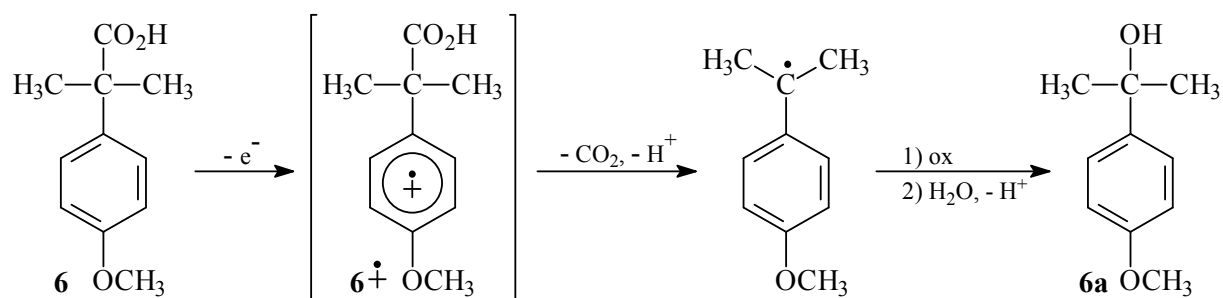
Scheme 2.2.12

BDEs calculated at the UB3LYP/6-31G(d) level of theory are sufficiently reliable for the discussion presented here, because it has been pointed out both that the B3LYP functional offers an attractive and seemingly accurate alternative to the expensive conventional ab initio methods for the computation of BDEs,<sup>17</sup> and that, thanks to the cancellation of errors, differences in BDEs ( $\Delta$ BDEs) within a closely related family of compounds are much more reliable than the absolute values.<sup>18</sup> BDE values were thus obtained from the energy differences between the radicals produced by homolytic C–H bond cleavage and the parent substrate ( $\text{BDE} = E(\text{H}^\bullet) + E(\text{subs}^\bullet) - E(\text{subs-H})$ , where  $\text{subs-H} = 4\text{-methoxycyclopropyl benzene or } 4\text{-methoxycumene}$ ). BDE values of 99.0 and 90.1 kcal mol<sup>-1</sup> were thus obtained for the benzylic C–H bond of 4-methoxycyclopropylbenzene and 4-methoxycumene, respectively

## Discussion

Product studies carried out on 2-(4-methoxyphenyl)-2-methyl propanoic acid (**6**) showed the formation of 2-(4-methoxyphenyl)propan-2-ol (**6a**) as the exclusive or predominant reaction product as described in Schemes 2.2.4 and 2.2.5. This product clearly derives from the oxidation of an intermediate 4-methoxycumyl radical formed after oxidative decarboxylation of **6**, as described previously for the one-electron oxidation of 4-methoxyphenylethanoic acid in acidic aqueous solution (see Chapter 2.1).<sup>2,19</sup> Along this line, the formation of 4-methoxyacetophenone in the  $\text{SO}_4^{\bullet-}$ -induced oxidation of **6** can be explained in terms of the further oxidation of the first formed alcohol **6a**, via an intermediate radical cation  $\text{6a}^{\bullet+}$ , a process that is known to be favored by the presence of a base.<sup>20</sup> LFP experiments carried out at pH = 1.7 did not provide any direct evidence for the formation of an intermediate radical cation  $\text{6}^{\bullet+}$ , showing instead the initial formation of  $\text{SO}_4^{\bullet-}$  whose decay (occurring with a first-order rate constant  $k_{\downarrow}(450 \text{ nm}) = 1.0 \times 10^7 \text{ s}^{-1}$ ) is accompanied by the corresponding buildup in absorption in the UV region of the spectrum ( $k_{\uparrow}(290 \text{ nm}) = 1.1 \times 10^7 \text{ s}^{-1}$ ) of a transient species (Figure 2.2.1). The decay of this species is accelerated by oxygen occurring with a second-order rate constant  $k = 1.7 \times 10^9 \text{ M}^{-1} \text{ s}^{-1}$ , a value that is similar to those measured previously for the reactions of carbon centered radicals with oxygen.<sup>21-23</sup> On the basis of this observation and of the results of product studies described above this transient can be assigned to the 4-methoxycumyl radical.

Overall, these results are consistent with those obtained previously for the one-electron oxidation 4-methoxyphenylethanoic acid (**1**), where no direct evidence for the formation of an intermediate radical cation  $\mathbf{1}^{\bullet+}$  but only of the 4-methoxybenzyl radical was obtained.<sup>2,19</sup> The mechanism of the one-electron oxidation of **6** can be thus described according to Scheme 2.2.13: the oxidation of **6** is coupled with the decarboxylation reaction, directly leading to the 4-methoxycumyl radical. Oxidation of this radical in the reaction medium gives **6a**.



Scheme 2.2.13

Clearly, even though no intermediate radical cation  $\mathbf{6}^{\bullet+}$  was detected in the LFP experiments, the kinetic data do not allow to exclude the possible intermediacy of  $\mathbf{6}^{\bullet+}$ , because its lifetime could be too short to allow detection under the experimental conditions employed: in other words, if  $\mathbf{6}^{\bullet+}$  is actually formed after one electron oxidation, its decarboxylation rate constant must be extremely fast ( $k > 5 \times 10^7 \text{ s}^{-1}$ ).

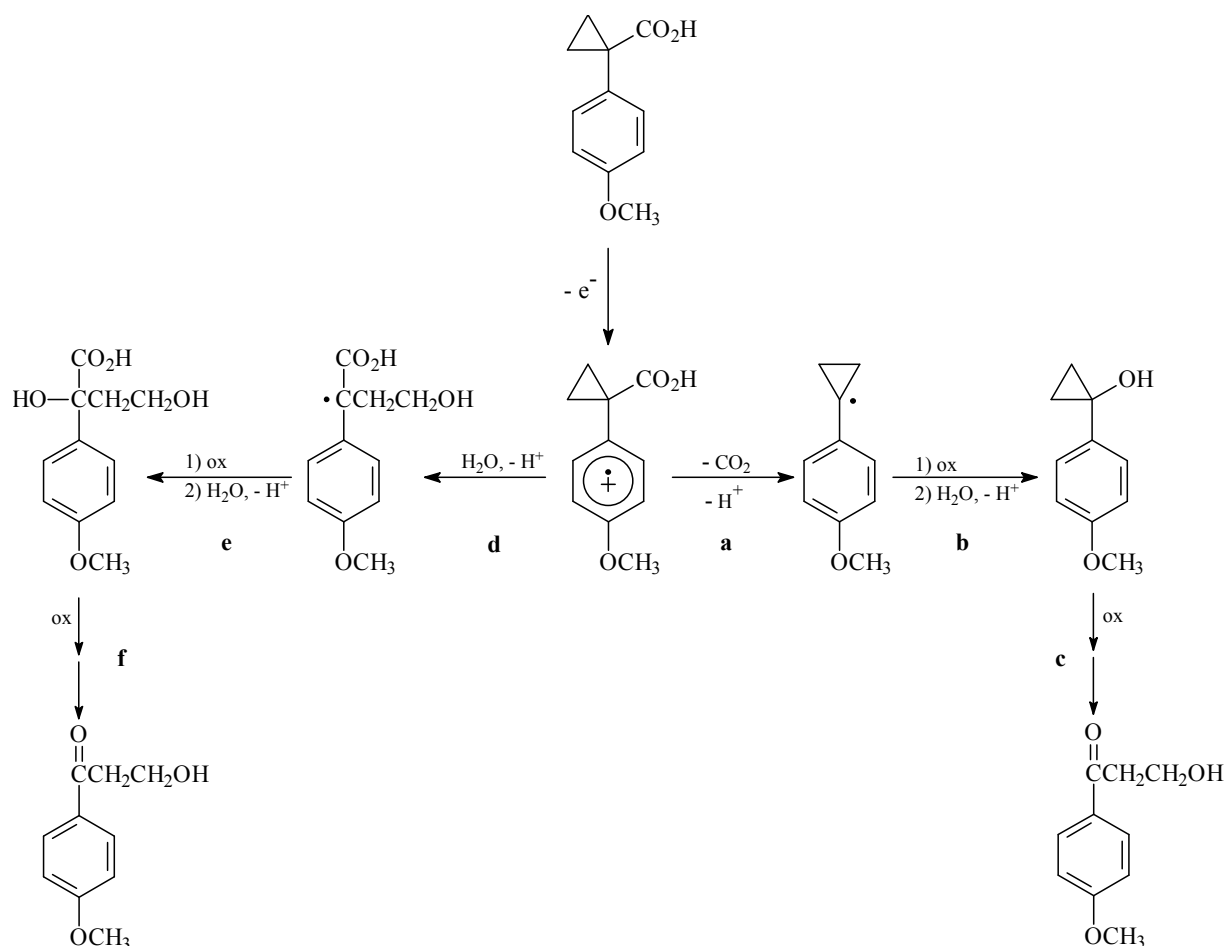
At least partial support to this hypothesis comes from the observation that the second order rate constant for reaction of  $\text{SO}_4^{\bullet-}$  with **6**, derived from the rate constant measured for the decay of  $\text{SO}_4^{\bullet-}$  ( $k_{\downarrow}(450 \text{ nm}) = 1.0 \times 10^7 \text{ s}^{-1}$ ) and the concentration of **6** ( $2.0 \times 10^{-3} \text{ M}$ ) as  $k = 5.0 \times 10^9 \text{ M}^{-1} \text{ s}^{-1}$ , is very similar to the rate constants measured previously for reaction of  $\text{SO}_4^{\bullet-}$  with monomethoxylated benzenes,<sup>7,11,24</sup> thus indicating that electron removal is very likely to occur from the aromatic nucleus. Along this line, the possibility that electron removal occurs from the carboxylic (or carboxylate) function, directly leading to an acyloxyl radical, can be discarded on the basis of the second-order rate constants determined for the reaction of  $\text{SO}_4^{\bullet-}$  with ethanoic acid at  $\text{pH} \approx 0$  and  $\text{pH} = 6.8$ :  $k = 8.8 \times 10^4$  and  $5.0 \times 10^6 \text{ M}^{-1} \text{ s}^{-1}$ , respectively.<sup>25,26</sup>

With methyl 2-(4-methoxyphenyl)-2-methyl propanoate (**10**), direct evidence for the formation of an intermediate radical cation  $\mathbf{10}^{\bullet+}$  after one-electron oxidation was obtained by LFP and PR, as clearly shown by the time-resolved spectrum displayed in Figure 2.2.3.  $\mathbf{10}^{\bullet+}$  displayed a very low reactivity, evidenced by the lack of oxidation observed when **10** was

reacted with Co(III)W, and by the upper limit determined for its decay rate constant ( $k < 10^3 \text{ s}^{-1}$ ). With this substrate, the presence of the  $\text{CO}_2\text{Me}$  group prevents the decarboxylation reaction of the corresponding radical cation, thus determining a dramatic depression in its reactivity as compared to **6**. Moreover, the presence of the two methyl groups in the  $\alpha$  position precludes the possibility of benzylic C–H deprotonation as an alternative decay pathway of  $\mathbf{10}^{\bullet+}$ .

With 1-(4-methoxyphenyl)cyclopropanecarboxylic acid (**7**), direct evidence for the formation of an intermediate radical cation  $\mathbf{7}^{\bullet+}$  or radical zwitterion  $^-\mathbf{7}^{\bullet+}$  after one-electron oxidation was obtained by LFP and PR, as clearly shown by the time-resolved spectra displayed in Figures 2.2.4 and 2.2.5. The Co(III)W induced oxidation of **7** showed, at  $\text{pH} = 6.7$ , the exclusive formation of 1-(4-methoxyphenyl)-3-hydroxypropan-1-one (**7b**) as described in Scheme 2.2.6. The same product, accompanied by 1,6-bis(4-methoxyphenyl)hexane-1,6-dione (**7c**) and 4-methoxypropiophenone (**7d**) was also observed after  $\text{SO}_4^{\bullet-}$ -induced oxidation of **7** at  $\text{pH} = 1.0$  and 6.7 (Scheme 2.2.7). The formation of **7b** can in principle be explained in terms of the two pathways described in Scheme 2.2.14 for the fragmentation of  $\mathbf{7}^{\bullet+}$ . In the mechanism described in paths **a-c**, the initially formed  $\mathbf{7}^{\bullet+}$  undergoes decarboxylation to give the 1-(4-methoxyphenyl)cyclopropyl radical (path **a**). Oxidation of this radical followed by reaction with the solvent water gives 1-(4-methoxyphenyl)cyclopropanol (**7a**) (path **b**) whose subsequent oxidation finally leads to **7b** (path **c**). As it is well known that arylcyclopropane radical cations undergo a facile ring-opening reaction by nucleophilic attack at the  $\text{C}_\beta$  carbon of the cyclopropane ring,<sup>9,27-29</sup> a possible mechanistic alternative is that described in paths **d-f** of Scheme 2.2.14.  $\mathbf{7}^{\bullet+}$  undergoes a water-induced ring-opening reaction to give a stabilized benzylic radical (path **d**). Oxidation of this radical followed by reaction with water gives 2,4-dihydroxy-2-(4-methoxyphenyl)butanoic acid (path **e**) whose subsequent oxidative decarboxylation finally leads to **7b** (path **f**).

However, the latter pathway can be discarded on the basis of the observation that methyl 1-(4-methoxyphenyl)cyclopropanecarboxylate (**11**), whose radical cation  $\mathbf{11}^{\bullet+}$  would be expected to display a reactivity towards ring-opening comparable to that of  $\mathbf{7}^{\bullet+}$ , showed instead a significantly lower reactivity (see Table 2.2.4). A result that indicates that water is not sufficiently nucleophilic to promote ring-opening of the cyclopropane ring.



Scheme 2.2.14

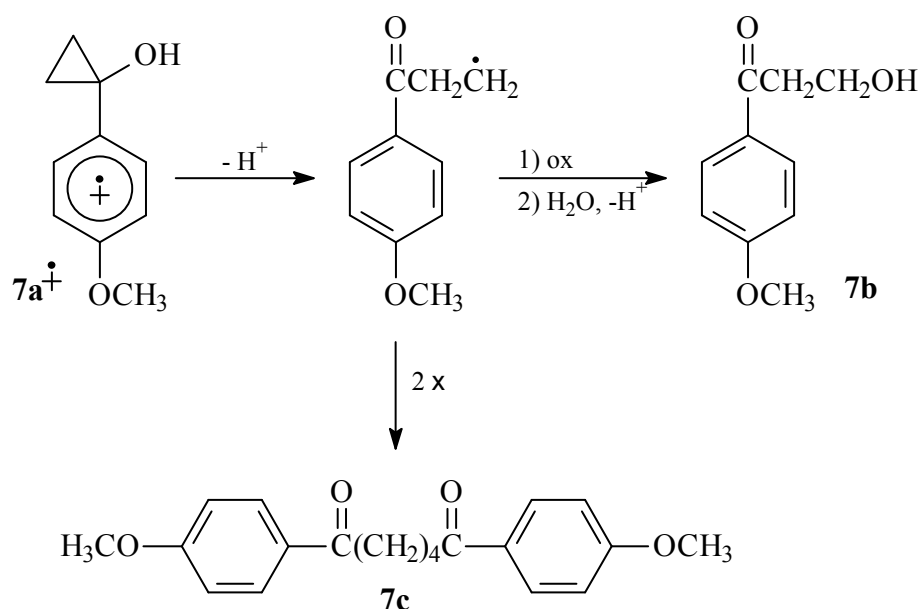
Also the observation that the decay rate constant increases on going from  $7^{\bullet+}$  to  $^{-}7^{\bullet+}$  is in line with a decarboxylation reaction (path **a**), as described in Chapter 2.1 for the one-electron oxidation of aryethanoic acids **2-5**, where the radical zwitterions were observed to be between 10 and 40 times more reactive than the corresponding radical cations. Last but not least, the mechanism described by paths **d-f** would not be able to account for the formation of products **7c** and **7d**.

On the other hand, in the one-electron oxidation of **7**, 1-(4-methoxyphenyl)cyclopropanol (**7a**) was never detected among the reaction products. This observation is however not surprising because **7a** was observed to be significantly more reactive than **7**, and in particular, given that the decarboxylation rate constants for  $7^{\bullet+}$  and  $^{-}7^{\bullet+}$  were measured as  $4.7 \times 10^3$  and  $2.2 \times 10^4$   $s^{-1}$ , respectively, the kinetic data obtained by PR indicate that if  $7a^{\bullet+}$  is actually formed, its decay rate constant must be  $> 1 \times 10^6$   $s^{-1}$ . Indirect evidence in favor of the intermediacy of **7a** comes from the observation that the same products were formed after one-electron oxidation of **7** and **7a**, and, more importantly, from the observation that 1-(4-methoxyphenyl)cyclopropyl acetate (**7e**) was detected among the reaction products when the Co(III)W-induced oxidation of **7** was carried out in AcOH/H<sub>2</sub>O 55:45, in the presence of

AcOK (Scheme 2.2.8); an observation that is in line with the previous indication that the conversion of 4-methoxybenzylalcohol into its acetate determines a significant decrease in reactivity in the corresponding radical cations.<sup>13</sup> Taken together, these evidences provide strong support to the hypothesis that the one-electron oxidation of **7** proceeds through the mechanism described by paths **a-c**.

Very interestingly, the data discussed above also provide indirect evidence on the involvement of an intermediate 1-(4-methoxyphenyl)cyclopropyl cation in this process.<sup>30</sup>

The formation of 1,6-bis(4-methoxyphenyl)hexane-1,6-dione (**7c**) can be explained according to Scheme 2.2.15, where **7a<sup>•+</sup>** undergoes ring-opening to give a radical that can either dimerize to give **7c**, or get oxidized in the reaction medium finally leading to **7b**.



Scheme 2.2.15

For what concerns instead 4-methoxypropiophenone (**7d**), it is well known that this product can derive from the acid catalyzed or thermal rearrangement of **7a**.<sup>34</sup> Blank experiments showed the stability towards rearrangement of **7a** above  $pH \approx 3$ . Accordingly, the observation that in aqueous solution ( $pH = 6.7$ ) the Co(III)W-induced oxidation of **7** led to the exclusive formation of **7b** (Scheme 2.2.6), whereas **7d** was also observed among the reaction products when the reaction was carried out in AcOH/ $H_2O$  55:45 (Scheme 2.2.8), indicates that in the latter experimental conditions the acid-catalyzed rearrangement of **7a** can compete efficiently with its one electron oxidation.

On the other hand, the formation of **7b** following  $\text{SO}_4^{\bullet-}$  induced oxidation of **7** at  $\text{pH} = 6.7$  (see Table 2.2.2) requires a different explanation and additional experiments in this respect will be necessary.

The direct comparison between the one-electron oxidation reactions of **6** and **7**, shows that the replacement of the  $\text{C}(\text{CH}_3)_2$  moiety with a cyclopropyl group, determines a decrease in decarboxylation rate constant in the corresponding radical cations of at least four orders of magnitude!<sup>35</sup> In order to rationalize this behavior, the relative contribution of several factors should be taken into account.

Previous studies have shown that the decarboxylation rate constant is influenced by the oxidation potential of the substrate,<sup>36</sup> as clearly shown for example in Chapter 2.1 for the one-electron oxidation of aryloethanoic acids (**2-5**). The radical cation decarboxylation rate constant was observed to be influenced by the stabilization of the positive charge on the aromatic ring, i.e. by the height of the kinetic barrier for side-chain to ring intramolecular electron transfer associated to decarboxylation. An increase in radical cation stability determines an increase in the height of the kinetic barrier for intramolecular electron transfer resulting in a corresponding decrease in decarboxylation rate constant.

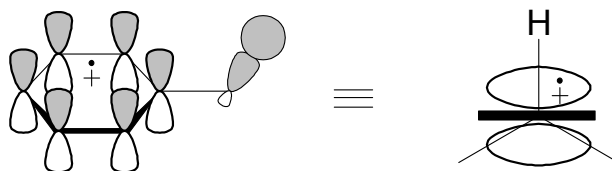
Along this line, the adiabatic ionization potentials calculated for **6** and **7** (7.48 and 7.33 eV, respectively) clearly indicate that  $7^{\bullet+}$  is more stable than  $6^{\bullet+}$ , a behavior that can be ascribed to the well known  $\pi$ -donor properties of the cyclopropyl group<sup>16,37</sup> (see for example in Scheme 2.2.10 the most stable conformation calculated for  $7^{\bullet+}$ ). Evidence in this respect is also provided by the analysis of the time-resolved spectrum obtained for  $7^{\bullet+}$ , shown in Figures 2.2.4 and 2.2.5, that resembles the spectra observed<sup>8,9,37</sup> for arylcyclopropane radical cations, rather than those observed for anisole derivatives.<sup>4,5,7,11</sup>

Another important factor is represented by the stability of the carbon centered radical formed after decarboxylation. In this context, Gould and Farid have clearly shown that in the decarboxylation of radical cations of anilino bis carboxylates characterized by comparable stabilities, the decarboxylation rate constants was influenced by the stability of the product radical, increasing with increasing radical stability.<sup>38</sup> Accordingly, as a consequence of the Hammond postulate,<sup>39</sup> an increase in stability of the product radical determines an increase in the reaction exothermicity and a corresponding decrease in activation energy. Along this line, the difference between the BDEs calculated for 4-methoxycyclopropylbenzene and 4-methoxycumene (see Scheme 2.2.12), allows the assessment of the relative stabilities of the 1-(4-methoxyphenyl)cyclopropyl and 4-methoxycumyl radicals.<sup>18</sup> Based on the BDEs calculated for 4-methoxycyclopropylbenzene and 4-methoxycumene (99.0 and 90.1 kcal mol<sup>-1</sup>, respectively), the 4-methoxycumyl radical appears to be  $\approx 9$  kcal mol<sup>-1</sup> more stable than



the 1-(4-methoxyphenyl)cyclopropyl radical,<sup>40</sup> a result that is in line with the relatively low stability of cyclopropyl radicals.<sup>41-43</sup> Clearly, the observed radical stabilities are in line with the decarboxylation rate constants reported above for **6**<sup>•+</sup> and **7**<sup>•+</sup>.

As final point of interest is represented by the possible role of stereoelectronic effects in these processes. It is well known that the side-chain fragmentation reactivity of alkylaromatic radical cations can be influenced by the relative orientation between the scissile bond and the  $\pi$  system (stereoelectronic effect).<sup>44-47</sup> As illustrated in Scheme 2.2.16 (where, for the sake of clarity, in the former structure only the benzylic C–H bond is shown), the most suitable orientation for cleavage is the one where the dihedral angle between the plane of the aromatic ring and the plane defined by the scissile bond and the atom of the aromatic ring to which this bond is connected is 90°. In this conformation the scissile bond is aligned with the  $\pi$  system bearing the unpaired electron, and the best orbital overlap for bond cleavage can be achieved.



Scheme 2.2.16

Along this line, in the most stable conformation calculated for **7**<sup>•+</sup>, (Scheme 2.2.10, structure I,  $\alpha = 180^\circ$ ,  $\beta = 0^\circ$ ) the carboxylic group is coplanar with the plane of the aromatic ring, and no efficient overlap between the scissile C–CO<sub>2</sub>H bond and the  $\pi$  system can be achieved. In order to reach the most stable conformation where the scissile bond is perpendicular to the plane of the aromatic ring (most suitable orientation for bond cleavage: structure **IV**,  $\alpha = 90^\circ$ ,  $\beta = 180^\circ$ ) an energy barrier of at least 4.63 kcal mol<sup>-1</sup> has to be overtaken.

On the other hand, in the most stable conformation calculated for **6**<sup>•+</sup>, (Scheme 2.2.11, structure V,  $\alpha = 300^\circ$ ,  $\beta = 0^\circ$ ) the scissile C–CO<sub>2</sub>H bond is very close to the most suitable orientation for cleavage ( $\alpha = 270^\circ$ ,  $\beta = 0^\circ$ ). In this case, moving on a relatively flat potential energy in order to reach the most suitable orientation for bond cleavage an energy barrier  $\leq 1.80$  kcal mol<sup>-1</sup> has to be overtaken.

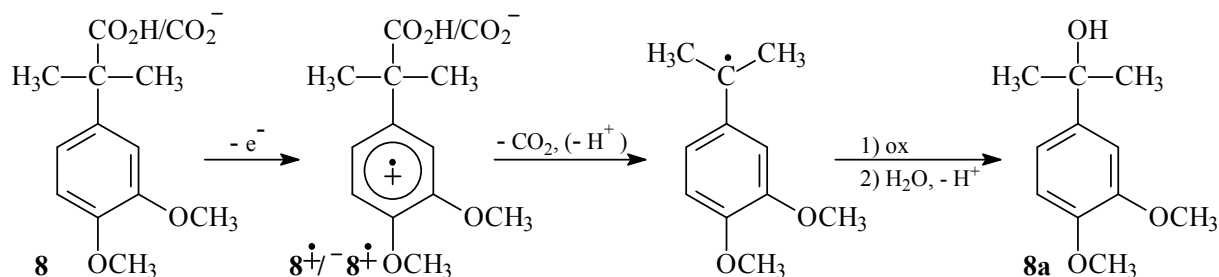
Thus, even though the observed differences in energy are relatively small, stereoelectronic requirements for C–CO<sub>2</sub>H bond cleavage are relatively more costly for **7**<sup>•+</sup> than for **6**<sup>•+</sup>.

In summary, when comparing the one-electron oxidation reactions of **6** and **7**, the factors discussed above clearly indicate that the stability of the radical cation, the stability of the carbon radical formed after decarboxylation and stereoelectronic requirements for

decarboxylation all exert their effect in the same direction that is by decreasing the decarboxylation rate constant of  $7^{\bullet+}$  as compared to that of  $6^{\bullet+}$ .

On going from **6** and **7** to the corresponding dimethoxylated substrates 2-(3,4-dimethoxyphenyl)-2-methyl propanoic acid (**8**) and 1-(3,4-dimethoxyphenyl)-1-cyclopropanecarboxylic acid (**9**), time-resolved studies showed in both cases the formation of the corresponding radical cations  $8^{\bullet+}$  and  $9^{\bullet+}$  at pH = 1.7 and radical zwitterions  $8^{\bullet-}$  and  $9^{\bullet-}$  at pH  $\approx$  7.

Product studies carried out on **8** showed the formation of 2-(3,4-dimethoxyphenyl)propan-2-ol (**8a**) as the exclusive reaction product both at pH = 1.0 and 6.7. Formation of this product can be explained in terms of the mechanism described in Scheme 2.2.17: oxidation of **8** leads to the formation of  $8^{\bullet+}$  (or  $8^{\bullet-}$ ) that undergoes decarboxylation to give the 3,4-dimethoxycumyl radical. Oxidation of this radical in the reaction medium gives **8a**.



Scheme 2.2.17

Decarboxylation rate constants  $k = 2.1 \times 10^5$  and  $2.6 \times 10^6 \text{ s}^{-1}$  were measured for  $8^{\bullet+}$  and  $8^{\bullet-}$ , respectively (see Table 2.2.4). Clearly, as compared to **6**, the presence of an additional methoxy ring substituent in **8** determines a significant stabilization of the radical cation that accordingly undergoes decarboxylation with a significantly lower rate constant.<sup>35</sup> An increase in decarboxylation rate constant on going from the radical cation to the corresponding radical zwitterion was also observed for  $2^{\bullet+}$ - $5^{\bullet+}$  (see Chapter 2.1) and for  $7^{\bullet+}$ . This behavior has been rationalized in terms of the kinetic barrier for intramolecular side-chain to ring electron transfer required for decarboxylation that is expected to be higher for the radical cation, because, as compared to the radical zwitterion an additional proton transfer to the medium is required.

Product studies carried out on **9** showed the formation of 1-(3,4-dimethoxyphenyl)-3-hydroxypropan-1-one (**9b**) as the exclusive reaction product both at pH = 1.0 and 6.7. Formation of this product can be explained in analogy with the mechanism described in

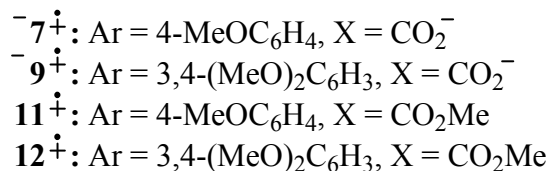
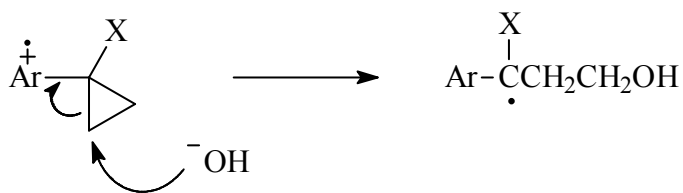
Schemes 2.2.14 (paths **a-c**) and 2.2.15 for the oxidation of **7**, in terms of the decarboxylation of the initially formed  $\mathbf{9}^{\bullet+}$  or  $\mathbf{9}^{\bullet-}$ .

Decarboxylation rate constants  $k = 1.1 \times 10^4$  and  $3.5 \times 10^4 \text{ s}^{-1}$  were measured for  $\mathbf{9}^{\bullet+}$  and  $\mathbf{9}^{\bullet-}$ , respectively (see Table 2.2.4). Quite surprisingly, these values are higher than those measured for  $\mathbf{7}^{\bullet+}$  and  $\mathbf{7}^{\bullet-}$  ( $k = 4.7 \times 10^3$  and  $2.2 \times 10^4 \text{ s}^{-1}$ , respectively). Even though the interplay between the relative stabilities of the radical cations and those of the decarboxylated radicals may play a role in this respect, no clear cut explanation for this observation can be envisaged. Further studies will be necessary in order to shed more light on this apparent discrepancy.

Table 2.2.5 displays the second-order rate constants for reaction of radical zwitterions  $\mathbf{7}^{\bullet-}$  and  $\mathbf{9}^{\bullet-}$  and of methyl ester radical cations  $\mathbf{11}^{\bullet+}$  and  $\mathbf{12}^{\bullet+}$  with  $\text{OH}^-$ . The  $k_{\text{OH}}$  values were observed to decrease on going from the monomethoxylated radical ions ( $k_{\text{OH}} = 7.1 \times 10^6$  and  $5.4 \times 10^7 \text{ M}^{-1} \text{ s}^{-1}$ , for  $\mathbf{7}^{\bullet-}$  and  $\mathbf{11}^{\bullet+}$ , respectively) to the dimethoxylated ones ( $k_{\text{OH}} = 1.0 \times 10^6$  and  $5.7 \times 10^6 \text{ M}^{-1} \text{ s}^{-1}$ , for  $\mathbf{9}^{\bullet-}$  and  $\mathbf{12}^{\bullet+}$ , respectively), and on going from the methyl ester radical cations to the corresponding carboxylic acid radical zwitterions.

At  $\text{pH} \approx 7$  radical zwitterions  $\mathbf{7}^{\bullet-}$  and  $\mathbf{9}^{\bullet-}$  were observed to undergo decarboxylation with  $k = 2.2 \times 10^4$  and  $3.5 \times 10^4 \text{ s}^{-1}$ , respectively (Table 2.2.4), whereas  $\mathbf{11}^{\bullet+}$  and  $\mathbf{12}^{\bullet+}$  displayed a significantly lower reactivity and only an upper limit for their decay rate constant could be obtained ( $k < 10^3 \text{ s}^{-1}$ ). In  $\mathbf{11}^{\bullet+}$  and  $\mathbf{12}^{\bullet+}$  the presence of the  $\text{CO}_2\text{Me}$  group prevents the decarboxylation reaction and moreover, the presence of the cyclopropyl group in the  $\alpha$  position precludes the possibility of benzylic C–H deprotonation as an alternative decay pathway. As mentioned above, ring-opening of the cyclopropane ring was not observed at  $\text{pH} \approx 7$ , indicating that water is not sufficiently nucleophilic to promote this reaction. In basic solution, however,  $\mathbf{11}^{\bullet+}$  and  $\mathbf{12}^{\bullet+}$  displayed a significantly higher reactivity than the corresponding carboxylic acid radical zwitterions  $\mathbf{7}^{\bullet-}$  and  $\mathbf{9}^{\bullet-}$ .

In order to explain this behavior it is reasonable to propose that under these conditions  $\mathbf{7}^{\bullet-}$ ,  $\mathbf{9}^{\bullet-}$ ,  $\mathbf{11}^{\bullet+}$  and  $\mathbf{12}^{\bullet+}$  undergo a  $\text{OH}^-$ -induced ring-opening of the cyclopropane ring, as described in Scheme 2.2.18. Quite importantly, the intercepts of the  $k_{\text{obs}}$  against  $[\text{NaOH}]$  plots for the reactions of  $\mathbf{7}^{\bullet-}$  and  $\mathbf{9}^{\bullet-}$  ( $1.6 \times 10^4$  and  $3.4 \times 10^4 \text{ s}^{-1}$ , see Figures 2.2.10 and 2.2.11, respectively), that represent the rate constants for the *uncatalyzed* reactions of  $\mathbf{7}^{\bullet-}$  and  $\mathbf{9}^{\bullet-}$ , are very close to the decarboxylation rate constants measured for these radical zwitterions at  $\text{pH} = 7.0$  ( $k = 2.2 \times 10^4$  and  $3.5 \times 10^4 \text{ s}^{-1}$ , see Table 2.2.4). On the basis of these observations it is reasonable to propose that at  $\text{pH} \geq 10$   $\mathbf{7}^{\bullet-}$  and  $\mathbf{9}^{\bullet-}$  undergo competition between decarboxylation and  $\text{OH}^-$ -induced ring-opening of the cyclopropane ring, with the latter process that becomes the major fragmentation pathway around  $\text{pH} 12$ .



Scheme 2.2.18.

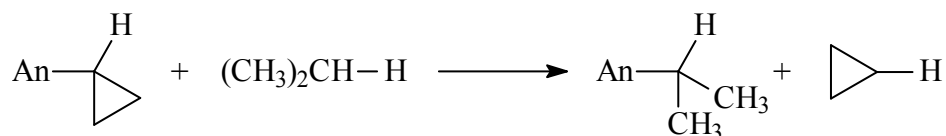
In this context, it has been shown that arylcyclopropane radical cations are characterized by a certain extent of positive charge at the C<sub>β</sub> carbon of the cyclopropane ring, and that nucleophilic attack generally occurs at this position.<sup>9,37</sup> Along this line, the *k*<sub>-OH</sub> values displayed in Table 2.2.5, can be rationalized in terms of the effect of the aromatic ring and of the cyclopropane ring substituent (CO<sub>2</sub><sup>-</sup> or CO<sub>2</sub>Me) on the stabilization of an incipient positive charge at C<sub>β</sub>, and consequently on the rate constant of the <sup>-</sup>OH-induced reaction. An increase in aromatic ring electron density determines a decrease in the extent of positive charge at C<sub>β</sub>, and accordingly *k*<sub>-OH</sub> is observed to decrease on going from  $\overset{-}{7}^{\dot{+}}$  to  $\overset{-}{9}^{\dot{+}}$  and from  $\mathbf{11}^{\dot{+}}$  to  $\mathbf{12}^{\dot{+}}$ . On the other hand, CO<sub>2</sub>Me is a relatively strong electron withdrawing group that is expected to increase the extent of positive charge at C<sub>β</sub> whereas the CO<sub>2</sub><sup>-</sup> group is expected to exert a negligible effect. Accordingly, as compared to  $\overset{-}{7}^{\dot{+}}$  and  $\overset{-}{9}^{\dot{+}}$ , significantly larger *k*<sub>-OH</sub> have been determined for  $\mathbf{11}^{\dot{+}}$  and  $\mathbf{12}^{\dot{+}}$ .

## References

- (1) Yu, X.-Y.; Bao, Z.-C.; Barker, J. R. *J. Phys. Chem. A* **2004**, *108*, 295-308.
- (2) Steenken, S.; Warren, C. J.; Gilbert, B. C. *J. Chem. Soc., Perkin Trans. 2* **1990**, 335-342.
- (3) Murov, S. L.; Carmichael, I.; Hug, G. L. *Handbook of Photochemistry* 2nd edition Marcel Dekker, New York 1993.
- (4) Baciocchi, E.; Bietti, M.; Ercolani, G.; Steenken, S. *Tetrahedron* **2003**, *59*, 613-618.
- (5) Baciocchi, E.; Bietti, M.; Steenken, S. *Chem. Eur. J.* **1999**, *5*, 1785-1793.
- (6) Baciocchi, E.; Bietti, M.; Manduchi, L.; Steenken, S. *J. Am. Chem. Soc.* **1999**, *121*, 6624-6629.
- (7) Baciocchi, E.; Bietti, M.; Putignani, L.; Steenken, S. *J. Am. Chem. Soc.* **1996**, *118*, 5952-5960.
- (8) Guirado, G.; Fleming, C. N.; Lingenfelter, T. G.; Williams, M. L.; Zuilhof, H.; Dinnocenzo, J. P. *J. Am. Chem. Soc.* **2004**, *126*, 14086-14094.
- (9) Dinnocenzo, J. P.; Zuilhof, H.; Lieberman, D. R.; Simpson, T. R.; McKechney, M. W. *J. Am. Chem. Soc.* **1997**, *119*, 994-1004.
- (10) This notation represents an oversimplification because, as compared to the radical cations, the corresponding radical zwitterions lack the presence of the carboxylic proton.
- (11) O'Neill, P.; Steenken, S.; Schulte-Frohlinde, D. *J. Phys. Chem.* **1975**, *79*, 2773-2779.
- (12) Baciocchi, E.; Bietti, M.; Gerini, M. F.; Manduchi, L.; Salamone, M.; Steenken, S. *Chem. Eur. J.* **2001**, *7*, 1408-1416.
- (13) Baciocchi, E.; Bietti, M.; Mattioli, M. *J. Org. Chem.* **1993**, *58*, 7106-7110.
- (14) Ebersson, L. *J. Am. Chem. Soc.* **1983**, *105*, 3192-3199.
- (15) It is important to point out that the time-resolution of the LFP equipment (8 ns laser pulse) is significantly lower than that of the PR equipment (300 ns electron pulse).
- (16) Drumright, R. E.; Mas, R. H.; Merola, J. S.; Tanko, J. M. *J. Org. Chem.* **1990**, *55*, 4098-4102.
- (17) Bally, T.; Borden, W. T. in *Reviews in Computational Chemistry, Vol. 13*; Lipkowitz, K. B., Boyd, D. B. Eds.; Wiley-VCH: New York, 1999, pp. 1-97.
- (18) Pratt, D. A.; Dilabio, G. A.; Mulder, P.; Ingold, K. U. *Acc. Chem. Res.* **2004**, *37*, 334-340 and references therein.
- (19) Baciocchi, E.; Bietti, M. *J. Chem. Soc., Perkin Trans. 2* **2002**, 720-722.

- (20) Baciocchi, E.; Bietti, M.; Lanzalunga, O.; Steenken, S. *J. Am. Chem. Soc.* **1998**, *120*, 11516-11517.
- (21) Font-Sanchis, E.; Aliaga, C.; Cornejo, R.; Scaiano, J. C. *Org. Lett.* **2003**, *5*, 1515-1518.
- (22) Scaiano, J. C.; Tanner, M.; Weir, D. *J. Am. Chem. Soc.* **1985**, *107*, 4396-4403.
- (23) Maillard, B.; Ingold, K. U.; Scaiano, J. C. *J. Am. Chem. Soc.* **1983**, *105*, 5095-5099.
- (24) Neta, P.; Madhavan, V.; Zemel, H.; Fessenden, R. W. *J. Am. Chem. Soc.* **1977**, *99*, 163-164.
- (25) Neta, P.; Huie, R. E.; Ross, A. B. *J. Phys. Chem. Ref. Data* **1988**, *17*, 1027-1284.
- (26) It is important to point out that whereas the results of an indirect kinetic study on the Co(III)W-induced oxidation of **1** were interpreted in terms of a rate-determining electron transfer from **1** to the relatively weak oxidant Co(III)W, leading to the conclusion that no aromatic radical cation  $\mathbf{1}^{\bullet+}$  was formed as a reaction intermediate (see reference 19 and Chapter 2.1), the mechanistic picture may be different with the significantly stronger oxidant  $\text{SO}_4^{\bullet-}$ .
- (27) Wang, Y.; Tanko, J. M. *J. Chem. Soc., Perkin Trans. 2* **1998**, 2705-2711.
- (28) Wang, Y.; Tanko, J. M. *J. Am. Chem. Soc.* **1997**, *119*, 8201-8208.
- (29) Dinnocenzo, J. P.; Simpson, T. R.; Zuilhof, H.; Todd, W. P.; Heinrich, T. *J. Am. Chem. Soc.* **1997**, *119*, 987-993.
- (30) In this respect, it is important to point out that clear evidence in favour of the formation of a cyclopropyl cation has been obtained only when the species is condensed in a rigid ring system,<sup>31,32</sup> or when the cationic center is bound to a strongly stabilizing ferrocenyl group.<sup>33</sup>
- (31) Schleyer, P. v. R.; Bremer, M. *J. Org. Chem.* **1988**, *53*, 2362-2364.
- (32) Olah, G. A.; Liang, G.; Ledlie, D. B.; Costopoulos, M. G. *J. Am. Chem. Soc.* **1977**, *99*, 4196-4198.
- (33) Surya Prakash, G. K.; Buchholz, H.; Prakash Reddy, V.; De Meijere, A.; Olah, G. A. *J. Am. Chem. Soc.* **1992**, *114*, 1097-1098.
- (34) DePuy, C. H.; Breitbeil, F. W.; DeBruin, K. R. *J. Am. Chem. Soc.* **1966**, *88*, 3347-3354.
- (35) Assuming that if  $\mathbf{6}^{\bullet+}$  is actually formed after one electron oxidation, it undergoes decarboxylation with  $k > 5 \times 10^7 \text{ s}^{-1}$ .
- (36) Gould, I. R.; Lenhard, J. R.; Muentner, A. A.; Godleski, S. A.; Farid, S. *J. Am. Chem. Soc.* **2000**, *122*, 11934-11943.
- (37) Dinnocenzo, J. P.; Merchán, M.; Roos, B. O.; Shaik, S.; Zuilhof, H. *J. Phys. Chem. A* **1998**, *102*, 8979-8987.
- (38) Gould, I. R.; Lenhard, J. R.; Farid, S. *J. Phys. Chem. A* **2004**, *108*, 10949-10956.

- (39) Hammond, G. S. *J. Am. Chem. Soc.* **1955**, *77*, 334-338.
- (40) It is however important to point out that this approach is based on the assumption that 4-methoxycyclopropylbenzene and 4-methoxycumene are characterized by the same energies. In order to validate this assumption, we have calculated, at the UB3LYP/6-31G(d) level of theory, the energy difference between products and reagents for the isodesmic reaction shown below (An = 4-MeOC<sub>6</sub>H<sub>4</sub>).



The energy difference thus obtained ( $\Delta E = -3.1 \text{ kcal mol}^{-1}$ ) is significantly smaller than the  $\Delta\text{BDE}$  of  $\approx 9 \text{ kcal mol}^{-1}$  reported above, and confirms that the 4-methoxycumyl radical is more stable than the 1-(4-methoxyphenyl)cyclopropyl radical.

- (41) Heinrich, M. R.; Zard, S. Z. *Org. Lett.* **2004**, *6*, 4969-4972.
- (42) Luo, Y.-R. *Handbook of Bond Dissociation Energies in Organic Compounds*. CRC Press LLC, Boca Raton, **2003**.
- (43) Walborsky, H. M. *Tetrahedron* **1981**, *37*, 1625-1651.
- (44) Bellanova, M.; Bietti, M.; Ercolani, G.; Salamone, M. *Tetrahedron* **2002**, *58*, 5039-5044.
- (45) Tolbert, L. M.; Li, Z.; Sirimanne, S. R.; VanDerveer, D. G. *J. Org. Chem.* **1997**, *62*, 3927-3930. Tolbert, L. M.; Khanna, R. K.; Popp, A. E.; Gelbaum, L.; Bottomley, L. A. *J. Am. Chem. Soc.* **1990**, *112*, 2373-2378.
- (46) Baciocchi, E.; D'Acunzo, F.; Galli, C.; Lanzaunga, O. *J. Chem. Soc., Perkin Trans. 2* **1996**, 133-140. Baciocchi, E.; Mattioli, M.; Romano, R.; Ruzziconi, R. *J. Org. Chem.* **1991**, *56*, 7154-7160.
- (47) Perrott, A. L.; Arnold, D. R. *Can. J. Chem.* **1992**, *70*, 272-279. Arnold, D. R.; Lamont, L. J.; Perrott, A. L. *Can. J. Chem.* **1991**, *69*, 225-233.





### 2.3 One-Electron Oxidation of Ring Methoxylated 1-Arylcycloalkanecarboxylic Acids. The Involvement of Aromatic Radical Cations and the Effect of Ring Size on the Decarboxylation Rate Constant.

Following the study of the one-electron oxidation reactions of ring-dimethoxylated phenylethanoic acids **2-5** discussed in Chapter 2.1, and of 2-aryl-2-methyl propanoic and 1-arylcyclopropanecarboxylic acids **6-9** discussed in Chapter 2.2, in order to obtain a deeper understanding of the role of structural effects on the one-electron oxidation of aryloethanoic acids and in particular on the possible involvement of aromatic radical cations in these processes, we have carried out a product and time-resolved kinetic study at different pH values on the one-electron oxidation of two related series of ring methoxylated 1-arylcycloalkanecarboxylic acids: 1-(4-methoxyphenyl)cyclobutanecarboxylic acid (**14**), 1-(4-methoxyphenyl)cyclopentanecarboxylic acid (**15**), 1-(4-methoxyphenyl)cyclohexanecarboxylic acid (**16**), 1-(3,4-dimethoxyphenyl)cyclobutanecarboxylic acid (**17**), 1-(3,4-dimethoxyphenyl)cyclopentanecarboxylic acid (**18**), and 1-(3,4-dimethoxyphenyl)cyclohexanecarboxylic acid (**19**), structurally related substrates derived from the side-chain modification of 4-methoxyphenylethanoic (**1**) and 3,4-dimethoxyphenylethanoic acids (**2**), respectively, whose structures are shown in Chart 2.3.1. As a matter of completeness, in this Chart, also the structures of 1-(4-methoxyphenyl)cyclopropanecarboxylic acid (**7**) and 1-(3,4-dimethoxyphenyl)cyclopropanecarboxylic acid (**9**), whose reactivities have been described in Chapter 2.2, have been included.

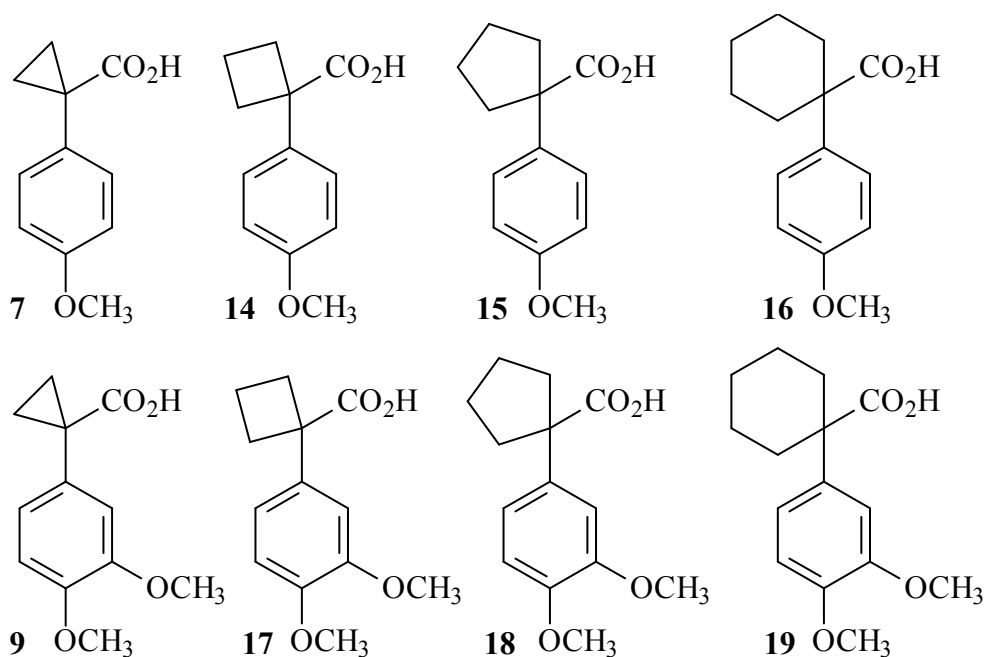
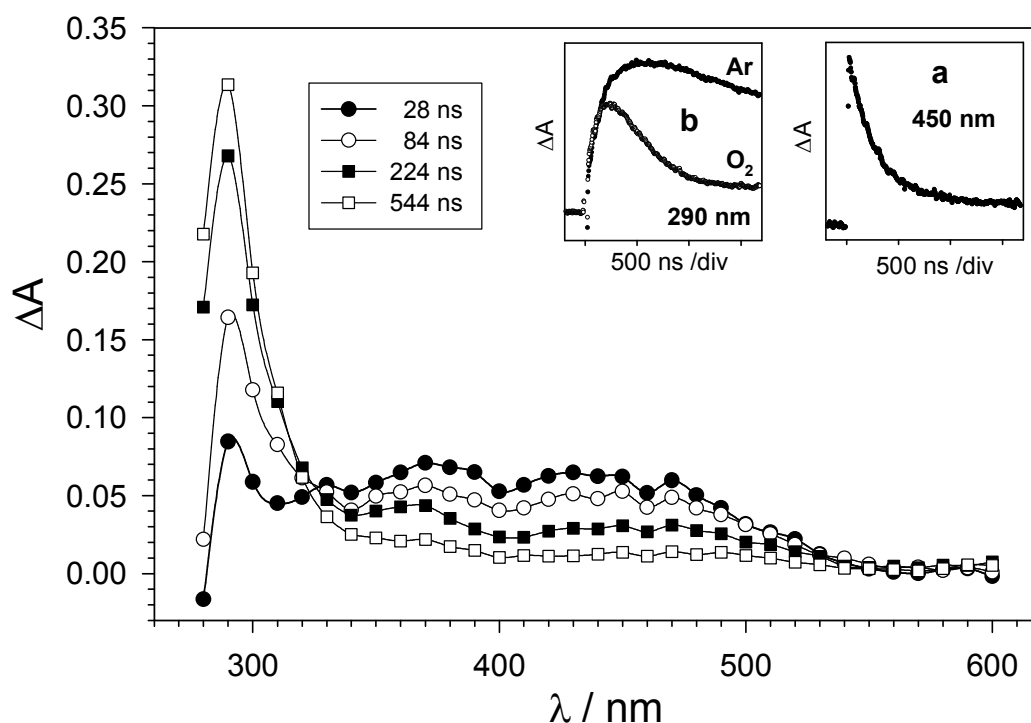


Chart 2.3.1

## Results

**Spectral properties.** Argon or nitrogen saturated aqueous solutions of substrates **14-19** (1.0-2.1 mM) were photolysed in the presence of 0.1 M  $K_2S_2O_8$  at  $pH \approx 2$  and  $pH \approx 7$ , employing 266 nm laser flash photolysis (LFP). Alternatively, time-resolved studies were carried out by pulse radiolysis (PR) of argon saturated aqueous solutions containing substrates **14-19** (0.5-1.0 mM),  $K_2S_2O_8$  (10 mM) and 2-methyl-2-propanol (0.2 M). Due to solubility problems, some experiments were carried out in the presence of 5-10 % (v/v) MeCN. The spectral properties of **7** and **9** were described previously in Chapter 2.2.

Figure 2.3.1 displays the time-resolved absorption spectra observed after LFP of an argon-saturated aqueous solution ( $pH = 1.7$ ) containing 1-(4-methoxyphenyl)cyclobutanecarboxylic acid (**14**) (2.1 mM),  $K_2S_2O_8$  (0.1 M) and 10 % MeCN (to improve the solubility of **14**).



**Figure 2.3.1.** Time-resolved absorption spectra observed after 266 nm LFP of an argon-saturated aqueous solution ( $T = 25\text{ }^\circ\text{C}$ ,  $pH = 1.7$ ) containing 10 % MeCN, 0.1 M  $K_2S_2O_8$  and 2.1 mM 1-(4-methoxyphenyl)cyclobutanecarboxylic acid (**14**), recorded at 28 (filled circles), 84 (empty circles), 224 (filled squares) and 544 ns (empty squares) after the 8 ns, 10 mJ laser flash. Insets: (a) First-order decay monitored at 450 nm. (b) Corresponding first-order buildup of absorption at 290 nm, measured under nitrogen (filled circles) and oxygen (empty circles).

The spectrum recorded 28 ns after the laser flash (filled circles) shows the formation of a broad absorption band between 340 and 530 nm, that by comparison with literature data,<sup>1,2</sup> and with the time-resolved absorption spectrum of  $SO_4^{\bullet-}$  (Chapter 2.2, Figure 2.2.2), can be assigned to  $SO_4^{\bullet-}$ , formed as described in Chapter 1, eq 1.2. The decay of this band (inset a)

occurs with  $k_{\downarrow}(450 \text{ nm}) = 3.9 \times 10^6 \text{ s}^{-1}$  and is accompanied by the formation of a species characterized by an absorption band at 290 nm (an isosbestic point is visible at 320 nm), whose decay is accelerated by the presence of oxygen (inset **b**).

An analogous behavior was observed after LFP of argon-saturated aqueous solutions (pH = 1.7) containing 1-(4-methoxyphenyl)cyclopentanecarboxylic acid (**15**) or 1-(4-methoxyphenyl)cyclohexanecarboxylic acid (**16**),  $\text{K}_2\text{S}_2\text{O}_8$  (0.1 M) and 10 % MeCN. Clearly no direct evidence for the formation of an intermediate was observed with substrates **14-16**, as described in Chapter 2.2 for 2-(4-methoxyphenyl)-2-methyl propanoic acid (**6**).

Figure 2.3.2 shows the time-resolved absorption spectra observed after LFP of a nitrogen-saturated aqueous solution (pH = 1.7) containing 0.1 M  $\text{K}_2\text{S}_2\text{O}_8$  and 1.1 mM 1-(3,4-dimethoxyphenyl)cyclobutanecarboxylic acid (**17**).

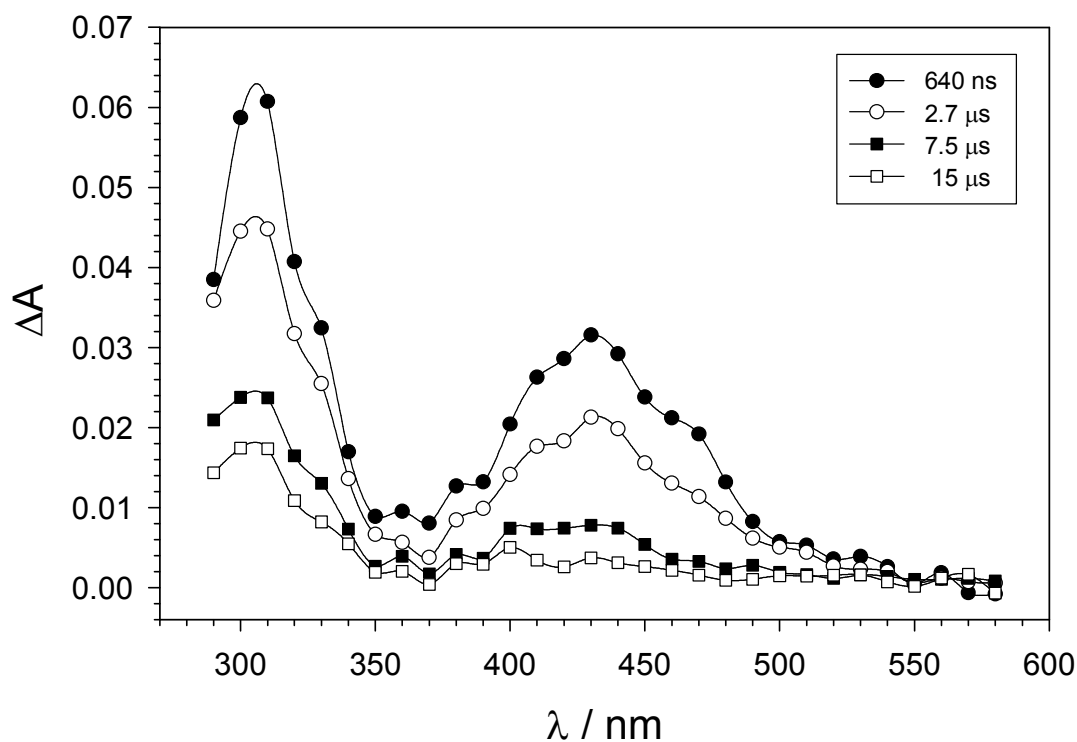
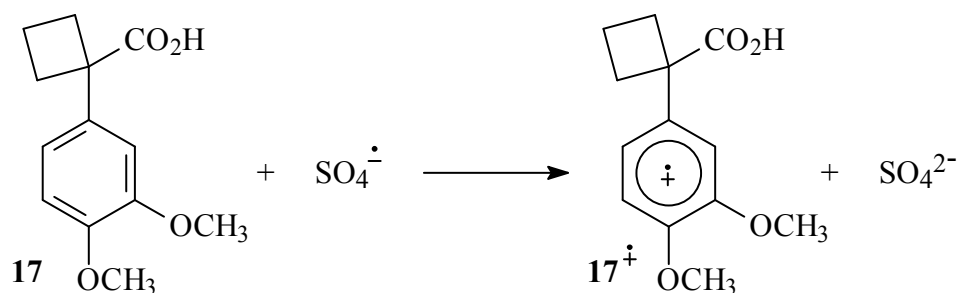


**Figure 2.3.2.** Time-resolved absorption spectra observed after 266 nm LFP of a nitrogen-saturated aqueous solution ( $T = 25 \text{ }^\circ\text{C}$ , pH = 1.7) containing 0.1 M  $\text{K}_2\text{S}_2\text{O}_8$  and 1.1 mM 1-(3,4-dimethoxyphenyl)cyclobutanecarboxylic acid (**17**), recorded 640 ns (filled circles), 2.7  $\mu\text{s}$  (empty circles), 7.5  $\mu\text{s}$  (filled squares) and 15  $\mu\text{s}$  (empty squares) after the 8 ns, 10 mJ laser flash.

The spectrum recorded 640 ns after the laser flash (filled circles) shows the formation of two bands, centered at 305 and 430 nm that are very similar to those observed previously for the radical cations of 1,2-dimethoxybenzene,<sup>3</sup> 1-(3,4-dimethoxyphenyl)alkanols,<sup>4</sup> and 3,4-dimethoxyphenylethanoic acid ( $\mathbf{2}^{\bullet+}$ ) (see Chapter 2.1).

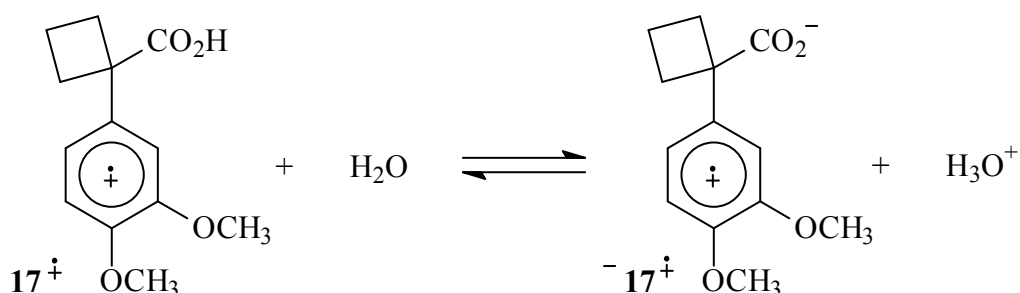
Similar spectra, characterized by two absorption bands centered at 310 and 430 nm were also observed after LFP of nitrogen-saturated aqueous solution (pH = 1.7) containing 5 % MeCN, 0.1 M  $K_2S_2O_8$  and 1.0 mM 1-(3,4-dimethoxyphenyl)cyclopentanecarboxylic acid (**18**) or 1-(3,4-dimethoxyphenyl)cyclohexanecarboxylic acid (**19**). In all cases, oxygen had no effect on the decay of the 310 and 430 nm bands.

On the basis of these observations, this transients described above can be reasonably assigned to the aromatic radical cation  $17^{\bullet+}$ - $19^{\bullet+}$ , formed by  $SO_4^{\bullet-}$  induced one-electron oxidation of the neutral substrates as described in Scheme 2.3.1 for **17**.



Scheme 2.3.1

By increasing the pH of the solution to  $\approx 7$ , the time-resolved spectrum obtained after  $SO_4^{\bullet-}$  induced one-electron oxidation of **17** was similar to those observed in acidic solution. However, as described previously (see Chapters 2.1 and 2.2), a broadening of the radical cation visible absorption band, accompanied by a 15 nm red-shift in its position was observed. This behavior is attributed to the formation of the radical zwitterions  $^{-}17^{\bullet+}$ ,<sup>5</sup> as described in Scheme 2.3.2.<sup>6</sup>



Scheme 2.3.2

Figure 2.3.3 shows the time-resolved absorption spectra observed after 266 nm LFP of an argon-saturated aqueous solution (pH = 6.9) containing **17** (2.0 mM) and  $K_2S_2O_8$  (0.1 M). The broadening of the visible absorption band is accompanied by a 15 nm red shift in its position

on going from  $17^{•+}$  to  $^{-}17^{•+}$ . Again, no effect of oxygen on the decay of the 310 and 445 nm bands was observed.

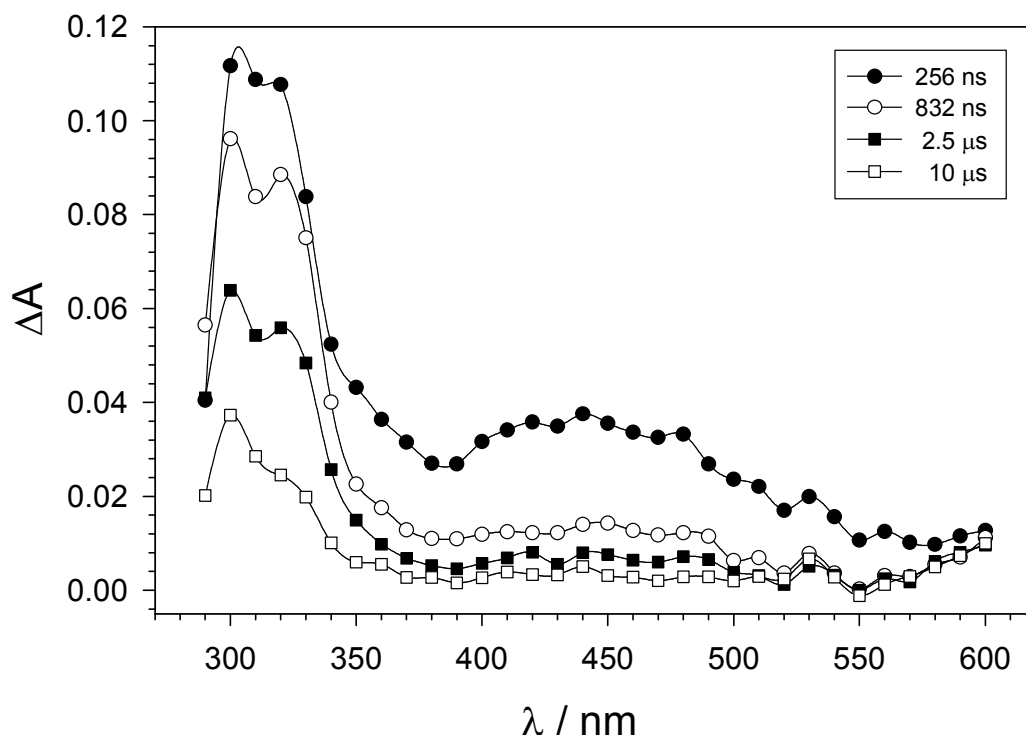
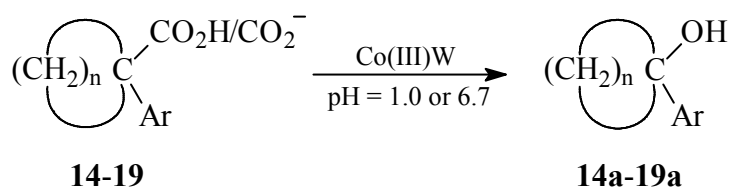


**Figure 2.3.3.** Time-resolved absorption spectra observed after 266 nm LFP of an argon-saturated aqueous solution ( $T = 25\text{ }^{\circ}\text{C}$ ,  $\text{pH} = 6.9$ ) containing  $0.1\text{ M K}_2\text{S}_2\text{O}_8$ ,  $2.0\text{ mM}$  1-(3,4-dimethoxyphenyl)cyclobutanecarboxylic acid (**17**) and  $10\text{ mM KH}_2\text{PO}_4$ , recorded at  $256\text{ ns}$  (filled circles),  $832\text{ ns}$  (empty circles),  $2.5\text{ }\mu\text{s}$  (filled squares) and  $10\text{ }\mu\text{s}$  (empty squares) after the  $8\text{ ns}$ ,  $10\text{ mJ}$  laser flash.

**Product studies.** The oxidation reactions of substrates **14-19** were carried out in argon saturated aqueous solution ( $\text{pH} = 1.0$  and  $6.7$ ) at  $T = 25\text{ }^{\circ}\text{C}$ , employing potassium 12-tungstocobalt(III)ate (Co(III)W) as the oxidant. Oxidations were generally carried out until complete conversion of the oxidant. For all substrates product analysis, both at  $\text{pH} = 1.0$  and  $6.7$ , showed the exclusive formation of the corresponding 1-arylcycloalkanol (**14a-19a**) as described in Scheme 2.3.3.



Scheme 2.3.3

The product distributions observed in the Co(III)W-induced oxidation reactions carried out on 1-arylcycloalkancarboxylic acids **14-19** are collected in Table 2.2.1.

**Table 2.2.1.** Product distributions observed in the Co(III)W-induced oxidation of 1-arylcycloalkanecarboxylic acids **14-19**, carried out in aqueous solution at  $T = 25\text{ }^{\circ}\text{C}$ .<sup>a</sup>

substrate	pH <sup>b</sup>	recovered substrate (%)	1-arylcycloalkanol (14a-19a) (%)
<b>14</b>	1.0 <sup>c</sup>	67	33
<b>14</b>	6.7 <sup>c</sup>	60	40
<b>15</b>	1.0 <sup>d</sup>	85	15
<b>15</b>	6.7 <sup>c</sup>	62	38
<b>16</b>	1.0 <sup>d</sup>	87	13
<b>16</b>	6.7 <sup>e</sup>	20	80
<b>17</b>	1.0 <sup>c</sup>	51	49
<b>17</b>	6.7 <sup>c</sup>	57	43
<b>18</b>	1.0 <sup>d</sup>	77	23
<b>18</b>	6.7 <sup>e</sup>	21	79
<b>19</b>	1.0 <sup>d</sup>	51	49
<b>19</b>	6.7 <sup>e</sup>	23	77

<sup>a</sup>Good to excellent mass balances ( $\geq 90\%$ ) were observed in all experiments. <sup>b</sup>pH = 1.0 (HClO<sub>4</sub> 0.1 M); pH = 6.7 (NaH<sub>2</sub>PO<sub>4</sub> 0.1 M, adjusted with NaOH). <sup>c</sup>[substrate] = 1 mM, [Co(III)W] = 2 mM. <sup>d</sup>[substrate] = 0.002 M, [Co(III)W] = 3 mM. <sup>e</sup>[substrate] = 0.001 M, [Co(III)W] = 1 mM, 20 % MeCN.

**Time-resolved kinetic studies.** As mentioned above, no intermediate radical cations were detected in the time-resolved studies carried out for 1-arylcycloalkanecarboxylic acids **14-16**. As discussed previously in Chapter 2.2 for 2-(4-methoxyphenyl)-2-methylpropanoic acid (**6**), the kinetic data obtained by LFP indicate that if intermediate radical cations are actually formed after one electron oxidation of **14-16**, their decay rate constants must be  $> 5 \times 10^7\text{ s}^{-1}$ . The decay of the radical cations **17**<sup>•+</sup>-**19**<sup>•+</sup> and of the radical zwitterion <sup>-</sup>**17**<sup>•+</sup> was measured spectrophotometrically in aqueous solution ( $T = 25\text{ }^{\circ}\text{C}$ , pH = 1.7 and  $\approx 7$ , respectively) following the decrease in optical density at the corresponding visible absorption band maximum (between 430 and 450 nm). In all cases the decay was observed to follow first order kinetics in a reaction that, on the basis of product analysis results, is assigned to decarboxylation. The rate constants thus obtained are collected in Table 2.3.2. As a matter of

comparison, the rate constants obtained analogously for  $\mathbf{2}^{\bullet+}$  (see Chapter 2.1),  $\mathbf{7}^{\bullet+}$ - $\mathbf{9}^{\bullet+}$  (see Chapter 2.2) and for the corresponding radical zwitterions have also been included

**Table 2.3.2.** First-order rate constants ( $k$ ) for the decay of radical cations and radical zwitterions generated after PR and/or LFP of the parent substrates **2**, **7-9**, **17-19** in aqueous solution, measured at  $T = 25$  °C.

substrate	pH <sup>a</sup>	transient	generation	$\lambda_{\text{det}}^{\text{b}}$ / nm	$k$ / s <sup>-1</sup>	
<b>2</b>	1.7	$\mathbf{2}^{\bullet+}$	PR, SO <sub>4</sub> <sup>•-</sup> , Ar	425	$5.2 \times 10^3$	
	7.1	$\text{-}\mathbf{2}^{\bullet+}$	PR, SO <sub>4</sub> <sup>•-</sup> , Ar	450	$6.5 \times 10^4$	
<b>7</b>	1.7	$\mathbf{7}^{\bullet+}$	PR, SO <sub>4</sub> <sup>•-</sup> , Ar	500	$4.7 \times 10^3$	
	7.0	$\text{-}\mathbf{7}^{\bullet+}$	PR, SO <sub>4</sub> <sup>•-</sup> , Ar	520	$2.2 \times 10^4$	
<b>8</b>	1.7	$\mathbf{8}^{\bullet+}$	PR, SO <sub>4</sub> <sup>•-</sup> , Ar	420	$2.1 \times 10^5$	
	6.8	$\text{-}\mathbf{8}^{\bullet+}$	LFP, SO <sub>4</sub> <sup>•-</sup> , N <sub>2</sub>	420	$2.6 \times 10^6$	
<b>9</b>	1.7	$\mathbf{9}^{\bullet+}$	PR, SO <sub>4</sub> <sup>•-</sup> , Ar	445	$1.1 \times 10^4$	
	7.0	$\text{-}\mathbf{9}^{\bullet+}$	PR, SO <sub>4</sub> <sup>•-</sup> , Ar	465	$3.5 \times 10^4$	
<b>17</b>	1.7	$\mathbf{17}^{\bullet+}$	PR, SO <sub>4</sub> <sup>•-</sup> , Ar	430	$3.1 \times 10^5$	
	1.7	$\mathbf{17}^{\bullet+}$	PR, SO <sub>4</sub> <sup>•-</sup> , O <sub>2</sub>	430	$3.4 \times 10^5$	
	1.7	$\mathbf{17}^{\bullet+}$	LFP, SO <sub>4</sub> <sup>•-</sup> , N <sub>2</sub>	430	$2.9 \times 10^5$	
	1.7	$\mathbf{17}^{\bullet+}$	LFP, SO <sub>4</sub> <sup>•-</sup> , O <sub>2</sub>	430	$2.9 \times 10^5$	
	1.7	5% MeCN	$\mathbf{17}^{\bullet+}$	LFP, SO <sub>4</sub> <sup>•-</sup> , N <sub>2</sub>	430	$4.0 \times 10^5$
	1.7	10% MeCN	$\mathbf{17}^{\bullet+}$	LFP, SO <sub>4</sub> <sup>•-</sup> , N <sub>2</sub>	430	$5.4 \times 10^5$
	1.7	10% MeCN	$\mathbf{17}^{\bullet+}$	LFP, SO <sub>4</sub> <sup>•-</sup> , O <sub>2</sub>	430	$5.4 \times 10^5$
	6.9		$\text{-}\mathbf{17}^{\bullet+}$	LFP, SO <sub>4</sub> <sup>•-</sup> , N <sub>2</sub>	450	$2.8 \times 10^6$
	6.9		$\text{-}\mathbf{17}^{\bullet+}$	LFP, SO <sub>4</sub> <sup>•-</sup> , O <sub>2</sub>	450	$2.8 \times 10^6$
	1.7		$\mathbf{18}^{\bullet+}$	PR, SO <sub>4</sub> <sup>•-</sup> , Ar	430	$\geq 8 \times 10^5$ <sup>c</sup>
<b>18</b>	1.7	$\mathbf{18}^{\bullet+}$	PR, SO <sub>4</sub> <sup>•-</sup> , O <sub>2</sub>	430	$\geq 8 \times 10^5$ <sup>c</sup>	
	1.7	5% MeCN	$\mathbf{18}^{\bullet+}$	LFP, SO <sub>4</sub> <sup>•-</sup> , N <sub>2</sub>	430	$1.1 \times 10^6$
	1.7	5% MeCN	$\mathbf{18}^{\bullet+}$	LFP, SO <sub>4</sub> <sup>•-</sup> , O <sub>2</sub>	430	$1.1 \times 10^6$
	1.7	10% MeCN	$\mathbf{18}^{\bullet+}$	LFP, SO <sub>4</sub> <sup>•-</sup> , N <sub>2</sub>	430	$1.4 \times 10^6$
	1.7	10% MeCN	$\mathbf{18}^{\bullet+}$	LFP, SO <sub>4</sub> <sup>•-</sup> , O <sub>2</sub>	430	$1.4 \times 10^6$
	1.7		$\mathbf{19}^{\bullet+}$	PR, SO <sub>4</sub> <sup>•-</sup> , Ar	430	$\geq 8 \times 10^5$ <sup>c</sup>
<b>19</b>	1.7	$\mathbf{19}^{\bullet+}$	PR, SO <sub>4</sub> <sup>•-</sup> , O <sub>2</sub>	430	$\geq 8 \times 10^5$ <sup>c</sup>	
	1.7	10% MeCN	$\mathbf{19}^{\bullet+}$	LFP, SO <sub>4</sub> <sup>•-</sup> , N <sub>2</sub>	430	$1.0 \times 10^6$
	1.7	10% MeCN	$\mathbf{19}^{\bullet+}$	LFP, SO <sub>4</sub> <sup>•-</sup> , O <sub>2</sub>	430	$1.1 \times 10^6$
	1.7	10% MeCN	$\mathbf{19}^{\bullet+}$	LFP, SO <sub>4</sub> <sup>•-</sup> , O <sub>2</sub>	430	$1.1 \times 10^6$

<sup>a</sup>pH = 1.7 (adjusted with HClO<sub>4</sub>); pH  $\approx$  7 (KH<sub>2</sub>PO<sub>4</sub> 10 mM, adjusted with NaOH).

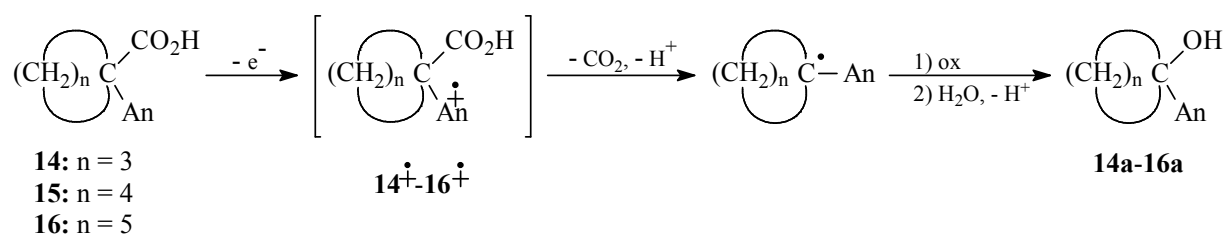
<sup>b</sup>Monitoring wavelength. <sup>c</sup>The time-resolution of the PR equipment did not allow a sufficiently reliable measurement of the decay rate constant and only a lower limit is given.

## Discussion

Product studies carried out on 1-(4-methoxyphenyl)cycloalkanecarboxylic acids **14-16** showed the exclusive formation of the corresponding 1-(4-methoxyphenyl)cycloalkanol **14a-16a** as described in Schemes 2.3.3. These products clearly derives from the oxidation of an intermediate 1-(4-methoxyphenyl)cycloalkyl radical formed after oxidative decarboxylation of **14-16**, as described previously for the one-electron oxidation of 4-methoxyphenylethanoic acid (**1**) and 2-(4-methoxyphenyl)-2-methylpropanoic acid (**6**) in acidic aqueous solution (see Chapters 2.1 and 2.2).<sup>7,8</sup>

LFP experiments carried out at pH = 1.7 did not provide any direct evidence for the formation of intermediate radical cations **14<sup>•+</sup>-16<sup>•+</sup>**, showing instead the initial formation of  $\text{SO}_4^{\bullet-}$  whose decay was in all cases accompanied by a corresponding buildup in absorption in the UV region of the spectrum of a transient species whose decay was accelerated by oxygen. On the basis of these observation and of the results of product studies described above these transients can be reasonably assigned to the 1-(4-methoxyphenyl)cycloalkyl radicals.

Overall, these results are consistent with those obtained previously for the one-electron oxidation of **1** and **6**, where no direct evidence for the formation of an intermediate radical cation but only of the 4-methoxybenzyl and 4-methoxycumyl radicals, respectively, was obtained.<sup>7,8</sup> The mechanism of the one-electron oxidation of **14-16** can be thus described according to Scheme 2.3.4 (An = 4-MeOC<sub>6</sub>H<sub>4</sub>): one-electron oxidation is coupled with the decarboxylation reaction, directly leading to the 1-(4-methoxyphenyl)cycloalkyl radical. Oxidation of this radical in the reaction medium gives **14a-16a**.



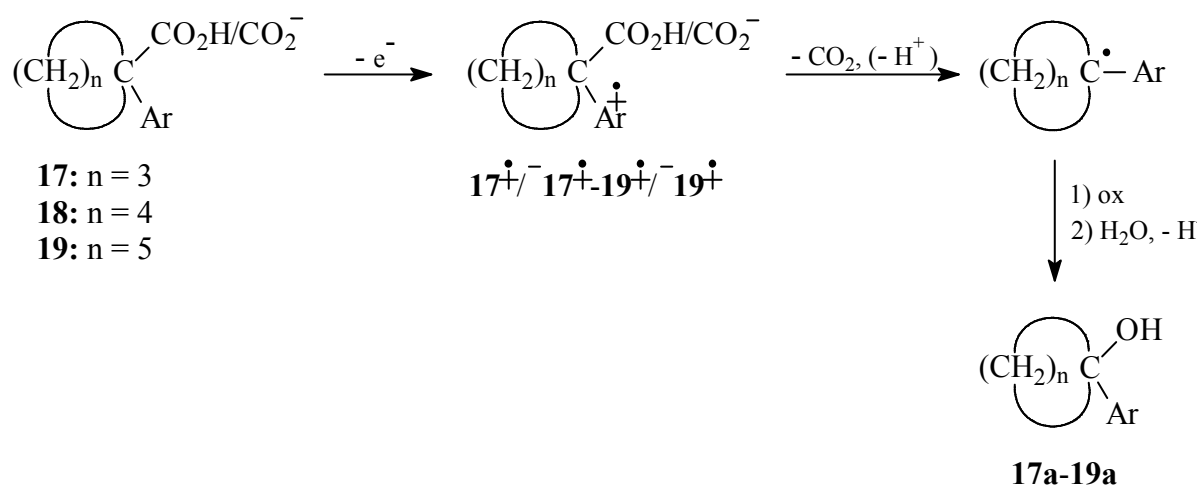
Scheme 2.3.4

Clearly, even though no intermediate radical cation was detected in the LFP experiments, the kinetic data do not allow to exclude the possible intermediacy of **14<sup>•+</sup>-16<sup>•+</sup>**, because their lifetime could be too short to allow detection under the experimental conditions employed: in other words, if **14<sup>•+</sup>-16<sup>•+</sup>** are actually formed after one electron oxidation, their decarboxylation rate constant must be extremely fast ( $k > 5 \times 10^7 \text{ s}^{-1}$ ).



On going from **14-16** to the corresponding dimethoxylated 1-arylcycloalkanoic acids **17-19**, time-resolved studies showed in all cases the formation of the corresponding radical cations **17<sup>•+</sup>-19<sup>•+</sup>** at pH = 1.7 and of the radical zwitterion **17<sup>•+</sup>** at pH ≈ 7.<sup>6</sup>

Product studies carried out on **17-19** showed the exclusive formation of the corresponding 1-(3,4-dimethoxyphenyl)cycloalkanol **17a-19a** both at pH = 1.0 and 6.7. Formation of these product can be explained in terms of the mechanism described in Scheme 2.3.5 (Ar = 3,4-(MeO)<sub>2</sub>C<sub>6</sub>H<sub>3</sub>): oxidation of **17-19** leads to the formation of **17<sup>•+</sup>-19<sup>•+</sup>** (or **17<sup>•+</sup>-19<sup>•+</sup>**) that undergo decarboxylation to give the corresponding 1-(3,4-dimethoxyphenyl)cycloalkyl radical. Oxidation of these radicals in the reaction medium gives **17a-19a**.



Scheme 2.3.5

Clearly, as compared to **14-16**, the presence of an additional methoxy ring substituent in **17-19** determines a significant stabilization of the radical cations that accordingly undergo decarboxylation with significantly lower rate constants.<sup>9</sup>

The first-order decarboxylation rate constants (*k*) measured for 1-(3,4-dimethoxyphenyl)cycloalkanecarboxylic acid radical cations **9<sup>•+</sup>**, **17<sup>•+</sup>-19<sup>•+</sup>** are collected in Table 2.3.2. Due to the low solubility of **18** and **19** in aqueous solution, some experiments were carried out in the presence of 5-10 % (v/v) MeCN. The decarboxylation rate constants were observed to increase with increasing the amount of MeCN (see the *k* values for **17<sup>•+</sup>** and **18<sup>•+</sup>** in Table 2.3.2), a behavior that was observed previously for the decarboxylation of anilino bis carboxylate radical cations.<sup>10</sup> An increase in the amount of MeCN determines a decrease in radical cation stability that results in turn in a corresponding increase in decarboxylation rate constant. The comparison between the rate constants measured for **9<sup>•+</sup>**, **17<sup>•+</sup>-19<sup>•+</sup>** shows that the decarboxylation is influenced by the size of the cycloalkane ring, following the order: **9<sup>•+</sup>**

$< \mathbf{17}^{\bullet+} < \mathbf{19}^{\bullet+} < \mathbf{18}^{\bullet+}$ . With the exclusion of  $\mathbf{9}^{\bullet+}$ , where the cyclopropyl group has been shown to increase the radical cation stability, comparable stabilities can be reasonably assumed for  $\mathbf{17}^{\bullet+}$ - $\mathbf{19}^{\bullet+}$ . Accordingly, the stability of the carbon centered radical formed after decarboxylation is expected to play an important role.<sup>11</sup> In this context, Gould and Farid have clearly shown that in the decarboxylation of radical cations characterized by comparable stabilities, the decarboxylation rate constants is influenced by the stability of the product radical, increasing with increasing radical stability.<sup>10</sup> Along this line, the differences between the C–H BDEs of cycloalkanes can be taken as simple models in order to assess the relative stabilities of the 1-(3,4-dimethoxyphenyl)cycloalkyl radicals formed after decarboxylation of  $\mathbf{9}^{\bullet+}$ ,  $\mathbf{17}^{\bullet+}$ - $\mathbf{19}^{\bullet+}$ . C–H BDEs of 106.3, 96.5, 94.5 and 95.5 kcal mol<sup>-1</sup> are available for cyclopropane, cyclobutane, cyclopentane and cyclohexane, respectively;<sup>12</sup> moreover, a similar order in BDE values has been obtained recently by means of accurate G3 calculations (109.2, 100.5, 96.4 and 100.0 for cyclopropane, cyclobutane, cyclopentane and cyclohexane, respectively).<sup>13</sup> Quite interestingly, these C–H BDE values are in line with the order in decarboxylation rate constants reported above for  $\mathbf{9}^{\bullet+}$ ,  $\mathbf{17}^{\bullet+}$ - $\mathbf{19}^{\bullet+}$ , suggesting that in this process the stability of the carbon centered radical formed after decarboxylation plays an important role. Clearly, in order to provide a more precise evaluation of the role of this effect, the calculation of the  $\alpha$ -C–H BDEs for the 1-arylcycloalkane series is certainly required.

It is also interesting to compare the decarboxylation rate constants for  $\mathbf{9}^{\bullet+}$ ,  $\mathbf{17}^{\bullet+}$ - $\mathbf{19}^{\bullet+}$ , with those measured for  $\mathbf{2}^{\bullet+}$ ,  $\mathbf{8}^{\bullet+}$  and  $\mathbf{9}^{\bullet+}$ .  $\mathbf{8}^{\bullet+}$  undergoes decarboxylation with a rate constant that is similar to the one measured for  $\mathbf{17}^{\bullet+}$  ( $k = 2.1 \times 10^5$  and  $3.1 \times 10^5$  s<sup>-1</sup>, respectively), in line with the similar stabilities of the corresponding decarboxylated radicals.<sup>12,13</sup>  $\mathbf{2}^{\bullet+}$  displays the lowest decarboxylation rate constant among the dimethoxylated radical cations shown in Table 2.3.2, an observation that likely reflects the relatively lower stability of a primary benzyl radical as compared to tertiary ones. Along this line, the observation that  $\mathbf{9}^{\bullet+}$  undergoes decarboxylation with a rate constant that is higher than the one measured for  $\mathbf{2}^{\bullet+}$  ( $k = 1.1 \times 10^4$  and  $5.2 \times 10^3$  s<sup>-1</sup>, respectively) is somewhat unexpected. As the relative stabilities of the radical cations and those of the decarboxylated carbon radicals are expected to exert their effect in the same direction that is by decreasing the decarboxylation rate constant of  $\mathbf{9}^{\bullet+}$  as compared to that of  $\mathbf{2}^{\bullet+}$ , in order to explain this behavior it can be suggested that the stereoelectronic requirements may play an important role in this respect. However, no clear cut explanation for this apparent discrepancy is presently available and further studies will surely be necessary.

Finally, with  $\mathbf{17}$  an increases in decarboxylation rate constant was observed on going from the radical cation to the corresponding radical zwitterion ( $k = 3.1 \times 10^5$  and  $2.8 \times 10^6$  s<sup>-1</sup>,

respectively).<sup>6</sup> This behavior was also observed for  $2^{\bullet+}$ - $5^{\bullet+}$  (Chapter 2.1) and for  $7^{\bullet+}$ - $9^{\bullet+}$  (Chapter 2.2), and has been rationalized in terms of the kinetic barrier for intramolecular side-chain to ring electron transfer required for decarboxylation that is expected to be higher for the radical cation, because, as compared to the radical zwitterion an additional proton transfer to the medium is required.

## References

- (1) Yu, X.-Y.; Bao, Z.-C.; Barker, J. R. *J. Phys. Chem. A* **2004**, *108*, 295-308.
- (2) Steenken, S.; Warren, C. J.; Gilbert, B. C. *J. Chem. Soc., Perkin Trans. 2* **1990**, 335-342.
- (3) O'Neill, P.; Steenken, S.; Schulte-Frohlinde, D. *J. Phys. Chem.* **1975**, *79*, 2773-2779.
- (4) Baciocchi, E.; Bietti, M.; Gerini, M. F.; Manduchi, L.; Salamone, M.; Steenken, S. *Chem. Eur. J.* **2001**, *7*, 1408-1416.
- (5) This notation represents an oversimplification because, as compared to the radical cations, the corresponding radical zwitterions lack the presence of the carboxylic proton.
- (6) Due to solubility problems and to the relatively high rate constants measured for the decarboxylation of  $\mathbf{18^{\bullet+}}$  and  $\mathbf{19^{\bullet+}}$  (see Table 2.3.2), time-resolved studies on these radical cations were limited to pH = 1.7.
- (7) Baciocchi, E.; Bietti, M. *J. Chem. Soc., Perkin Trans. 2* **2002**, 720-722.
- (8) Steenken, S.; Warren, C. J.; Gilbert, B. C. *J. Chem. Soc., Perkin Trans. 2* **1990**, 335-342.
- (9) Assuming that if  $\mathbf{14^{\bullet+}}$ - $\mathbf{16^{\bullet+}}$  are actually formed after one electron oxidation, they undergoes decarboxylation with  $k > 5 \times 10^7 \text{ s}^{-1}$ .
- (10) Gould, I. R.; Lenhard, J. R.; Farid, S. *J. Phys. Chem. A* **2004**, *108*, 10949-10956.
- (11) In the following discussion, the possible role of stereoelectronic effects on the rate of decarboxylation has been neglected.
- (12) McMillen, D. F.; Golden, D. M. *Annu. Rev. Phys. Chem.* **1982**, *33*, 493-532.
- (13) Tian, Z.; Fattahi, A.; Lis, L.; Kass, S. R. *J. Am. Chem. Soc.* **2006**, *128*, 17087-17092.